UNDERGROUND EXCAVATION IN JOINTED ROCKS

JIAO XUGUANG

NATIONAL UNIVERSITY OF SINGAPORE

2014

UNDERGROUND EXCAVATION IN JOINTED ROCKS

JIAO XUGUANG

(B.Eng.(Hons.),NUS)

A THESIS SUBMITTED

FOR THE DEGREE OF MASTER OF ENGINEERING

DEPARTMENT OF CIVIL AND ENVIRONMENTAL ENGINEERING

NATIONAL UNIVERSITY OF SINGAPORE

2014

DECLARATION

I hereby declare that the thesis is my original work and it has been written by me in its entirety. I have duly acknowledged all the sources of information which have been used in the thesis.

This thesis has also not been submitted for any degree in any university previously.

_____

Jiao Xuguang

30 July 2014

Acknowledgements

I would like to express the deepest appreciation to my supervisors, Professor Leung Chun Fai and Assistant Professor Ong Ghim Ping, Raymond for their patient guidance, encouragement and useful critiques of this research work. I am extremely blessed by their unconditional support. I also wish to thank them for revising the English of my thesis.

I would also like to thank the fellow colleagues, in particular Ay Lee, Kok Shien, Yang Yu, Zongrui, Junhui for their company through this journey. Also, I would like to thank my good friends for their support and continuing belief in me. Special thanks to Yanyan for her encouragement.

Last but not the least, an honorable mention goes to my family for always being there for me.

Table of Contents

Acknowledgements ..... **i**

Table of Contents ..... **ii**

Summary ..... **v**

List of Tables ..... **vii**

List of Figures ..... **ix**

List of Symbols ..... **xiii**

Chapter 1 Introduction **1**

1.1 Research Objective 5

1.2 Thesis Organization 5

Chapter 2 Literature Review **7**

2.1 Introduction 7

2.2Rock Reinforcement Design Methods 8

2.2.1 Empirical Method 8

2.2.2 Analytical Design Methods 14

2.2.3 Probabilistic Approach 29

2.3 Variation of Rock Parameters 35

2.3.1 Joint Orientation 36

2.3.2 Size Parameters 42

2.4 Summary 46

2.4 Scope of Work 47

Chapter 3 Joint Orientation Simulation **49**

3.1 Introduction 49

3.2 Methodology 50

3.3 Joint Set Classification 51

3.4 Goodness of Fit Test 54

3.5 Parameter Estimation of Kent Distribution 64

3.6 Simulation of Kent Distribution 67

3.7 Rotation Matrix 73

3.8 Case Study 75
3.9 Summary 85
Chapter 4 Unstable Block Identification 87
4.1 Introduction 87
4.2 Methodology for Probabilistic Unstable Block Identification 89
4.3 Basic Assumptions and Rock Parameter distributions 90
4.3.1 Ubiquitous Approach 91
4.3.2 Discontinuity Orientation 91
4.3.3 Trace Length 92
4.3.4 Discontinuities Spacing 93
4.3.5 Friction Angle and Cohesion 94
4.3.6 Water Pressure 95
4.4 Deterministic Block Analysis Model 95
4.4.1 Scaling Factor 96
4.4.2 Case Study- Louvicourt Mine in Northeastern Canada 101
4.5 Probability of Joint Set Combination 106
4.6 Iteration Times for Monte Carlo Simulation 108
4.7 Case Study 112
4.7.1 Louvicourt Mine in Northeastern Canada 113
4.7.2 Singapore Jurong Formation 121
4.7.3 Singapore Kent Ridge data 128
4.7.4 Hypothetical Case 132
4.8 Summary 146
Chapter 5 Rock Support Design 148
5.1 Introduction 148
5.2 Reinforcement Design 151
5.2.1 Rock Bolt Length 151
5.2.2 Number of Bolts 153
5.2.3 Resultant Force 154
5.2.4 Rock Bolt Capacity 158

5.2.5 Bolt Angle 159
5.2.6 Rock Bolt Spacing 160
5.4 Design Criteria 161
5.4.1 Introduction 161
5.4.2 Factor of Safety vs. Probability of Failure 163
5.5 Model for Reliability Assessment 165
5.5.1 Model setup Assumptions 171
5.6 Case study 172
5.6.1 Singapore Jurong formation (1) 172
5.6.2 Singapore Jurong Formation (2) 182
5.7 Summary 187
Chapter 6 Conclusion 190
6.1 Summary of Findings 190
6.2 Recommendations for Further Studies 192
Reference 194
Appendix 201

Summary

When excavating jointed rocks underground, unstable rock blocks may be formed due to unfavorable orientation of the rock joints. The characteristics of unstable rock block define the magnitude of rock support and reinforcement required in the design of underground rock excavations. Variation in rock parameters may result in uncertainties on the identification of these unstable rock blocks. In view of the above, this study aims to investigate the effects of variation in rock parameters on rock block identification. Reliability-based design with probability of failure is adopted to evaluate the stability of rock block in underground excavations. The effects of scatter of various rock parameters are examined in detail using Monte Carlo simulation. It is found that the occurrence of non-symmetrical distributed joint sets is dominant with 15 joint sets out of 21 joint sets gathered in the field from Singapore and overseas. The commonly assumed Fisher distribution fails to simulate these non-symmetrical joint sets. Thus, a more flexible Kent distribution was investigated for joint orientation simulation. A parametric study has been conducted and the results show that joint set concentration, ovalness and position have significant effects on the failure mode and volume of unstable rock blocks. As such, Kent distribution which can handle non-symmetrical data should be adopted for joint orientation simulation instead of Fisher distribution. In addition, reliability assessment of reinforced rock block shows that rock reinforcement design using conventional deterministic rock block

analysis with a Factor of Safety (FoS) may not be reliable. Reliability-based design with considering Probability of Failure (PoF) was investigated and a parametric study has been conducted revealing that increasing rock bolt length, bolt capacity and decrease in bolt spacing will result in a more stable rock block. The results of probabilistic block analysis and parametric study are presented as an aid to conduct reliability-based rock reinforcement design.

List of Tables

Table 2.1 Rock Mass Rating System (After Bieniawski, 1989) 10

Table 3.1 Joint set classification result 58

Table 3.2 Probability plot result and Goodness of fit test result by Mardia and Jupp (2009)'s method 63

Table 3.3 Joint orientation of EXAMPFLD 79

Table 3.4 Joint orientation of Joint Set 3 80

Table 3.5 Parameter estimation and Goodness of fit test results 81

Table 4.1 Spacing distribution model used in literature 93

Table 4.2 Statistical analysis result of site #1 of Louvicourt mine 103

Table 4.3 Deterministic analysis result with size parameters 104

Table 4.4 Values of zc for different confidence levels 110

Table 4.5 Probability of each failure mode out of total simulation number (%) 115

Table 4.6 Goodness of fit test result and statistical parameter estimation 122

Table 4.7 Deterministic analysis result 123

Table 4.8 Probability of each failure mode out of total simulation number (%) 124

Table 4.9 Goodness of fit test result and statistical parameter estimation 129

Table 4.10 Deterministic analysis result 130

Table 4.11 Probability (%) of rock blocks failure under different joint combinations 131

Table 4.12 Goodness of fit test result and statistical parameter estimation 134

Table 4.13 Probabilistic block analysis with pure Fisher distribution 135

Table 4.14 Probabilistic block analysis with pure Kent distribution 136

Table 4.15 Combinations of varying concentration parameter κ 142

Table 4.16 Percentage of each failure mode and statistical parameter of different case 145

Table 5.1 Deterministic analysis result 173

Table 5.2 Preliminary design parameters 176

Table 5.3 Alternative design parameters and corresponding POF 181

Table 5.4 Deterministic block analysis result 184

Table 5.5 Probability of each failure mode out of total simulation number (%) 187

List of Figures

Figure 1.1 Unstable rock wedges 2

Figure 2.1 Applicability of Q rock support chart (after Palmstron and Broch, 2006) 13

Figure 2.2 Equal area projection (After Brady and Brown, 1993) 16

Figure 2.3 Equal area projection (DIPS) 17

Figure 2.4 Equal area stereonet 18

Figure 2.5 Equal area stereonet 19

Figure 2.6 Data plotting on stereonet 20

Figure 2.7 Contour plot for joint orientation 21

Figure 2.8 Gravity Fall Wedge (after Hoek and Brown, 1980) 24

Figure 2.9 Sliding Wedge (after Hoek and Brown, 1980) 25

Figure 2.10 Stable Wedge (after Hoek and Brown, 1980) 25

Figure 2.11 Three Intersecting Planes forming a Wedge (after Hoek and Brown, 1980) 28

Figure 2.12 Wedge Dimensions Generated Within Tunnel Span (after Hoek and Brown, 1980) 28

Figure 2.13 The intersection of three circular discontinuities in plan (a and b) and in isometric (c) (After Windsor, 1999) 32

Figure 2.14 Relationship between bolt length and roof span (after Lang and Bischoff, 1982) 35

Figure 3.1 Pole plot and contour plot of stereographic projection of discontinuity data mapped on the South Crofty mine (after Tyler et al., 1991) 53

Figure 3.2 Steronet plotting for Kent Ridge rock joint data 57

Figure 3.3 Graphical test for Kent Ridge data set 2 59

Figure 3.4 Graphical test for Kent Ridge data set 1 60

Figure 3.5 Concentration parameter κ vs ovalness β 67

Figure 3.6 Effect of ovalness β 72

Figure 3.7 Euler angle for 3D rotation 74

Figure 3.8 Lower hemispherical projection of EXMPFLD data..... 78

Figure 3.9 Rock joint data before and after conjugate set combination..... 82

Figure 3.10 Data simulation with Kent distribution (a), Fisher distribution (b) 83

Figure 4.1 Probabilistic simulation steps 88

Figure 4.2 Trace length limited block size..... 98

Figure 4.3 Spacing limited block size..... 101

Figure 4.4 Contour plot of Louvicourt mine data (Grenon and Hadjigeorgiou, 2003) 102

Figure 4.5 Deterministic analysis result..... 105

Figure 4.6 Spherical triangles produced by five planes that mutually intersect 107

Figure 4.7 Time vs number of iteration 109

Figure 4.8 Number of iterations required vs. Trial simulation number 112

Figure 4.9 CDF of block size considering different size parameters..... 116

Figure 4.10 CDF of apex height considering different size parameters 117

Figure 4.11 CDF of excavation face area considering different size parameters 117

Figure 4.12 Volume distribution CDF according to different failure mode (a) span limited analysis result (b) trace length limited analysis result (c) spacing limited analysis result..... 118

Figure 4.13 Same volume block in different failure modes..... 120

Figure 4.14 Contour plotting and joint set identification (pole plot) 122

Figure 4.15 CDF of block size considering different size parameters..... 125

Figure 4.16 CDF of apex height considering different size parameters 125

Figure 4.17 CDF of excavation face area considering different size parameters 126

Figure 4.18 Volume distribution CDF according to different failure mode (a) span limited analysis result (b) trace length limited analysis result (c) spacing limited analysis result..... 127

Figure 4.19 Contour plotting and joint set identification..... 129

Figure 4.20 Contour plotting and joint set identification..... 133

Figure 4.21 Comparison of unstable block size (span limited) generated by simulation with pure Fisher distribution and simulation with pure Kent distribution 136

Figure 4.22 Block size distributions $\beta = 50$ and with different κ values 138

Figure 4.23 Block size distribution $\kappa = 100$ and with different β values 138

Figure 4.24 Block size distribution $\kappa = 100$ $\beta = 50$ with different Γ 139

Figure 4.25 Block size distribution by vary concentration parameter κ of each joint set 143

Figure 5.1 Procedure for reinforcement design of single blocks 149

Figure 5.2 A tetrahedral block with its associate reinforcement (after Windsor and Thompson, 1992) 150

Figure 5.3 The reinforcement design length relative to block size (after Windsor and Thompson, 1992) 150

Figure 5.4 Design of length of rock support (after Chen, 1994) 152

Figure 5.5 Varying the relative position of the block with in a reinforcement array (after Windsor, 1999) 154

Figure 5.6 Fallout failure 155

Figure 5.7 Sliding along a single discontinuity 156

Figure 5.8 Sliding along intersection of two discontinuities (after Hoek and Bray, 1979) 157

Figure 5.9 Rock bolt deformation with unfavorable bolt angle (after Windsor and Thompson, 1992) 160

Figure 5.10 Probability of Failure concept 162

Figure 5.11 PDF of FS distribution 163

Figure 5.12 High probability of failure 164

Figure 5.13 Variation effect on PoF with different FS 164

Figure 5.14 Size parameter limited blocks 166

Figure 5.15 Rock design procedure 168

Figure 5.16 Number of active rock bolt determination 170

Figure 5.17 CDF of block size considering different size parameters 173

Figure 5.18 CDF of excavation face area considering different size parameters 174

Figure 5.19 CDF of apex height considering different size parameters 174

Figure 5.20 Contour plotting and joint set identification (pole plot) 175

Figure 5.21 PoF of deterministic design with span limited block..... 177

Figure 5.22 FS distribution of 30kN rock bolt installed with 1m by 1m square pattern and various bolt length..... 178

Figure 5.23 FS distribution of 5 m rock bolt installed with 1m by 1m square installation pattern and various bolt capacity..... 180

Figure 5.24 FS distribution of 5 m rock bolt installed with capacity 30 kN and different installation spacing..... 180

Figure 5.25 Comparison of PoF for two different designs 181

Figure 5.26 Contour plotting and joint set identification (pole plot) 183

Figure 5.27 Span limited block..... 183

Figure 5.28 CDF of block size considering different size parameters..... 184

Figure 5.29 CDF of apex height considering different size parameters 185

Figure 5.30 CDF of excavation face area considering different size parameters 185

Figure 5.31 Figure 5.31 Volume distribution CDF according to different failure mode (a) span limited analysis result (b) trace length limited analysis result (c) spacing limited analysis result 186

List of Symbols

A1	Rating for uniaxial unconfined compressive strength of the rock material
A2	Rating from rock quality designation (RQD)
A3	Rating for spacing of joints
A4	Rating for condition of joints
A5	Rating for ground water conditions
A_b	Cross section of a single bolt
A_{base}	Excavation face area
A_i	Triangular area of discontinuity plane *i*
A_j	Triangular area of discontinuity plane *j*
A_k	Triangular area of discontinuity plane *k*
A_{ri}	Area of the i-th plane
B	Rating for orientation of joints
B_l	Total rock bolt length
B_s/b	Bolt spacing
C_i	Cohesion coefficient of i-th plane
C_j	Cohesion coefficient of j-th plane
C_{ijk}	Apex of tetrahedral defined by discontinuity planes *i*, *j* and *k*
C_{ij}	Corner of the intersection of discontinuity planes *i* and *j*
C_{jk}	Corner of the intersection of discontinuity planes *j* and *k*
C_{ki}	Corner of the intersection of discontinuity planes *i* and *k*
$C_p(\kappa)$	Normalizing constant
d	Diameter of rock bolt/borehole

E	Reinforcement effectiveness factor
F_s /FS	Factor of safety
F_t	Resultant force
H_w	Apex height of the unstable block
h	apex height
I_d	Modified Bessel function of the first kind
I_{ij}	Edge vector defined by discontinuity planes *i* and *j*
I_{jk}	Edge vector defined by discontinuity planes *j* and *k*
I_{ki}	Edge vector defined by discontinuity planes *i* and *k*
$I_{0.5}(\kappa)$	Modified Bessel function of the first kind and order 0.5
$I_{2.5}(\kappa)$	Modified Bessel function of the first kind and order 2.5
J_n	Joint set number
J_r	Joint roughness
J_a	Joint alteration
J_w	Joint water
K	Fisher constant
l	Bolt length
L	Roof span
L_1	Minimum anchor length
L_2	Length in zone to be stabilized
N	Number of discontinuities in a joint set
N_b	Required number of bolts

P_A	Bolt load
$P(b_{123})$	Probability of b_{123} formed
$P(b_{123})_{fallout}$	Probability of b_{123} fails by fallout failure
POF	Probability of failure
R	Rotation matrix
R_i	Resolved normal force on discontinuity *i*
R_j	Resolved normal force on discontinuity *j*
RMR	Rock Mass Rating
RQD	Rock quality designation
SRF	Stress reduction factor
Sx	Standard deviation
r_{ni}	Discontinuity normal
V	Span limited block size
W	Weight of the unstable block
z_c	Value of confidence coefficient
α	Significance level
α_i	Dip of the i_{th} plane
α_{in}	Dip direction of i_{th} conjugate set
β_{in}	Dip angle of i_{th} conjugate set
β	Ovalness
Γ	Rotation matrix
$\gamma_{(1)}$	Mean direction or pole
$\gamma_{(2)}$	Major axis
$\gamma_{(3)}$	Minor axis

γ_{ij}	Dip angle of the intersection along which the wedge slides
γ_{ti}	Trace length limit scaling factor defined by discontinuity *i*
γ_{tj}	Trace length limit scaling factor defined by discontinuity *j*
γ_{tk}	Trace length limit scaling factor defined by discontinuity *k*
γ_t	Overall trace length limit scaling factor
γ_{si}	Spacing limit scaling factor defined by discontinuity *i*
γ_{sj}	Spacing limit scaling factor defined by discontinuity *j*
γ_{sk}	Spacing limit scaling factor defined by discontinuity *k*
γ_t	Overall Spacing limit scaling factor
δ_t	Axial tension of reinforcement
δ_B	Block displacement resolved onto the discontinuity
$\lvert\delta_s\rvert$	Block displacement vector resolved onto the discontinuity.
τ_{bond}	Average working bond stress between grout and borehole/between grout and bolt
κ	Concentration
σ	Tensile strength of bolts
σ_a	Yield strength of steel
Ω	Directional vector
θ	Dip angle
φ	Dip direction
ψ_i	Angle between planes i and the vertical plane passing through the intersection of planes i and j
ψ_j	Angle between planes i and the vertical plane passing through the intersection of planes i and j
θ_o	Mean dip angle
Φ_i	Friction angle of the i-th plane

Φ_j	Friction angle of the j-th plane
φ_o	Mean dip direction
μ	Mean direction

Chapter 1 Introduction

In many urban areas, ground space has become increasingly precious. It is hence attractive to relocate less productive surface facilities (e.g. warehouse) underground so as to free up the surface land for housing or commercial buildings. In addition, due to land use restriction, it becomes necessary to place potentially noxious operations to underground (Berthelsen, 1992). For example, rock caverns can be built to meet the liquid hydrocarbons storage needs. Large scale underground rock excavations are built in countries such as Norway and Sweden. Safety is a prime consideration of cavern development. As rock caverns are built deep below ground, rock mass is good often and there is little stability. However, if rock parameters become highly variable, adequate design of reinforcement becomes a major challenge. Reinforcement design without proper consideration to rock conditions will lead to economical loss or fatal accidents. For example, a tunnel collapse due to rock fall in Siberia Russia was reported with three miners trapped (RIAnovosti, 2012). As such, it is important to consider all possible rock parameter variation when designing rock reinforcement.

When an excavation was performed on jointed rocks, an unstable rock block may fail either by falling or sliding. This occurs when rock joint orientations are unfavorable (as shown in Figure 1.1). The primary concern when designing reinforcement is the size and the failure mode of rock blocks formed

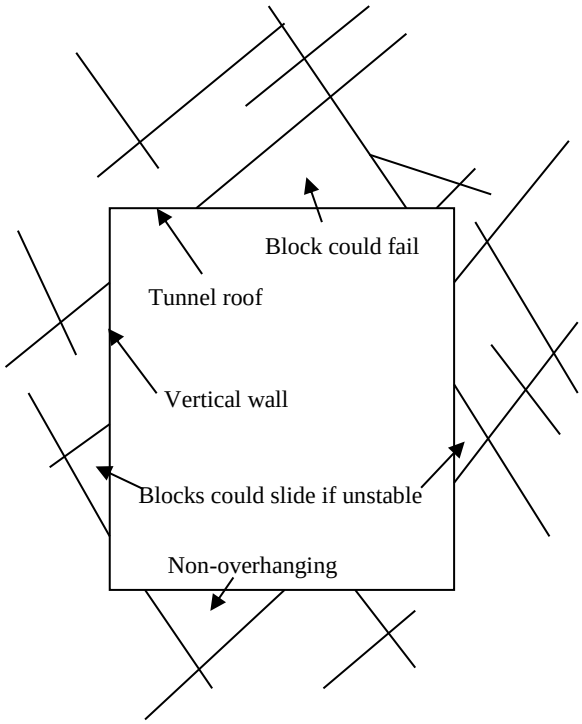

Figure 1.1 Unstable rock wedges

by the rock joints and the excavation face. In order to create a safe working environment, unstable rock masses are usually reinforced by rock bolts before or immediately after excavation. The required bolt capacity, spacing and length depend largely on characteristics of key blocks. For example, the design capacity of anchors embedded in fractured rock depends largely on key block size (Mauldon, 1995). However, rock block features are largely affected by the natural fractures of jointed rocks (such as discontinuity spacing, persistence and orientation). Therefore, a close study on rock joint characteristics is an important element for unstable block identification.

It is well known that discontinuities have a degree of natural scatter in joint orientation due to rupturing of the rock material. (Mandl, 2005). The orientation of discontinuities, though not always parallel, is also not purely random. Usually, many of the discontinuities recorded in a borehole coring are approximately parallel to one or several planes. These discontinuities, which have approximately the same orientation, could be gathered as a joint set. Traditionally, joint sets are usually analyzed using mean joint orientation value. However, the dispersion of joint orientation was found to have an important effect on unstable rock block volume and failure mode prediction (Leung and Quek, 1995). When studying the effect of joint orientation dispersion, Priest (1993) stated that Fisher distribution (Fisher, 1953) can be assumed if statistical property of the distribution was required. In geotechnical engineering, joint sets are often modeled using Fisher distribution (Priest, 1993; Song et al., 2001; Kemeny and Post, 2003; Engelder and Delteil, 2004). However, some researchers (Peel et al., 2001; Whitaker and Engelder, 2005) reported that Fisher distribution is not suitable for non-symmetrical rock joint orientation data. Whitaker and Enelder (2005) concluded that if a non-symmetrical joint distribution is modelled using a Fisher distribution, significant errors could occur. Therefore, a more flexible distribution such as the Kent distribution which can handle non-symmetrical density contours should be considered for joint orientation simulation.

Block size is largely affected by variation of jointed rock parameters. In conventional block stability assessment, it is customary to use the mean joint orientation of each joint set to determine the block shape and use the excavation span to estimate the block size across the tunnel width. The rock support is designed based on the factored span limited block size. The scale factor is commonly derived based on field observations or engineering design. This leads to the major limitation where traditional deterministic analysis is unable to identify all possible block types and geometries. In addition, the support reinforcement design from deterministic result may not be adequate for all circumstances. Conventional deterministic reinforcement design based on mean values might be less stable if joint orientation dispersion was considered. Therefore, probabilistic design on reinforcement is necessary.

Variation of rock parameters and unavailable ground information make it difficult for unstable block identification. Therefore, it is necessary to use some sort of criterion in deciding whether a design is acceptable. A factor of safety (F.S or FoS) is commonly used in engineering to consider the uncertainties involved in design. Since safety is of prime importance in cavern development, a high FoS value is commonly selected for rock reinforcement design. However, Dunn (2013) noted design with a higher FoS may have a higher chance to fail when the standard deviation increases. Therefore, the reinforcement design criteria should be carefully selected and the reliability of proposed design should be assessed.

1.1 Research Objective

The successful design of rock bolt reinforcement depends upon two factors: the identification of blocks that are free to move into the excavation, and the installation of rock bolts that are long enough and of sufficient capacity to anchor the block. However, scatter of rock parameters have a great effect on unstable rock wedge determination. Conventional rock support design based on deterministic wedge analysis may not reliable. Hence, the objectives of this thesis are as follow:

1. To determine a suitable distribution for rock joint parameters simulation based on available actual field data from (Singapore or overseas) and to evaluate the effect of scatter of joint parameters on unstable rock block size determination.
2. To assess the reliability of rock support design based on deterministic wedge analysis
3. To propose a suitable scheme for rock support design in the feasibility study stage using probabilistic wedge analysis.

1.2 Thesis Organization

Chapter 1: This chapter gives a brief introduction to the research and the arrangement of the thesis.

Chapter 2: This chapter introduces the basic concept for joint data recording in joint mechanics and reviews previous studies including rock reinforcement design, unstable rock block identification and scatter of joint parameters.

Chapter 3: In this chapter, the basics on directional statistics are introduced. The need for directional statistics in describing joint orientations was thoroughly explained. The Fisher distribution and the Kent distribution are described in detail. Different parameter estimation procedures and randomization of vectors based on two distributions are compared. Besides, goodness of fit test is used to exam real rock joint data worldwide. The two models are verified in terms of their accuracy in characterizing the distribution of joint orientation.

Chapter 4: In this chapter, several examples are conducted for block size analysis. Results from both conventional deterministic approach and probabilistic approach are compared to illustrate the importance of probabilistic approach considering joint parameter dispersions.

Chapter 5: In this chapter, rock support design method is discussed in detail. The reliability of rock support design based on both deterministic and probabilistic analysis results are assessed. A more rigorous rock support design based on probability of failure is attempted.

Chapter 6: In this chapter, the findings and contributions of this thesis are presented.

Chapter 2 Literature Review

2.1 Introduction

Underground facilities are usually built for a long service life and safety is the prime concern in rock engineering. Adequate supporting system should be carefully designed. A successful design of rock support depends on the proper identification of potential rock instability and a proper design and installation of rock bolts to stabilize such instability (Tyler et al, 1991). Therefore, identification of unstable block features such as size and failure mode is essential in reinforcement design. Current rock support design can be broadly divided into two categories: (1) empirical design with design indices and charts (2) analytical design such as key block analysis. Key block analysis can be further categorize into conventional deterministic analysis and probabilistic analysis which considering variations of rock parameters. However, as mentioned in Chapter 1, statistical dispersion of rock parameters such as joint orientation has a great impact on rock block identification. Monte Carlo simulation is commonly adopted to include statistical variation of parameters on rock block identification or to assess reliability of a proposed design. Each rock parameter data is represented by its Probability Density Function (PDF) defined with key statistics such as mean and standard deviation. Various distributions have been assumed for these rock parameters simulations (Latham et al., 2006). However, block analysis with misspecified distribution could lead to error. For example, if non-symmetrical joint orientation data is

forced into the symmetrical Fisher distribution, significant errors would occur (Whitaker and Enelder, 2005). Besides, a preliminary reinforcement scheme has to be proposed prior to excavation. Parameters such as trace length which cannot be quantified before excavation must be reasonably assumed. Therefore, this chapter shall review the literature related to rock reinforcement design methods and rock parameter distributions.

2.2Rock Reinforcement Design Methods

Adequate reinforcements need to be provided for underground excavation. However, design with different methods might lead to different reinforcement schemes. Therefore, the pros and cons of each reinforcement design methods need to be carefully studied.

2.2.1 Empirical Method

Reinforcement design based on empirical chart is commonly practiced in the industry as it is easy to implement. Rock features are normalized to indices and are then recommended reinforcement parameters can be determined from empirical charts. The most common empirical methods are Rock Mass Rating (RMR) and Q system.

2.2.1.1 RMR Classification System

The RMR system or Geomechanics Classification was developed by Bieniawski (1974). It is commonly used for rock mass classification. Five rock features (i.e. rock strength, RQD, spacing of discontinuities, condition of

discontinuities and ground water) are considered and rated as shown in Table 2.1. Sum of the rated values of these rock properties is defined as RMR for a specific rock. Then, this RMR value can be used for rock reinforcement estimation based on empirical charts or tables. RMR can also be used to crudely estimate the deformation modulus of rock mass. The overall rating system is as follow

$$RMR = A1 + A2 + A3 + A4 + A5 + B \tag{2.1}$$

where A1=rating for uniaxial unconfined compressive strength of the rock material; A2 = rating from rock quality designation (RQD); A3 = rating for spacing of joints; A4 = rating for condition of joints; A5 = rating for ground water conditions and B = rating for orientation of joints.

Changes and modifications have been made over the years. However, reinforcement design tables are only developed for tunnels of 10m span. Therefore, Bieniawski (1989) noted that a great deal of judgment is needed in the application of RMR for rock reinforcement design.

Table 2.1 Rock Mass Rating System (After Bieniawski, 1989)

A. CLASSIFICATION PARAMETERS AND THEIR RATINGS									
Parameter			Range of values						
1	Strength of intact rock material	Point-load strength index	>10 MPa	4 - 10 MPa	2 - 4 MPa	1 - 2 MPa	For this low range - uniaxial compressive test is preferred		
		Uniaxial comp. strength	>250 MPa	100 - 250 MPa	50 - 100 MPa	25 - 50 MPa	5 - 25 MPa	1 - 5 MPa	< 1 MPa
	Rating		15	12	7	4	2	1	0
2	Drill core Quality *RQD*		90% - 100%	75% - 90%	50% - 75%	25% - 50%	< 25%		
	Rating		20	17	13	8	3		
3	Spacing of discontinuities		> 2 m	0.6 - 2 . m	200 - 600 mm	60 - 200 mm	< 60 mm		
	Rating		20	15	10	8	5		
4	Condition of discontinuities (See E)		Very rough surfaces Not continuous No separation Unweathered wall rock	Slightly rough surfaces Separation < 1 mm Slightly weathered walls	Slightly rough surfaces Separation < 1 mm Highly weathered walls	Slickensided surfaces or Gouge < 5 mm thick or Separation 1-5 mm Continuous	Soft gouge >5 mm thick or Separation > 5 mm Continuous		
	Rating		30	25	20	10	0		
5	Groundwater	Inflow per 10 m tunnel length (l/m)	None	< 10	10 - 25	25 - 125	> 125		
		(Joint water press)/ (Major principal σ)	0	< 0.1	0.1, - 0.2	0.2 - 0.5	> 0.5		
		General conditions	Completely dry	Damp	Wet	Dripping	Flowing		
	Rating		15	10	7	4	0		
B. RATING ADJUSTMENT FOR DISCONTINUITY ORIENTATIONS (See F)									
Strike and dip orientations			Very favourable	Favourable	Fair	Unfavourable	Very Unfavourable		
Ratings		Tunnels & mines	0	-2	-5	-10	-12		
		Foundations	0	-2	-7	-15	-25		
		Slopes	0	-5	-25	-50			

Table 2.1 (con't) Rock Mass Rating System (After Bieniawski, 1989)

C. ROCK MASS CLASSES DETERMINED FROM TOTAL RATINGS					
Rating	100 ← 81	80 ← 61	60 ← 41	40 ← 21	< 21
Class number	I	II	III	IV	V
Description	Very good rock	Good rock	Fair rock	Poor rock	Very poor rock
D. MEANING OF ROCK CLASSES					
Class number	I	II	III	IV	V
Average stand-up time	20 yrs for 15 m span	1 year for 10 m span	1 week for 5 m span	10 hrs for 2.5 m span	30 min for 1 m span
Cohesion of rock mass (kPa)	> 400	300 - 400	200 - 300	100 - 200	< 100
Friction angle of rock mass (deg)	> 45	35 - 45	25 - 35	15 - 25	< 15
E. GUIDELINES FOR CLASSIFICATION OF DISCONTINUITY conditions					
Discontinuity length (persistence)	< 1 m	1 - 3 m	3 - 10 m	10 - 20 m	> 20 m
Rating	6	4	2	1	0
Separation (aperture)	None	< 0.1 mm	0.1 - 1.0 mm	1 - 5 mm	> 5 mm
Rating	6	5	4	1	0
Roughness	Very rough	Rough	Slightly rough	Smooth	Slickensided
Rating	6	5	3	1	0
Infilling (gouge)	None	Hard filling < 5 mm	Hard filling > 5 mm	Soft filling < 5 mm	Soft filling > 5 mm
Rating	6	4	2	2	0
Weathering	Unweathered	Slightly weathered	Moderately weathered	Highly weathered	Decomposed
Ratings	6	5	3	1	0

F. EFFECT OF DISCONTINUITY STRIKE AND DIP ORIENTATION IN TUNNELLING**			
Strike perpendicular to tunnel axis		Strike parallel to tunnel axis	
Drive with dip - Dip 45 - 90°	Drive with dip - Dip 20 - 45°	Dip 45 - 90°	Dip 20 - 45°
Very favourable	Favourable	Very unfavourable	Fair
Drive against dip - Dip 45-90°	Drive against dip - Dip 20-45°	Dip 0-20 - Irrespective of strike°	
Fair	Unfavourable	Fair	

2.2.1.2 Q system

The Q system is another empirical design method for estimating rock support. Barton et al. (1974) of Norwegian geotechnical institute proposed the Q system based on a large database of tunnel projects. Q system is popular in industry application. The Q value is determined from the following relationship:

$$Q = \left(\frac{RQD}{J_n} \right) \times \left(\frac{J_r}{J_a} \right) \times \left(\frac{J_w}{SRF} \right) \tag{2.2}$$

where RQD = rock quality designation; J_n = joint set number; J_r = joint roughness; J_a = joint alteration; J_w = joint water; SRF = stress reduction factor. RQD / J_n represents the block size, J_r / J_a represents the minimum inter-block shear strength and J_w / SRF represents the active stress. Q system is applicable to various tunnel span and height. Once the tunnel span is fixed, reinforcement required can be determined from Figure 2.1.

Empirical classification systems (RMR and Q system) are useful in estimating the need for reinforcement element in preliminary design stages, when very little detailed information on the rock mass is available (Palmstron and Broch, 2006). However, Loset (1990) pointed out that the rock classification methods only give an indication of the kind of support to be applied in a tunnel and the details of design (such as instance the placing of rock bolts) is not covered by the empirical classification system. In addition, the input parameters of Q

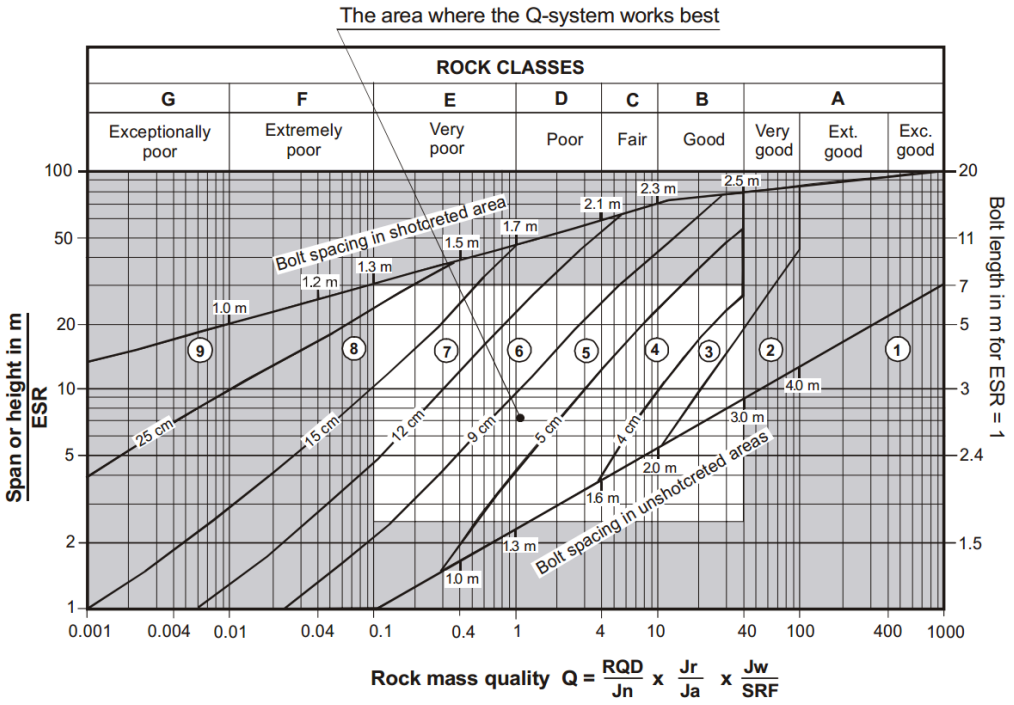

Figure 2.1 Applicability of Q rock support chart (after Palmstron and Broch, 2006)

system are critiqued by many researchers. RQD is found not sufficient to provide an adequate description of rock mass (Bieniawski, 1984; Milne et al., 1998). RQD/J_n is not suitable to indicate block size (Grenon and Hadjigeorgiou, 2003; Palmstron and Broch, 2006). Palmstron and Broch (2006) carried out a critical evaluation of the parameters used in the Q system and pointed out that the Q system can only work well within a limited range as shown in Figure 2.1. If Q value is outside the arrange, supplementary methods or evaluations should be applied (Palmstrom et al., 2002). Palmstron and Broch (2006) stated that important rock features (i.e. joint orientation, joint size, joint persistence, joint aperture, rock strength) should be included in rock

analysis. Besides, Pell and Bertuzzi (2007) also pointed out tunnel design should be done by methods of applied mechanics, like any other structural design.

2.2.2 Analytical Design Methods

In the analytical design approach, rock reinforcement scheme is proposed to stabilize the predicted unstable rock block. Thus, identification of unstable block is essential in analytical design. Conventional deterministic block analysis is commonly used to predict the key rock block. Important rock features such as joint orientation, size and spacing are considered. The mean value of each rock features is commonly adopted for key rock block identification. The stereographic projection technique is used for rock block stability analysis and identification of key rock block features (Hoek and Brown, 1980; Brady and Brown, 1993; Goodman and Shi, 1985; Priest, 1985). However, statistical dispersion of rock parameters has a great impact on rock block identification (Leung and Quek, 1995). Therefore, the probabilistic rock block analysis which considers variation of rock parameters is also studied by many researchers (Tyler, et al., 1991; Dunn, et al., 2008; Grenon and Hadjigeorgiou, 2012).

2.2.2.1 Representation of geological data

In rock block analysis, the most important parameter is joint orientation (Hoek and Brown, 1980). There are several types of spherical projection which can be used for the representation of joint orientation. The equal area and equal

angle projection techniques are the most commonly used projection methods for the interpretation of joint orientation data. In rock engineering, equal angle projection is commonly used due to its simplicity to draw and formulate based on Goodman and Shi (1985). However, equal area projection is good at showing the joint density distribution. Equal area projection preserves areas which allows user to more accurately compare joint sets on the projection without distortion of area. In terms of programming, there is no significant advantage in either method. Therefore, equal area projection is selected and used throughout this thesis for data plotting due to its accuracy in contouring.

Discontinuity planes are recorded by the dip angle and dip direction. Dip angle is an acute angle measured vertically between a given plane and the horizontal and dip direction is geographical azimuth measured in clockwise rotation from North containing the given line of dip. The great circle which is traced by the intersection of the plane and the sphere will define uniquely the inclination and orientation of the plane in space. Since the same information is included in the upper and lower parts of the sphere, only one of them needs to be used and the lower hemisphere is used in this study. In addition to great circle, the inclination and orientation of the plane can also be defined by pole of the plane. The pole is the intersection of discontinuity plane normal which pass through the center of reference sphere with the reference sphere surface, as shown in Figure 2.2.

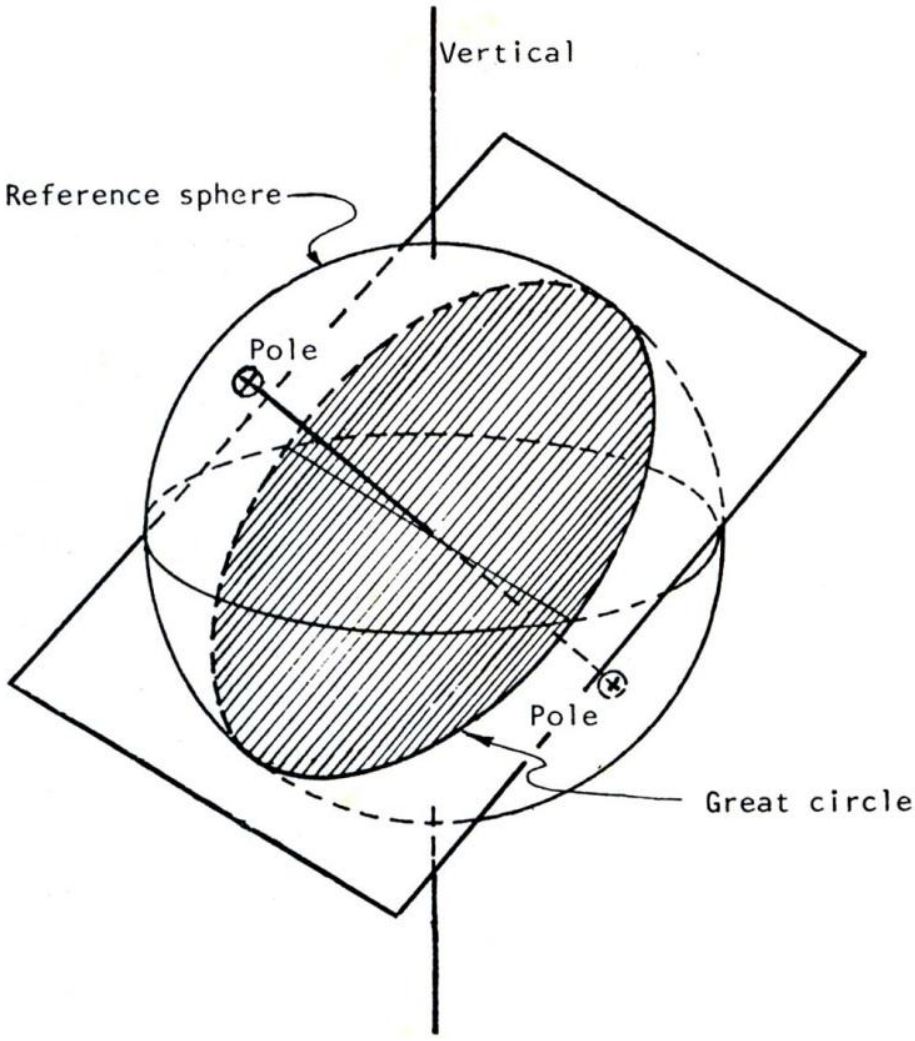

Figure 2.2 Equal area projection (After Brady and Brown, 1993)

Three dimensional presentation of discontinuity plane or pole is difficult to shown on two dimensional paper. Therefore, hemispherical projection is proposed to represent joint discontinuity orientations. As shown in Figure 2.3, point A on the surface of the sphere is projected to point B by swinging it in an arc which is centered at the point of contact of the sphere and a horizontal surface upon which stands. If this process is repeated for a number of points,

defined by the intersection of equally spaced longitude and latitude circles on the surface of the sphere, an equal area net will be obtained. The stereonets used in rock engineering are shown in Figures 2.4 and 2.5.

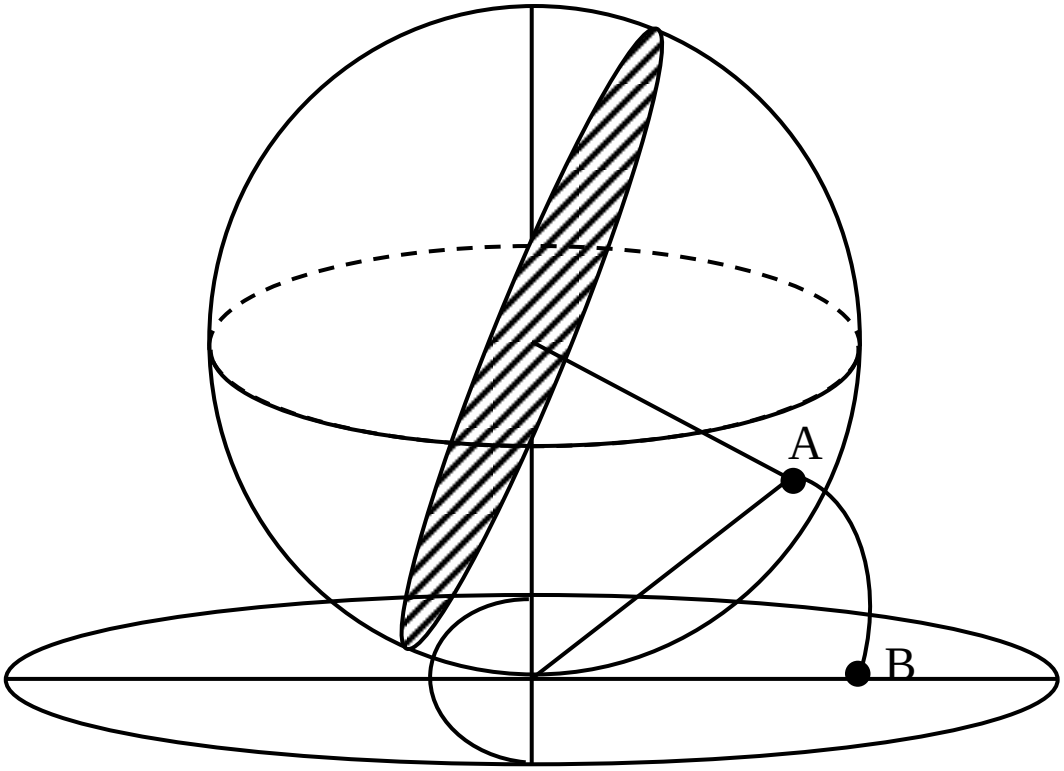

Figure 2.3 Equal area projection (DIPS)

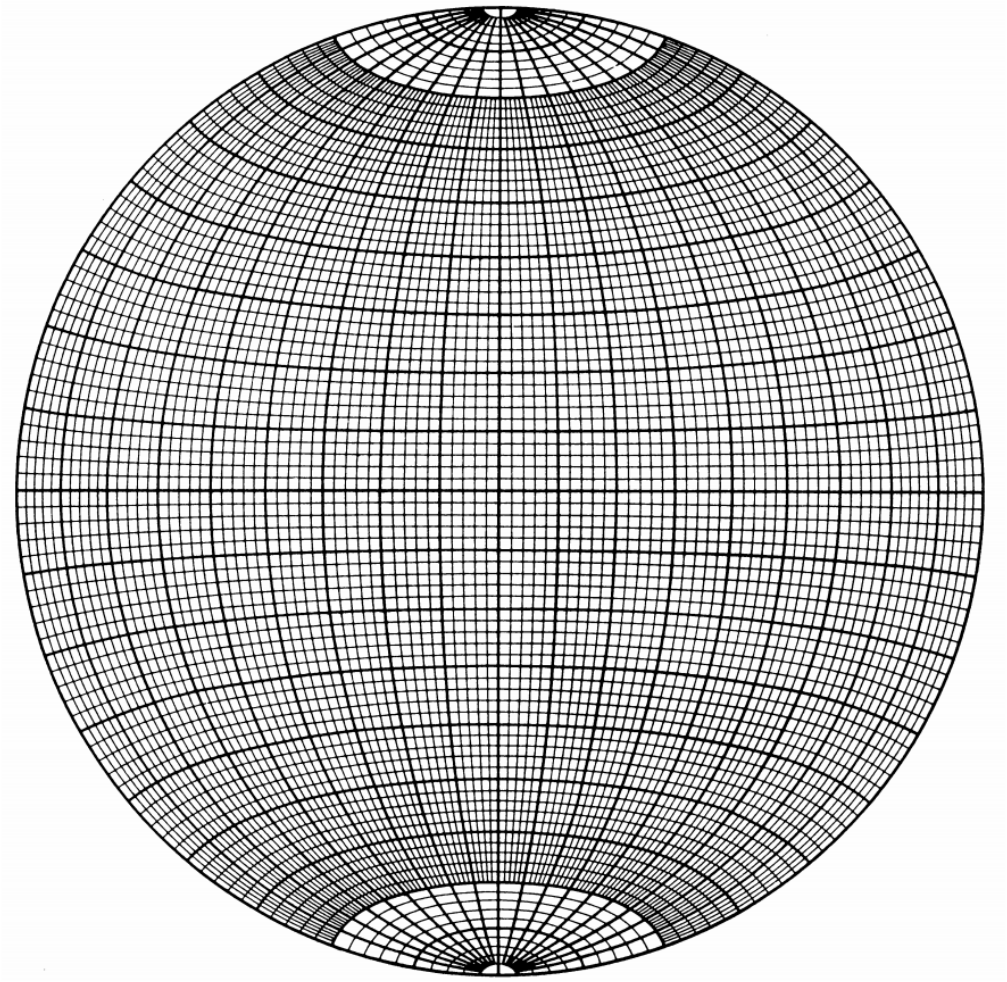

Figure 2.4 Equal area stereonet

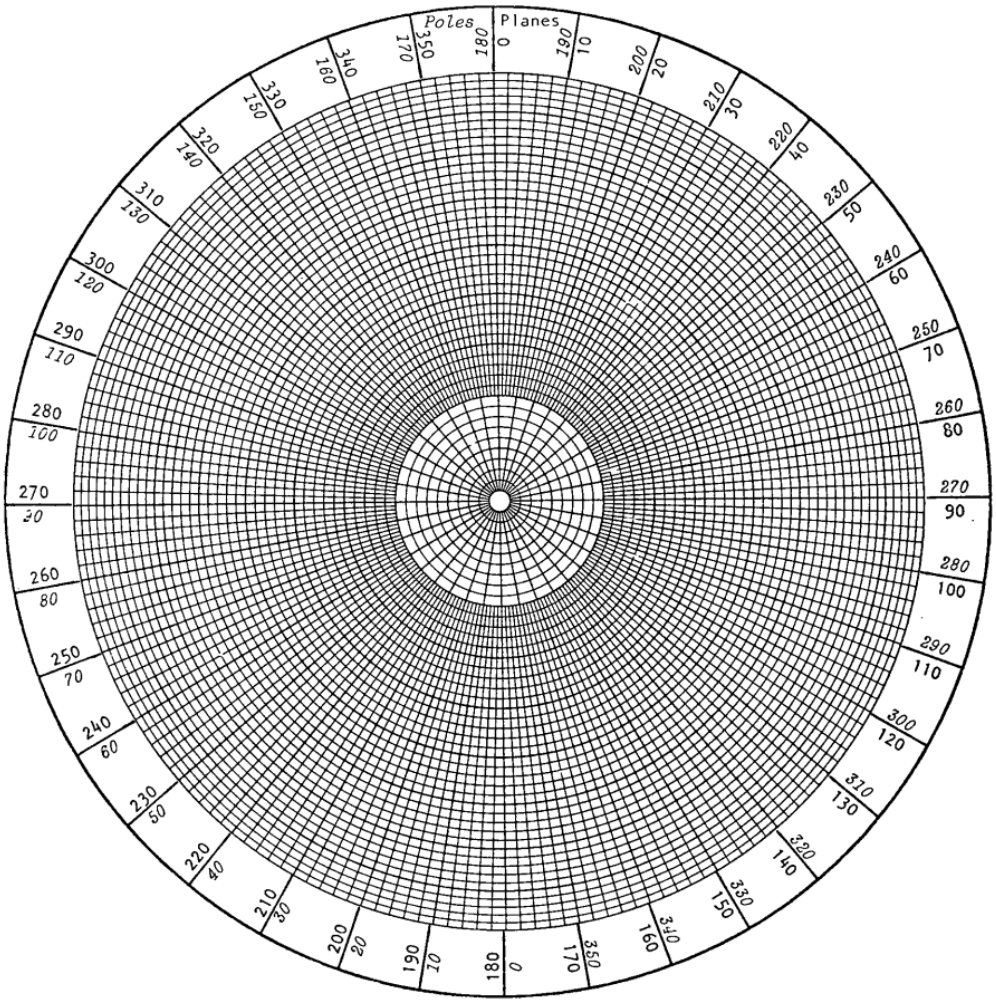

Figure 2.5 Equal area stereonet

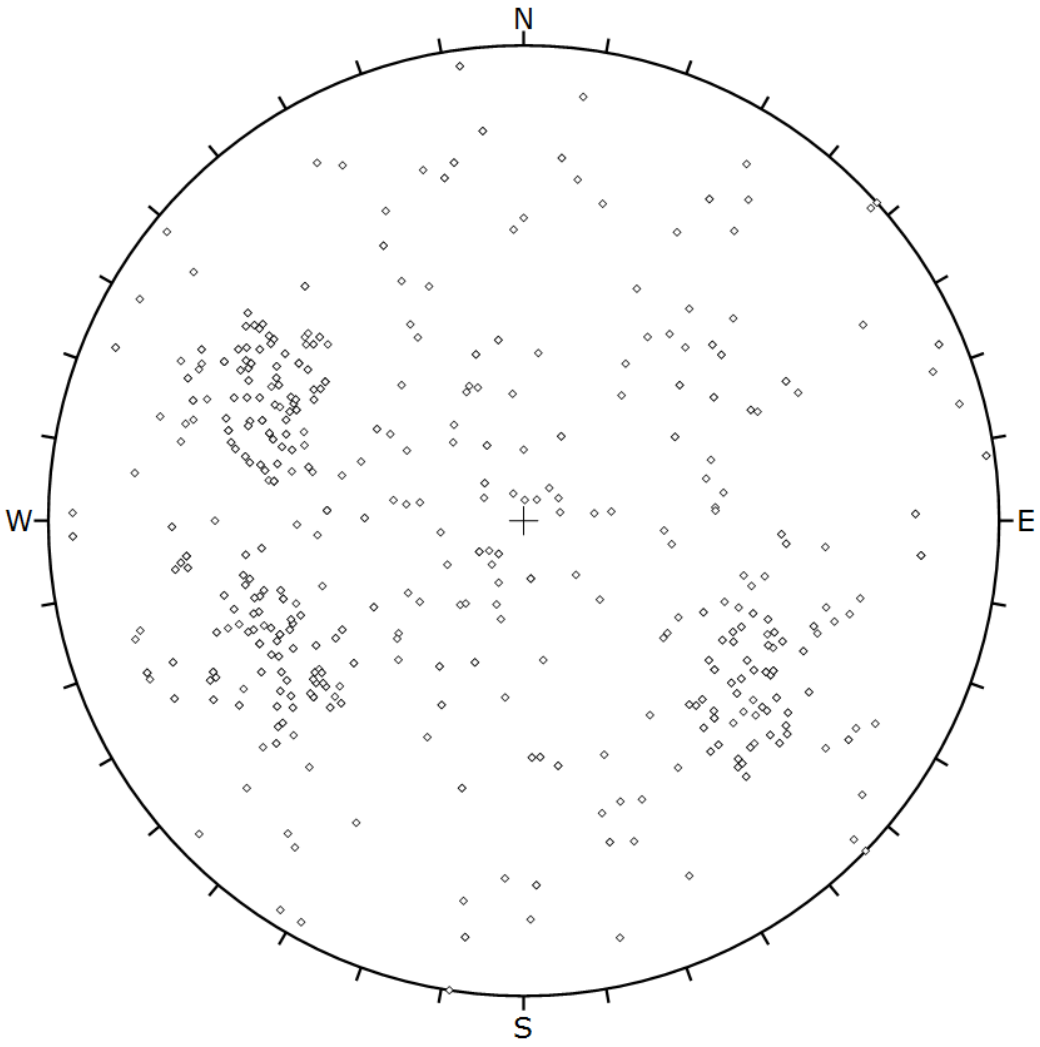

Figure 2.6 Data plotting on stereonet

To present orientation data in a stereonet, it is convenient to work with poles rather than great circles. This is because the poles can be plotted directly on a polar stereonet as shown in Figure 2.6. After all the orientation data have been plotted on the stereonet, the pole density is determined by using a counting cell to count the number of the poles that fall in the cell. The points with the

same pole density are connected to form a contouring diagram, as shown in Figure 2.7. Details of the procedure are given in Priest (1985).

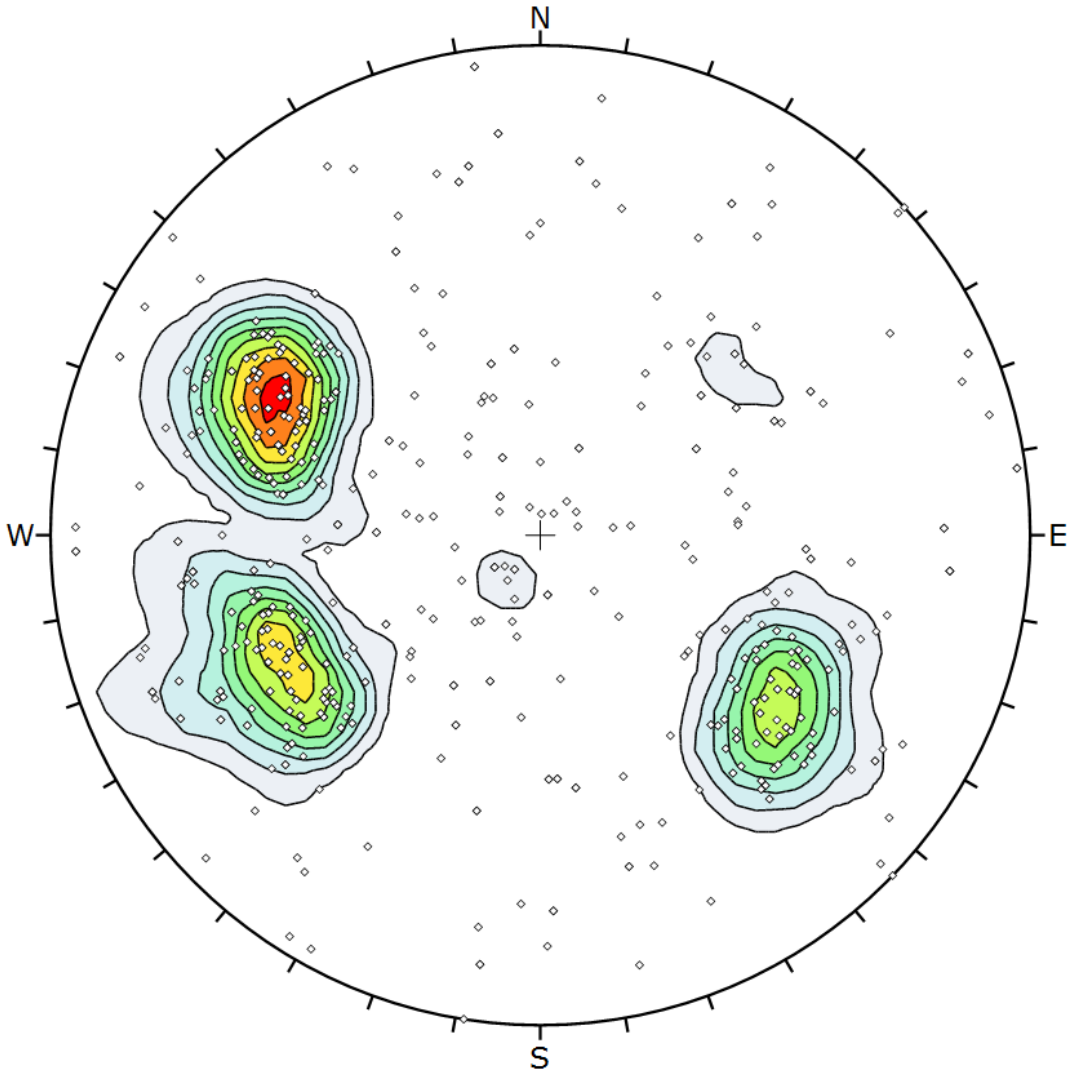

Figure 2.7 Contour plot for joint orientation

Statistically significant discontinuity clusters can be visually observed from the contour plot. With the aid of a computer software, joint cluster based on classification can be identified using algorithms such as the K-means (Forgy,

1965; McQueen, 1967), improved K-means (Zhang et al., 2008), the Fuzzy C mean (Hammah and Curran, 1998) and the Gustafson-Kessel algorithm (Gustafson and Kessel, 1978). The basic concept of these pattern recognition algorithms is to minimize the defined objective function which is used for distance measurement. Data points from the same cluster should produce the minimum error. A predefined number of clusters is required to initiate the calculation. After joint classification is performed, the validity indices can be used as a criterion to determine the optimal number of joint sets. However, different algorithms with different validity indices may produce different results. Therefore in the field, joint set clustering produced by experienced engineer is treated as the accurate result. In this thesis, visual identification is adopted for joint clustering.

Once the major joint sets are classified, the mean discontinuity orientation is commonly used to represent each joint set. Stereographic projection technique can be applied for subsequent stability analysis which will be elaborated in Section 2.2.2.2. Figure 2.8 shows a wedge of rock falling from the roof of an excavation. The vertical line *l* drawn through the apex of the wedge *O* must fall within the base of the wedge *AB*. This also means that the center of stereonet must fall within the closed area formed by 3 great circles on the stereographic projection plot. However, if a wedge is formed in the roof or sidewalls of an underground excavation but the vertical line *l* through its apex does not fall within its base *AB*, then sliding may occur along one of the discontinuity or along the intersection of two discontinuities. The

stereographic plot of this condition indicates that intersection figure formed by the three great circles falls to one side of the center of the net. Another condition for failure is that the sliding plane or line of intersection must be steeper than the angle of friction angle. This condition is satisfied if at least part of the intersection figure falls within the friction circles shown in Figure 2.9. In this case, the wedge formed will fail by sliding. When the entire intersection figure falls outside the friction circle, as shown in Figure 2.10, the weight of the block is not enough to overcome the frictional resistance of the plane and sliding failure would not take place. Under these conditions, the wedge is stable. Therefore, cohesion and friction of joint discontinuities have a great impact on rock block stability. Representative mean orientations should be derived from stereographic projection analysis. With a predefined tunnel width, the excavation span limited block size could be determined with conventional wedge analysis.

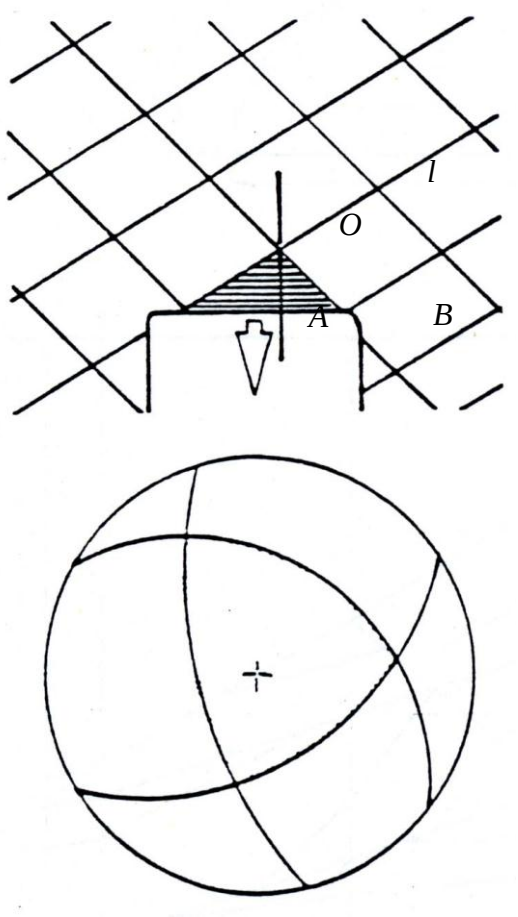

Figure 2.8 Gravity Fall Wedge (after Hoek and Brown, 1980)

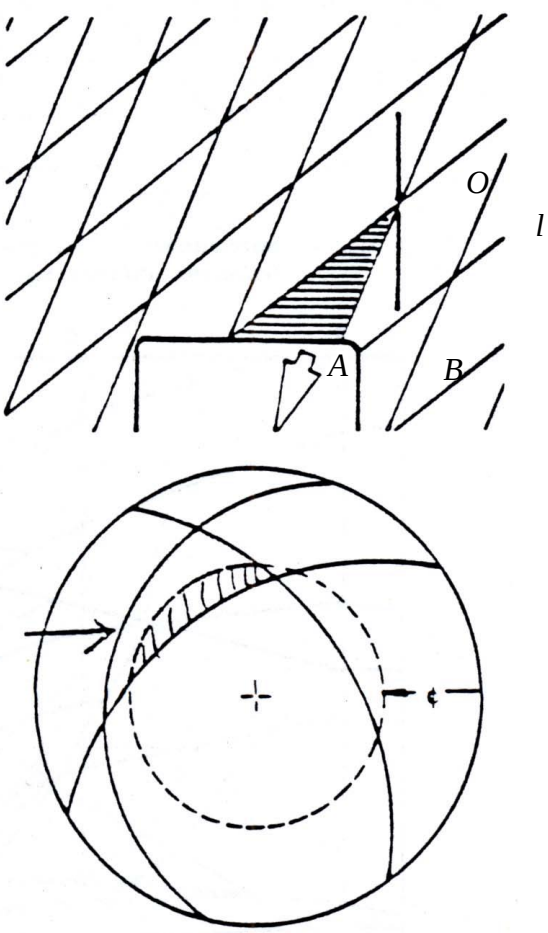

Figure 2.9 Sliding Wedge (after Hoek and Brown, 1980)

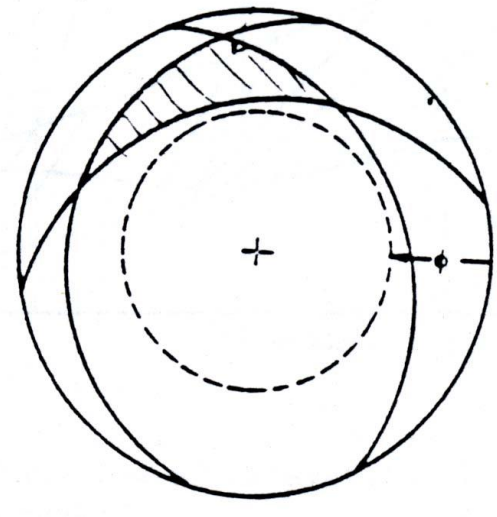

Figure 2.10 Stable Wedge (after Hoek and Brown, 1980)

2.2.2.2 Determination of size and shape of rock block

Stereographic plot can not only be used to perform simple stability checks, but can also be used to estimate the size and shape of a potentially unstable wedge. Ubiquitous approach is commonly assumed in rock block analysis (Hoek and Brown, 1980). It assumes that rock discontinuities and excavation surface can occur everywhere and anywhere in spacing. This assumption makes it possible for discontinuity planes to intersect with each other to form rock blocks. The representative orientations of classified joint sets are used to determine the excavation span limited block size which is the largest potential unstable rock block. Unstable rock wedges may range from tetrahedral through to high order polyhedral. Many researchers (e.g. Grenon and Hadjigeorgiou, 2003; Windsor, 1999; Kuszmaul, 1999; Mauldon, 1995) pointed out lower order tetrahedral blocks are more likely to be removable compared to polyhedral blocks. Therefore, this study focuses on stability of the unstable tetrahedral blocks. In addition, stereographical projection technique is very time consuming and prone to human errors (Priest, 1985). It is more practical to perform the kinematic analysis of stability of a three-dimensional rock block based on vector approach as it is programmable. A block analysis program code is provided in Hoek and Brown (1980). The principle of block analysis is shown in Figure 2.11 and 2.12.

Three planes are represented by their corresponding great circles in Figure 2.11. Lines *a*, *b* and *c* represent the strike lines and Lines *ab*, *ac* and *bc*

represent the traces of the vertical planes through the center of the net and great circle intersections. The wedge formed by the intersecting planes will be free to separate from the surrounding rock masses. A typical tetrahedral rock block wedge can be described in Figure 2.12 with X-X as the cross section view of tunnel width. The length through the volumetric centroid of the wedge to the exposed face is the apex height (h). Having found the shape of the base of the wedge, its area A_{base} can be obtained. The volume of span limited wedge (V) is given by

$$V = \frac{1}{3} \times h \times A_{base} \tag{2.3}$$

The corresponding failure mode can be determined as well. Details are given in Hoek and Brown (1980).

The commercial software UNWEDGE programme (Rocscience, 2005) which applies Goodman and Shi (1985) block theory can be used to assess the stability of wedges. This software can be used to analyze block failure due to excavations in hard rock. UNWEDGE is restricted to analyze rock block formed by three discontinuity planes. Combined with tunnel axis and tunnel opening dimensions, UNWEDGE can calculate the maximum sized wedges which can form around an excavation. The user can scale the size of the wedges based on experience and field observations. Then, the block properties can be used for reinforcement design. However, the procedure to scale the analysis result can be rather empirical.

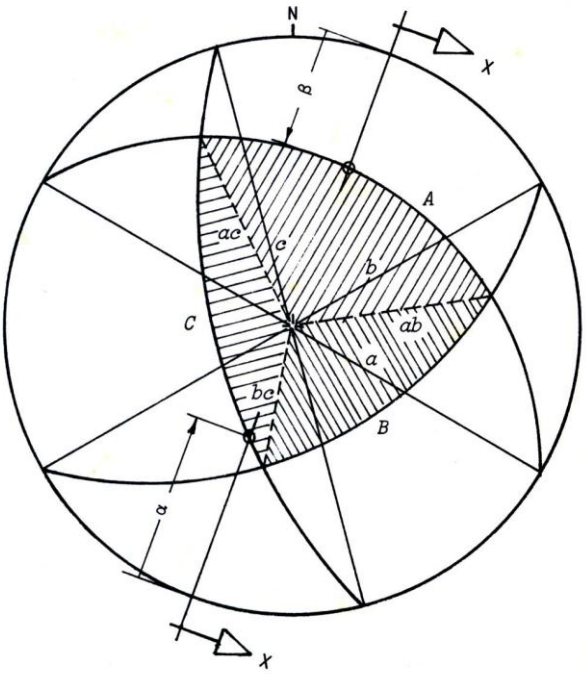

Figure 2.11 Three Intersecting Planes forming a Wedge (after Hoek and Brown, 1980)

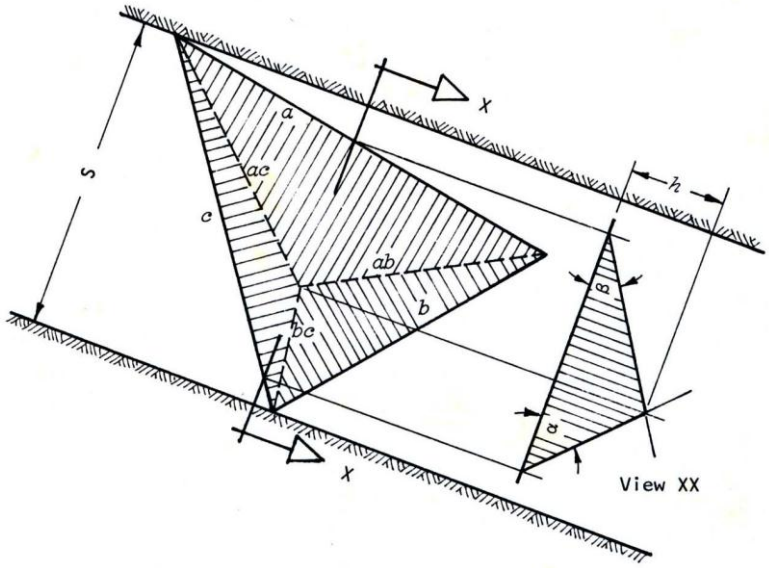

Figure 2.12 Wedge Dimensions Generated Within Tunnel Span (after Hoek and Brown, 1980)

When designers apply different scale factors, the designed volume can vary tens or hundreds of cube meters. In addition, as mentioned in Chapter 1, rock discontinuity is formed by rupturing of the rock material. Moreover uncertainty is involved in rock parameters and the mean orientation may not be able to capture the discontinuity distribution. If a rock reinforcement design is proposed based on the deterministic theory, there is no way to ascertain the reliability of the design. Therefore, various joint orientation values such as the worst values are adopted to determine block size. The predicted rock block could be very different from the analysis with mean values. The use of worst case values can result in a very conservative design (Diederichs et al., 2000; Thompson and Windsor, 2007). In addition, it is necessary to conduct multiple analyses on combinations of planes if more than three discontinuity planes are present. UNWEDGE can only take three representative discontinuities from each joint cluster as inputs for unstable block determination without considering variation of joint orientations. This is the main weakness of UNWEDGE as well as deterministic analysis approach.

2.2.3 Probabilistic Approach

Traditionally a combination of empirical and deterministic approaches has been used for tunnel support design (Dunn et al 2008). Recent support design reviews (Earl, 2007; Watson, 2007) presented an opportunity to include a probabilistic approach to determine potential block sizes and frequency. Probabilistic key block analysis has been applied to overcome simplification

limitations of deterministic analyses by many researchers (Tyler et al., 1991; Dunnet al., 2008; Grenon and Hadjigeorgiou, 2012). The advantage of probabilistic method is that the probability distribution for the rock bolt design is obtained if the Probability Density Function (PDF) of input parameters is assessed precisely and correlation between the input parameters is estimated. The overall procedure of probabilistic analysis is as follow.

A deterministic model for unstable rock block identification is required for unstable block analysis. The Hoek and Brown (1980) model is commonly used to determine tetrahedral block properties. After calculation model is selected and the probabilistic properties of input parameters are assumed, the probability of failure can be evaluated by many different risk analysis procedures. The Monte Carlo simulation method is commonly used to evaluate reliability of rock support system when direct integration of the system function is not practical. The PDF of each component variable is completely prescribed. In this procedure, values of each rock parameter are generated randomly by its respective PDFs and then these values are used to determine characteristics of unstable rock block. By repeating this calculation, the probability of critical parameter for rock bolt design such as rock bolt capacity, length and installation pattern can be estimated. This probabilistic approach can provide great flexibility to take parameter uncertainties into consideration. This will be discussed in detail in chapter 4.

The conventional deterministic model only considers discontinuity orientations for stability analysis. The block size restriction depends on the scale factor used which is selected based on experience or field observation. However, prediction of representative size is important for rock bolt design. Therefore, discontinuity size should be considered for unstable block size in probabilistic analysis. Disc model proposed by Baecher et al (1977), is commonly used for joint plane simulation. It assumes all joints are finite circular planes distributed in space. Windsor (1999) gave a detail description on how to use circular joint to determine the potential unstable rock blocks. They are as follow.

The basic assumption is that discontinuities are circular and a maximum possible trace length can be estimated for each set. This result in discontinuities of either infinite or finite radii defined by the maximum trace length attributed to each of the associated sets. Figure 2.13 shows the intersection of three circular-shaped discontinuities in plan view. The discontinuities are arranged to intersect on their extreme edges at the point (C_{ijk}). There are three lines of mutual intersection of the planes, radiating from C_{ijk} to the other three bounding intersections between each pair of planes at C_{ij}, C_{jk} and C_{ki}. These lines are vectors with magnitudes given by the distance from the point of common intersection C_{ijk} to C_{ij}, C_{jk} and C_{ki} respectively and orientations and senses given by the three unit vectors I_{ij}, I_{jk} and I_{ki} respectively, as shown in Figure 2.13(b).

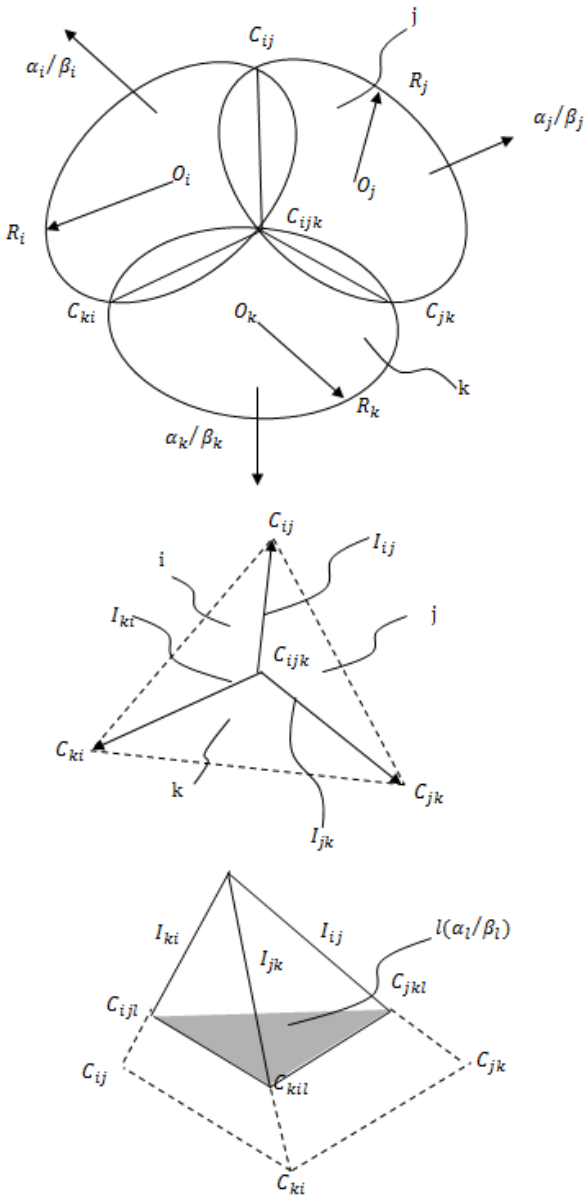

Figure 2.13 The intersection of three circular discontinuities in plan (a and b) and in isometric (c) (After Windsor, 1999)

The three vectors form a vector triple and an open tetrahedral shape – 'open' because the fourth plane of C_{ijk} is such that all three vectors do intersect the excavation face (labelled *l*) in Figure 2.13(c) at the points C_{ij}, C_{jk} and C_{ki}

respectively; then the open tetrahedral is completed and becomes a fully formed tetrahedron block with apex. The shape and size of the block is fully defined by the orientation of the four planes (*i*, *j*, *k* and *l*) and by the block edge vectors I_{ij}, I_{jk} and I_{ki}.

The position of point C_{ijk}, the three discontinuities and the excavation surface are all assumed to be ubiquitous. This allows the three discontinuities to intersect at their extreme edges at C_{ijk} and the excavation plane to intersect the circular planes *i*, *j* and *k* anywhere. The intersection of plane *l* with plane *i* produces a line in plane *i* of given direction. The intersection of plane *l* with the other two lines of intersection (associated with the other two planes *j* and *k*) forms two corners C_{ijl} and C_{ikl}. The three corners form the triangular face of a potential block. There are 3 triangular areas A_i, A_j and A_k that can form within discontinuities *i*, *j* and *k*, one of these will control the trace length limited block (Windsor, 1999).

Three candidate block volumes can be determined from the maximum plane triangular areas of faces *i*, *j* and *k* and a scaling parameter K. The minimum block size from the three solutions defines the maximum trace length limited block size. This is usually found to be controlled by the persistence of one of the joint sets. The maximum trace length limited block size is defined in Figure 2.13 by setting the discontinuity diameters to the maximum trace length and having them intersect at their extremities. This arrangement is extremely unlikely but not impossible. In fact, if the characteristics of the discontinuities

are independent, their trace lengths may vary independently and the point of common intersection C_{ijk} may occur anywhere within the plane and boundary of each. This has significant implications for the magnitudes of the vectors representing the lines of intersection between the planes and the ability of the vector triple and the excavation surface to form a valid, closed tetrahedral shape.

Trace length variation together with variations in orientation form the basis of the probabilistic simulation. Both variations can affect block sizes and must be considered when determining potential unstable block size. If the maximum trace length can used, an upper bound of unstable block size can be obtained.

Rock bolt length is the major design factor and it is based on the total thickness of unstable strata. Bolt length design is related to apex height of the target unstable block. Lang and Bischoff (1982) proposed a relationship between bolt length and roof span as shown in Figure 2.14, which is usually used as a guideline to determine bolt length. It shows that required bolt length increases with excavation span. Biron and Arioglu (1982) simplified this relationship to be linear. Tyler et al. (1991) proposed a probabilistic rock support design for underground tunneling. Rock parameters (e.g. joint orientations, trace length, spacing) are generated systematically from their PDFs. Their results showed that the apex height of unstable rock block distribution tends to be stable after maximum critical block volume is achieved, if trace length and spacing distribution were considered. In other

words, rock bolt length design has an upper limit. Beyond this maximum length, increase of rock bolt length does not enhance the stability of the block. Based on their field observations, they found that probabilistic analysis fits field observation much better than the empirical methods. Tyler et al.(1991) established correlations to determine rock bolt length with considering factored risk and drive width. However, rock bolt diameter and capacity are also important parameters for rock bolt design which are closely related to unstable rock block size and weight. They can be further studied with consideration to rock parameter variation.

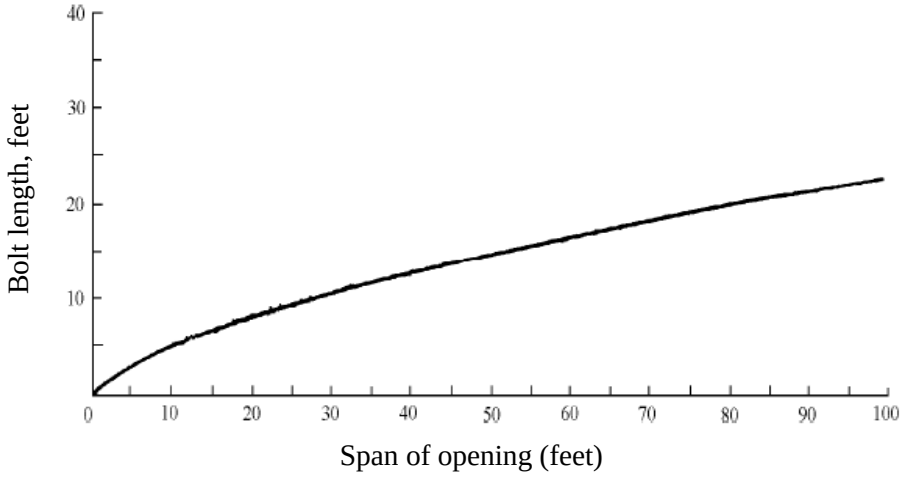

Figure 2.14 Relationship between bolt length and roof span (after Lang and Bischoff, 1982)

2.3 Variation of Rock Parameters

Different distributions are used to capture variation of rock parameters in rock block identification. Such that, JBlock program is used for rockfall hazard

evaluation (Estherhuizen, 1996; Esterhuizen and Streuders, 1998; Dun et al., 2008). Minimum, mean and maximum values of each rock parameter are needed as inputs. Windsor (1999) assumed Fisher distribution for joint orientation and exponential distribution for trace length in his probabilistic rock support analysis. Grenon and Hadjigeorgiou (2003) found Fisher distribution fits their joint orientation data and lognormal distribution shows a good fit for trace length distribution. These assumptions are necessary as durns the design stage, parameters such as trace length and spacing cannot be quantified before excavation and has to be reasonably assumed. Therefore, the distribution of rock parameters has to be investigated when performing probabilistic block analysis.

2.3.1 Joint Orientation

It is well known that rock discontinuities were formed by tectonic movement. Unfavorable joint orientation can lead to rock blocks sliding or falling during excavation. Discontinuity orientation is considered to be one of the controlling factors in key block analysis (Hoek and Brown, 1980). Joint orientations have a relatively high degree of natural scatter; therefore, it has usually been performed using mean values are adopted in conventional deterministic analysis. Priest (1993) suggested that Fisher distribution can be assumed if statistical property of the distribution was required. Fisher distribution is usually assumed for joint orientation simulation due to its simplicity (Leung and Quek, 1995; Song et al., 2001; Kemeny and Post, 2003; Engelder and

Delteil, 2004). However, some researchers treated joint orientation as two variables: dip angle and dip direction. Dip angle and dip direcction are simulated separately from a normal distribution or uniform distribution and then combine together as joint orientation (Tyler et al., 1991; Esterhuizen, 1996; Esterhuizen and Streuders, 1998; Dunn, 2008). This method forces a 3 D distribution which distributed on the reference sphere into a 2 D plane distribution. Distortion is inevitable. Therefore, Fisher distribution is still recommended in literature. However, very few researchers (e.g. Grenon and Hadjigeorgiou, 2003) provided goodness of fit test to show the appropriateness of using Fisher distribution in their case study.

2.3.1.1 Fisher distribution

In geotechnical engineering, past studies have often modeled joint sets using Fisher distribution (e.g. Priest, 1993; Song et al., 2001; Kemeny and Post, 2003; Engelder and Delteil, 2004). The Fisher distribution is defined as follows: each directional vector Ω represents the trend and plunge of the normal of each rock discontinuity plane. In this thesis, a Ω vector is used to represent discontinuity normal consistently. A unit random vector Ω could follow the 3-dimensional Fisher distribution and its probability density function is given by Mardia & Jupp (2009) as

$$f = C_p(\kappa) exp^{\kappa\mu^T} sin\theta \tag{2.4}$$

$$C_p(\kappa) = \frac{\kappa^d}{2\pi^{d+1} I_d(\kappa)} \tag{2.5}$$

where I_d denotes the modified Bessel function of the first kind and order d where d=p/2 -1. If p=3 the normalizing constant $C_p(\kappa)$ can be simplified as

$$C_p(\kappa) = \frac{\kappa}{4\pi \sinh(\kappa)} \tag{2.6}$$

where μ is a unit mean vector pointing into the center of the target cluster and its spherical coordinates are given by

$$\mu = \left[sin\theta_0 cos\varphi_0 \;\; sin\theta_0 sin\varphi_0 \;\; cos\theta_0 \right]^T \tag{2.7}$$

The concentration parameter κ is a measure of the concentration of the distribution about the mean orientation vector. In other words κ indicates the degree of directional dispersion. Since the Fisher distribution is the analogue of the Gaussian distribution on the sphere, it has to relate to some of its properties. In particular, $1/\sqrt{\kappa}$ plays the same role as the variance in a Gaussian normal distribution. Hence, as κ increases, the distribution becomes more concentrated in a specific direction. As κ approaches infinity, the scatter becomes extremely non-isotropic and concentrates in the mean orientation specified by θ_0, φ_0; and when κ=0 uniform scattering occurs (Mammasis and Stewart, 2009). Therefore, κ controls the radius of circular contour shape on the surface of the reference sphere. Taking the product of μ and Ω yields

$$\mu^T \Omega = sin\theta_0 sin\theta cos(\varphi - \varphi_0) + cos\theta_0 cos\theta \tag{2.8}$$

By substitution of the $\mu^T \Omega$ term into Equation (2.4), the Fisher distribution PDF is given by

$$f = \frac{\kappa}{4\pi \sinh(\kappa)} exp^{\kappa\left[sin\theta_0 sin\theta \cos(\varphi-\varphi_0)+cos\theta_0 cos\theta\right]} sin\theta \quad (2.9)$$

Equation (2.9) is the general form of Fisher distribution (Mammasis and Stewart, 2009). The form of distribution is dependent on the mean orientation (axis of symmetry) as specified by μ. The concentration parameter κ and the sample mean orientation are key statistics of Fisher distribution.

For the Fisher distribution, there is an interesting property that the azimuth and colatitude are independently distributed only if the mean orientation vector μ points towards the North Pole,[0 0 1], of the coordinate system. To derive this, let us assume that $(\theta_0, \varphi_0) = (0°, 0°)$, which implies that the axis of symmetry is the z-axis with Cartesian coordinates. This fact greatly simplifies the Fisher PDF expression in Equation (2.9) which can be rewritten as follows

$$f = \frac{\kappa}{4\pi \sinh(\kappa)} exp^{\kappa cos\theta} sin\theta \quad (2.10)$$

where θ denotes the angle between the mean orientation and 'true orientation'. Equation (2.10) is known as the standardized form of the Fisher distribution.

The Fisher distribution works well with rotational symmetric data. Geological and engineering studies have often modeled joint sets using the Fisher distribution; however, any joint set with statistically greater variation in either the strike or dip direction does not meet this criterion. Some researchers (e.g. Peel et al., 2001; Whitaker and Engelder, 2005) pointed out that Fisher distribution is not suitable for non-symmetrical joint data. Whitaker and

Enelder (2005) concluded that if a non-symmetrical joint distribution is modelled using Fisher distribution, significant errors could be involved. Therefore, a more flexible distribution which can accommodate non-symmetrical density contours has to be considered.

2.3.1.2Kent distribution

The Fisher-Bingham 5-parameter distribution (also known as the Kent distribution) can provide greater flexibility in non-symmetric joint data representation (Kent, 1982). More parameters are involved in describing joint clustering. The Kent distribution is a generalization of the Fisher distribution (which is a spherical analogue of the general bivariate normal distribution). It allows for distributions of any elliptical shape, size, and orientation on the surface of the sphere.

The density function of Kent distribution is defined as follow

$$f\left(\bar{\boldsymbol{x}}\right)=c\left(\kappa,\beta\right)^{-1}\exp\left\{\kappa\gamma_{(1)}^{'}\bar{\boldsymbol{x}}+\beta\left[\left(\gamma_{(2)}^{'}\bar{\boldsymbol{x}}\right)^{2}-\left(\gamma_{(3)}^{'}\bar{\boldsymbol{x}}\right)^{2}\right]\right\} \qquad (2.11)$$

where

$$\bar{\boldsymbol{x}}\in R^{3}:x_{1}^{2}+x_{2}^{2}+x_{3}^{2}=1 \qquad (2.12)$$

where $\bar{\boldsymbol{x}}$ denotes a point on the unit sphere in R^3, $\kappa \geq 0$ represents the concentration, $\beta \geq 0$ describes the ovalness, $\gamma_{(1)}$ is the mean direction or pole, $\gamma_{(2)}$ is the major axis and $\gamma_{(3)}$ is the minor axis. $\gamma_{(1)},\gamma_{(2)}\ and\ \gamma_{(3)}$ are perpendicular to each other, therefore a (3×3) orthogonal matrix $\Gamma =$

$(\gamma_{(1)}, \gamma_{(2)}, \gamma_{(3)})$ could be formed. If the original distribution is rotated to the frame of reference defined by the orthogonal matrix Γ to the population standard frame of reference, the probability density function $f(x)$ could take a simple form. Transform from origin data point $\boldsymbol{x}$ to $\boldsymbol{x}^*=\Gamma'\boldsymbol{x}$. The probability density function for $\boldsymbol{x}^*$takes the form

$$f(x) = c(\kappa,\beta)^{-1} \exp\left\{\kappa x_1^* + \beta\left[x_2^{*2} - x_3^{*2}\right]\right\} \tag{2.13}$$

In terms of polar coordinates (θ, φ), where $0 \le \theta \le \pi$ is plunge of discontinuity normal and $0 \le \varphi \le 2\pi$ is the trend of discontinuity normal.

$$x_1^* = cos\theta, x_2^* = sin\theta cos\varphi, x_3^* = sin\theta sin\varphi \tag{2.14}$$

The probability density function takes the form

$$g(\theta,\varphi) = c(\kappa,\beta)^{-1} \exp\left\{\kappa\cos\theta + \beta\sin^2\theta cos2\varphi\right\} \tag{2.15}$$

$$0 \le \theta \le \pi, 0 \le \varphi \le 2\pi \tag{2.16}$$

The normalizing constant of Kent distribution is given by

$$c(\kappa,\beta) \cong 2\pi e^{\kappa}\left[(\kappa-2\beta)(\kappa+2\beta)\right]^{-\frac{1}{2}} \tag{2.17}$$

If concentration parameter κ is large and $\kappa > 2\beta$.

In short, Kent distribution is the general form of Fisher distribution and involves more parameters to describe the shape and location of directional data. If the shape factor β reduced to zero, the eccentricity of the elliptical contour would equal to 1. The Kent distribution will then be simplified to a

Fisher distribution. Kent distribution can describe non-symmetrical joint data unlike Fisher distribution is only suitable for symmetrical data. Lewis and Fisher (1982) proposed a convenient probability plot to judge whether a data set is originated from Fisher distribution. A statistical goodness to fit test was also proposed by Mardia and Jupp (2009). Kent and Hamelryck (2005) developed an effective method for data generation following Kent distribution. Data points were simulated by acceptance-rejection using an exponential envelope on an equal area stereonet, and then reject data points out of stereonet circumference. The details of simulation will be discussed in Chapter 3.

2.3.2 Size Parameters

The excavation span limited block size is the largest block that can move into the excavation by assuming rock discontinuity size is infinite and rock discontinuity can happen anywhere along excavation. It is customary to use the factored excavation span limited block size for design. However, in many circumstances the maximum block size is governed by the trace length limited block size. A block larger than the trace length limited block size will only be partially formed. Furthermore, the spacing value limited block size could also be smaller than the trace length limited block size. The spacing value limited block size defines the largest individual block size for the given block shape. However, uncertainties are involved in both parameters and has to be estimated for unstable rock block identification.

2.3.2.1 Trace length

Joint discontinuities are 3-dimensional planes. Their size are not finite and they do not cut through entire rock mass. If a rock block face is greater than the largest discontinuity plane of the corresponding joint set. The unstable block can only be partially formed, which means that the tetrahedral block cannot be formed to fall or slide into excavation. Therefore, size of rock discontinuities is important for potential unstable rock block volume prediction. However, it is impossible to obtain the size of 3-dimensional discontinuity through borehole sampling. It is because borehole coring diameter is commonly 75mm to 300mm. It can be treated as a 1-dimensional sampling and it is impossible to derive the rock information in the other two dimensions. Therefore, some simplifications and assumptions are necessary (such as using 2-dimensional trace length to calculate joint discontinuity size).

Trace length is defined as the intersection length of rock discontinuity and the sampling face (it is usually excavation wall or roof). Trace length distribution can be used to estimate rock size distribution. There are two types of sampling method which can be used to measure trace length: Sampling the traces that intersect a line drawn on the exposure, which is known as scanline sampling (Priest and Hudson, 1981). The principle of this method is to place a line which is near right angle to discontinuities and record trace length of all discontinuity lines which intersect this sampling line. This method is usually adopted by exposure rock sampling. However, it can be difficult for

underground excavation due to limited sampling orientation and size. It is difficult to draw a sample line containing sever hundred discontinuities to provide a meaningful overall picture or the rock mass. Alternatively sampling the traces within a finite size area (usually rectangular or circular shape) on the exposure, which is known as window sampling can be adopted (Pahl, 1981). The principle for window sampling is to measure all discontinuities that have a portion of their trace length within a defined area of rock face, rather than only those intersect the scanline. Circular windows are preferred to rectangular cells, because they eliminate orientation bias along the mapped surface (Mauldon et al., 2001).

The trace length distribution in the field has been studied by many researchers (Tyler et al., 1991; Song et al., 2001; Park and West, 2001; Hadjigeorgiou et al., 2002; Grenon and Hadjigeorgiou, 2012). Lognormal distribution was found adequate to represent trace length distribution in most cases (Hadjigeorgiou and Grenon, 2003). On the other hand, Park and West (2001) stated that trace length distribution follows an exponential distribution. Tyler et al, (1991) found that different joint sets collected from same borehole may follow different distributions. In their goodness to fit test, 2 out of total 3 joint sets follow lognormal distribution; while the other one follows a negative exponential distribution.

2.3.2.2 Joint Spacing

Joint spacing limits the largest block that can form without it being intersected by additional discontinuities that may result in other blocks being formed within that block. An estimate of this volume is determined by considering the spacing values of the discontinuity sets. For each discontinuity set, one discontinuity is placed to intersect the apex and form the block face associated with that set. The block is then scaled such that the vertex opposite the first discontinuity lies in the plane of a second discontinuity from the same set. This second discontinuity is placed at a perpendicular distance from the first equal to the set spacing. If the spacing chosen is minimum likely spacing, it is unlikely that this block volume will be penetrated by additional discontinuities from this set. Spacing determines the maximum individual block which might form during excavation. However, the normal distance between two discontinuities is not equal. Therefore, some uncertainty is involved. In literature, spacing distribution is commonly assumed in the design stage (Windsor, 1999). Exponential (Grenon and Hadjigeorgiou, 2003), lognormal (Tyler et al., 1990; Parker and West, 2001) or more rarely uniform distribution (Windsor, 1999) were all used for describing spacing distribution (Latham et al., 2006). However, negative exponential distribution is usually assumed proper for joint spacing simulation (Lu and Latham, 1999).

2.4 Summary

Rock reinforcement design methods have been reviewed. Empirical classification systems (RMR and Q system) are useful in estimating the need for reinforcement element in preliminary design stages. However, empirical classification method can only give indication of what kind of support to be applied in an excavation without detailed design (Loset, 1997). Whereas, conventional deterministic approach can give a good estimation of key block shape and largest possible block size based on mean joint orientations. However, scatter is inherent in each rock parameter. Results from conventional deterministic design may not be representative or even conservative. In addition, rock size parameters (trace length and spacing) have great effect on potential unstable rock block identification. If trace length is taken into consideration, the excavation span limited rock block may only be partially formed, whereas joint spacing may further restrain block volume to smaller size. Therefore, the probabilistic approach is applied to overcome the over-simplification of the empirical approach and deterministic approach (Tyler et al., 1991; Dunnet al., 2008; Grenon and Hadjigeorgiou, 2012). The fisher distribution is commonly assumed for joint orientation distribution in literature and it may fail to capture the joint orientation distribution (Peel et al., 2001; Whitaker and Engelder, 2005). The use of Fisher distribution for joint orientation simulation has to be further investigated. In addition, the reliability

aspect of preliminary reinforcement design is not carried out in literature and is investigated in this thesis.

2.4 Scope of Work

An adequate rock reinforcement design is related closely to the identification of unstable block characteristics. However, variation of rock parameters has a great impact on unstable block prediction. Rock features need to be carefully studied and the reliability of proposed design needs to be assessed. Therefore, the scope of work of this study is as follow:

- To investigate whether Fisher distribution is capable to capture the variation of rock discontinuity orientations through probability plot and statistical goodness to fit test based on available actual data form Singapore and overseas.
- To select a suitable distribution for joint orientation simulation and develop Matlab code for statistical distribution parameter estimation and data generation
- To develop Matlab code for probabilistic block analysis with considering the effect of trace length and joint spacing on rock block size determination
- To evaluate the effect of variation of joint parameters on unstable rock block identification with case studies
- To compare different criteria used in rock reinforcement design and to determine suitable design criterion for underground excavation

- To assess the reliability of rock reinforcement design based on conventional deterministic block analysis
- To determine the proper rock reinforcement design parameters based on parametric study of the effect of rock parameter variation.

Chapter 3 Joint Orientation Simulation

3.1 Introduction

As mentioned in the previous chapter, uncertainty is inevitable in rock parameters. Variation in joint orientation has shown tremendous impact on rock block identification (Leung and Quek, 1995). Thus, joint orientation dispersion has to be properly simulated. In literature, Fisher distribution is commonly assumed for joint orientation simulation (Priest, 1993). However, Fisher distribution is only suitable for data that is symmetric in nature. If non-symmetrical joint orientation data assumed to follow a symmetrical Fisher distribution, significant errors in unstable rock block prediction can occur (Whitaker and Enelder, 2005). Therefore, a more flexible distribution such as Kent distribution should be used for joint orientation simulation. Kent distribution is a general bivariate normal distribution which is suitable for the simulation of non-symmetrical data. It allows for distributions of any elliptical shape, size, and orientation on the surface of a sphere. Inferential statistics is adopted to test whether Kent distribution is suitable for a particular rock joint orientation distribution simulation as compared to Fisher distribution. Goodness of fit tests were performed. A case study was established to test the goodness of fit of chosen distribution. The properties of Kent distribution and parameter estimation are also presented.

3.2 Methodology

Discontinuity orientation data is commonly presented graphically on a stereonet by hemispherical projection. Sub-parallel discontinuities are grouped as joint sets. These joint sets have an important influence on the behavior of the rock mass (Priest, 1985). Different joint set classifications can lead to different result for rock block stability analysis. Hence, joint set classification should be carefully carried out. Many classification algorithms had been developed for auto-identification of joint sets (Shanley and Mahtab, 1976; Hammah and Curran, 1998; Gustafson and Kessel, 1978; Bahuka and Veen, 2002). However, as discussed in Chapter 2, the use of different algorithms with different validity indices can produce different results. As a result of this disparity, joint set clustering produced by an experienced engineer in the field is often as accurate and preferred over these algorithms. Therefore, visual identification is used for joint set classification in this research. Subsequently, the suitability of Fisher distribution for joint orientation simulation should be investigated. Probability plot from Lewis and Fisher (1982) is used to test the fitness of Fisher distribution and statistical goodness of fit test from Mardia and Jupp (2009) are commonly adopted to test whether a particular joint set originates from Fisher distribution or Kent distribuion (Peel, et al., 2001). The formulation details shall be provided in Section 3.4. In modern Monte Carlo statistical methods, distributions such as Kent distribution are simulated with a large number of iteration, and efficient algorithms are needed to simulate from such distribution. Kent and Hamelryck (2005) proposed an exact simulation

method with good efficiency properties for the whole range of concentration (κ) and ovalness (β) values. Their method is adopted in this study. This is discussed in detail in Section 3.7. A case study is presented to compare Fisher distribution and Kent distribution.

3.3 Joint Set Classification

For most joint data available from the field, the joint set can be easily identified. However, if two concentrated sets are opposite to each other in dip direction and are distributed along the circumference of stereonet, precaution must be taken to avoid erroneous results. This is because the two sets may belong to the same joint set. This condition occur when dip angle of joint planes are nearly vertical (plunge of its pole is near horizontal) and only lower pole is used to record joint direction during site investigation. If a joint set sit on the equator of reference sphere, data points in the upper hemisphere sphere were replaced by their opposite lower poles. That is the reason why two conjugate clusters which are opposite to each other along the stereonet circumference may belong to one joint set. However, it is necessary to combine conjugate sets for later goodness of fit test and data fitting. In the literature, few conjugate sets were studied to check if the sets is to be combined. Tyler et.al (1991) treated conjugate sets separately during simulation without prof. Figure 3.1 shows an example of lower hemispherical stereographic projections of discontinuity data mapped on the South Crofty

mine (Tyler et.al., 1991). Three main joint sets were visually identified. Joint set 1 was deliberately divided into conjugate sets 1a and 1b. Then these two conjugate sets were simulated separately by their dip angle and dip direction distribution. it is to note that the same joint set is usually formed during the same tectonic activity and in this case it may be improper to analyze a joint set by two conjugate sets. This is further complicated by the effect of sampling during data recording. Here, we check if the conjugate joint sets need to be combined before data analysis. Then it can be combined with the other set to form back the original single joint set for joint data analysis.

Let us assume $N_1=(\alpha_{11},\beta_{11})$, (α_{12},β_{12}), …, (α_{1n},β_{1n}) are lower poles from conjugate set 1 and $N_2=(\alpha_{21},\beta_{21})$, (α_{22},β_{22}), …, (α_{2n},β_{2n}), are lower poles from conjugate set 2. α_{1n} and β_{1n} are dip direction and dip angle of conjugate set 1. α_{2n} and β_{2n} are dip direction and dip angle of conjugate set 2. Conjugate set 1 and 2 belong to the same joint set.

The following equations can be used to determine the opposite upper pole of the conjugate set 1 and conjugate set 2

$$\begin{aligned}
\alpha_{1n(upper)} &= \alpha_{1n} \pm 180° \ (0° \le \alpha_{1n(upper)} \le 360°) \\
\beta_{1n(upper)} &= 90° \pm \beta_{1n} \ (0° \le \beta_{1n(upper)} \le 90°) \\
\alpha_{2n(upper)} &= \alpha_{2n} \pm 180° \ (0° \le \alpha_{2n(upper)} \le 360°) \\
\beta_{2n(upper)} &= 90° \pm \beta_{2n} \ (0° \le \beta_{2n(upper)} \le 90°)
\end{aligned} \tag{3.1}$$

The lower poles of conjugate set 1 and upper poles of conjugate set 2 are combined to form a complete joint set Ω_{12} which is distributed on the whole

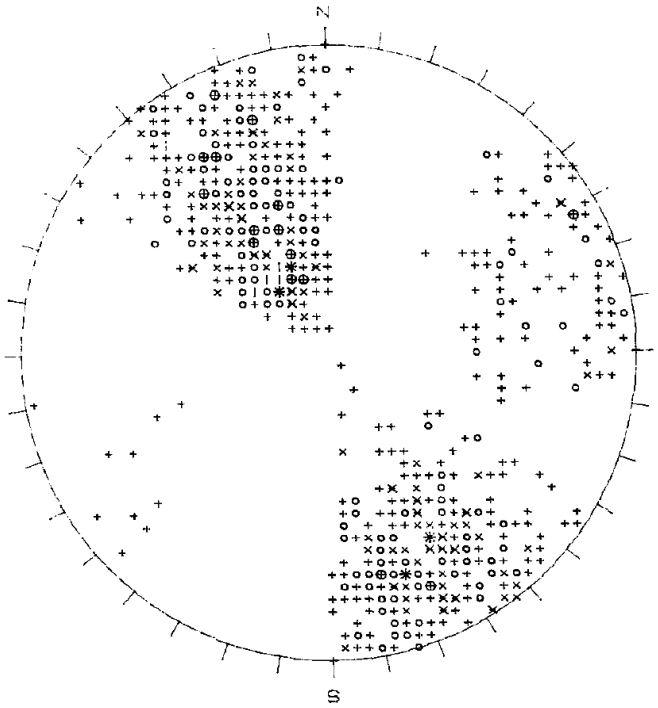

(a) Scatter plot

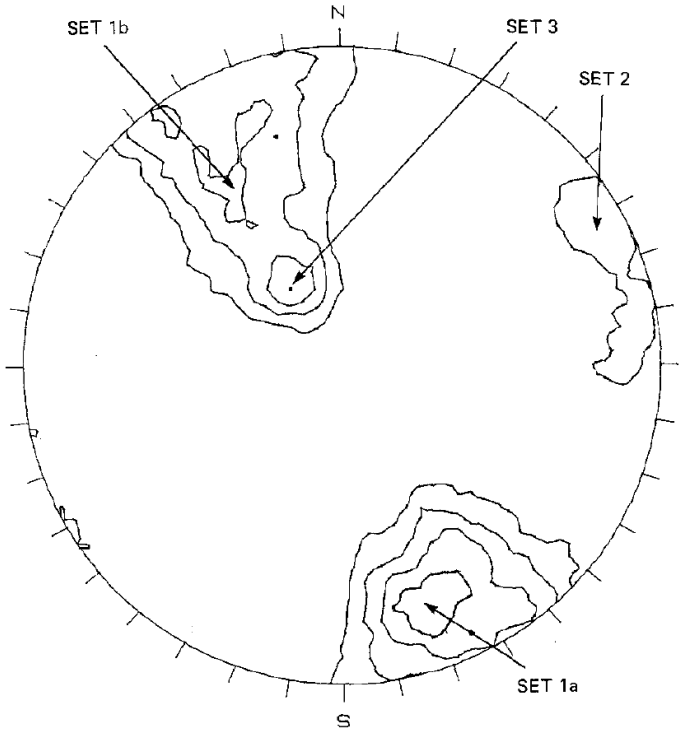

(b) Contour plot

Figure 3.1 Pole plot and contour plot of stereographic projection of discontinuity data mapped on the South Crofty mine (after Tyler et al., 1991)

reference sphere. Otherwise, the conjugate set 2 with upper poles of conjugate set 1 are combined to form joint set Ω_{21}. Ω_{12} and Ω_{21} that are opposite to each other on the reference surface. Thus, they carry the same joint orientation information. Either joint set Ω_{12} or Ω_{21} can be used for joint data analysis.

3.4 Goodness of Fit Test

As mentioned in Chapter 2, Fisher distribution is commonly assumed for joint data analysis. However, the suitability of Fisher distribution to describe joint scatter needs to be investigated. Inferential statistics is involved in this case. Inferential statistics is concerned with the use of statistical concepts in order to make inferences regarding some unknown property of a population. Whereas, descriptive statistics tends to describe the basic features of data gathered from field study and provide summary measures about the samples. On the contrary, statistical inference addresses the problem of inferring properties of an unknown distribution from data generated by that distribution. The most common type of inference involves approximating the unknown distribution with a distribution from a restricted family of distributions. Statistical inference includes point estimation and hypothesis testing. Priest (1985) provided details of point estimation using the maximum likelihood method. This method is adopted for estimating Fisher distribution generation. Probability plots are used to test whether a sample was generated from a particular distribution or not. In the following section, graphical hypothesis

testing for the Fisher distribution and formal formulation of the goodness of fit test are briefly introduced.

Let us assume points Ω_1 and Ω_2 on S^2 with $\Omega_1 \neq \Omega_2$. The point Ω_1 can be rotated to point Ω_2 by multiplying it with matrix $H(\Omega_1, \Omega_2)$ as follows

$$H\left(\Omega_1, \Omega_1\right) = \frac{\left(\Omega_1 + \Omega_1\right)\left(\Omega_1 + \Omega_1\right)^T}{1 + \Omega_1{}^T + \Omega_1} - I_p \tag{3.2}$$

Assume $\Omega_1, \Omega_2, \ldots, \Omega_N$ are points on unit sphere which might have come from Fisher distribution. Further, let (θ_n', φ_n') denote the spherical polar coordinates of the sample data point Ω_n and the sample mean direction vector $\bar{\Omega}_0$is the north pole. A particularly useful arrangement is as the spherical polar coodinates of $H(\bar{\Omega}_0, z)\Omega_n$, where $H(\bar{\Omega}_0, z)$ is the rotation given (3.2), it takes the sample mean orientation vector to the north pole with coordinates $z = (0, 0, 1)^T$. Now define a second data point Ω_n on the unit sphere whose spherical polar coordinates are now given by $(\theta_n'', \varphi_n'')$. In this case, however, the sample mean direction vector has spherical polar coordinates given by $(\theta_0'', \varphi_0'') = (\pi/2, 0)$. More specifically, we define a rotation matrix A by

$$A = \begin{bmatrix} sin\theta cos\varphi & \sin\theta sin\varphi & cos\theta \\ sin\theta & -cos\theta & 0 \\ cos\theta cos\varphi & cos\theta sin\theta & -sin\theta \end{bmatrix} \tag{3.3}$$

where

$$\bar{\Omega}_0 = \begin{bmatrix} sin\theta cos\varphi \\ sin\theta sin\varphi \\ cos\theta \end{bmatrix} \tag{3.4}$$

The spherical polar coordinates $(\theta_n'', \varphi_n'')$ are defined by

$$A\bar{\Omega}_n = \begin{bmatrix} sin\theta_n^{"} cos\varphi_n^{"} \\ sin\theta_n^{"} sin\varphi_n^{"} \\ cos\theta_n^{"} \end{bmatrix} \tag{3.5}$$

with φ_n'' in the range (-π,π]. It is now easy to construct the probability plots for a Fisher distribution to test whether a data set has originated from this distribution. The probability plots can be constructed using the following graphical plot assessments (Lewis and Fisher, 1982):

a) Co-latitude plot: plots the ordered values of 1-cos $\theta_n^{'}$ against –log(1-(n-0.5)/N). If κ is not too small (κ>2), this plot should be close to a straight line through the origin with slope 1/κ.

b) Azimuth plot: otherwise known as longitude plot, plots the ordered values of $\varphi_n^{'}$ against (n-0.5)/N. This follows the symmetry of Fisher distribution that this plot should be close to a straight line through the origin with unit slope gradient.

Mammasis and Stewart (2009) used this probability plot to test whether the electrical signal from an antenna fits Fisher distribution. This graphical goodness of fit test works well with electrical signal. Rock joint orientations were tested by this method as well. Figure 3.2 shows the pole plot of sedimentary rock data from Kent Ridge, Singapore. There are 162 rock discontinuities recorded in the borehole core. After contouring is performed, 4 joint sets are classified. They are shown on Figure 3.2 and the detailed joint

orientation data is shown in Table 3.1. Joint sets 2 and 1 are used as examples and the results are shown in Figure 3.3 and Figure 3.4 accordingly.

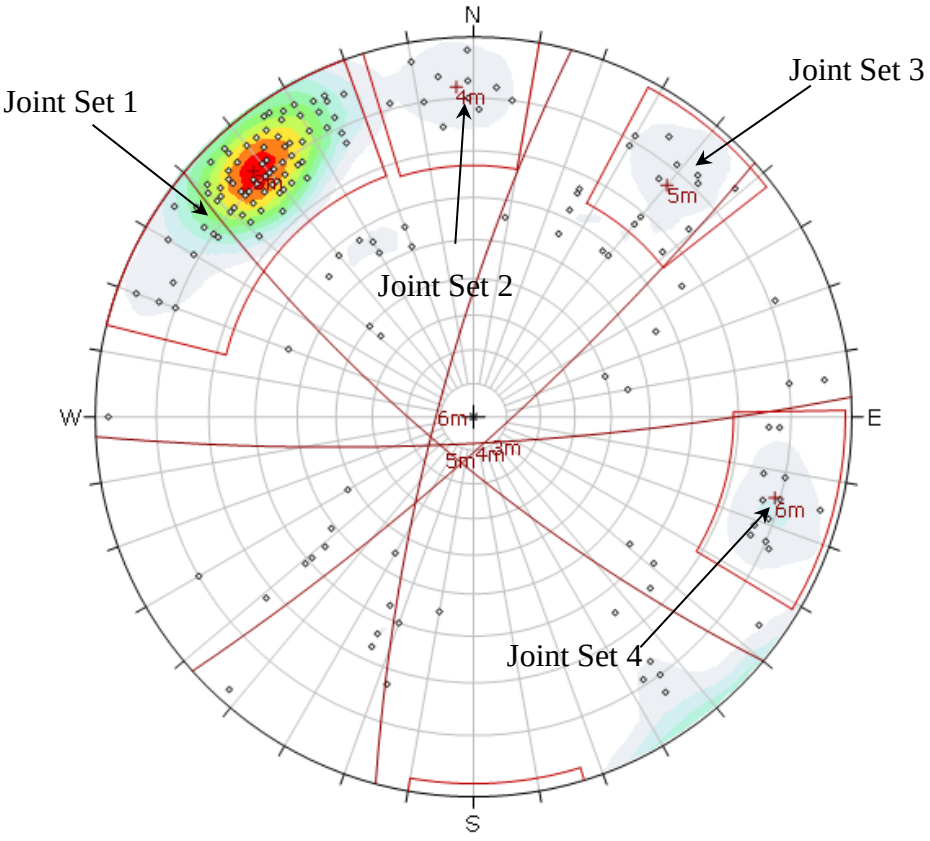

Figure 3.2 Steronet plotting for Kent Ridge rock joint data

Table 3.1 Joint set classification result

Joint set 1									
Dip angle°	Dip direction°	Dip angle°	Dip direction°	Dip angle°	Dip direction°	Dip angle°	Dip direction°	Dip angle°	Dip direction°
85	158	84	153	86	147	82	145	78	142
82	155	86	153	82	146	78	145	76	142
85	155	82	150	88	146	75	145	82	141
86	155	85	150	78	146	86	144	80	141
79	155	87	150	88	145	80	143	86	140
77	155	87	148	84	145	86	142	82	140
81	153	81	148	80	145	84	142	80	140
78	140	87	137	85	135	78	134	80	131
76	140	85	137	80	135	76	134	78	131
78	139	81	137	83	134	88	134	76	131
76	139	80	137	84	134	84	132	85	130
80	139	78	137	81	134	86	131	83	130
88	137	73	137	80	134	83	131	80	130
73	130	88	125	80	125	86	120	82	114
85	127	82	125	79	125	81	120	87	110
83	110	80	110						
Joint set 2									
Dip angle°	Dip direction°	Dip angle°	Dip direction°	Dip angle°	Dip direction°	Dip angle°	Dip direction°	Dip angle°	Dip direction°
80	179	88	179	75	174	87	170	80	187
83	179	84	174	80	171	81	165	82	184
78	181								
Joint set 3									
Dip angle°	Dip direction°	Dip angle°	Dip direction°	Dip angle°	Dip direction°	Dip angle°	Dip direction°	Dip angle°	Dip direction°
85	229	81	224	81	219	84	215	69	220
74	229	82	223	77	218	81	210	67	220
79	210								
Joint set 4									
Dip angle°	Dip direction°	Dip angle°	Dip direction°	Dip angle°	Dip direction°	Dip angle°	Dip direction°	Dip angle°	Dip direction°
76	272	80	281	77	286	77	291	80	293
78	272	80	285	79	289	77	293	81	294
76	281	87	285						

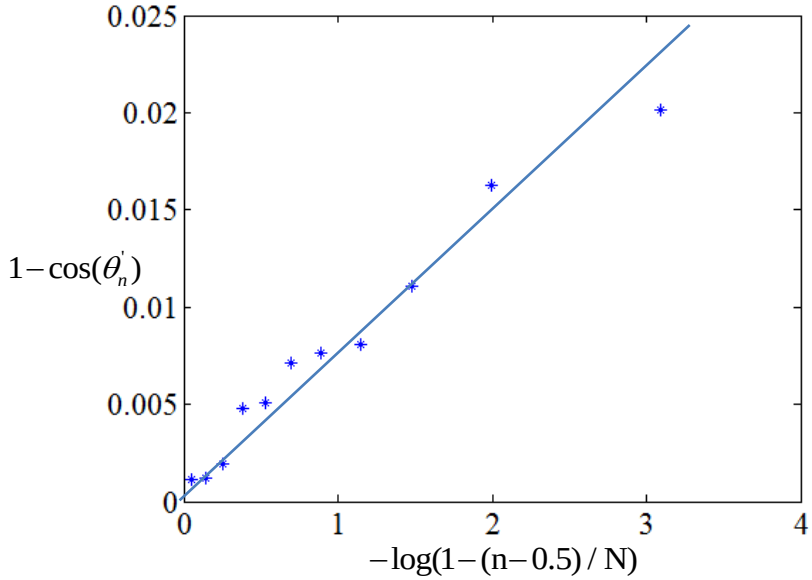

(a) Colatitude plot

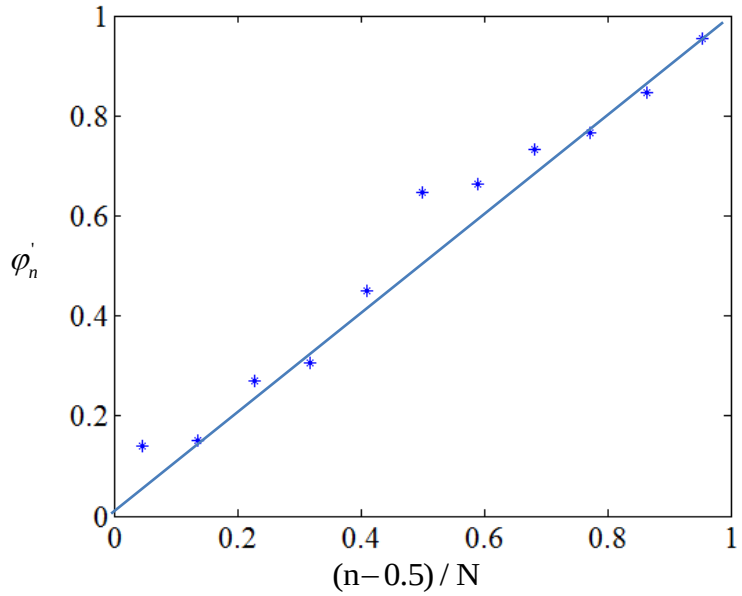

(b) Longitude plot

Figure 3.3 Graphical test for Kent Ridge data set 2

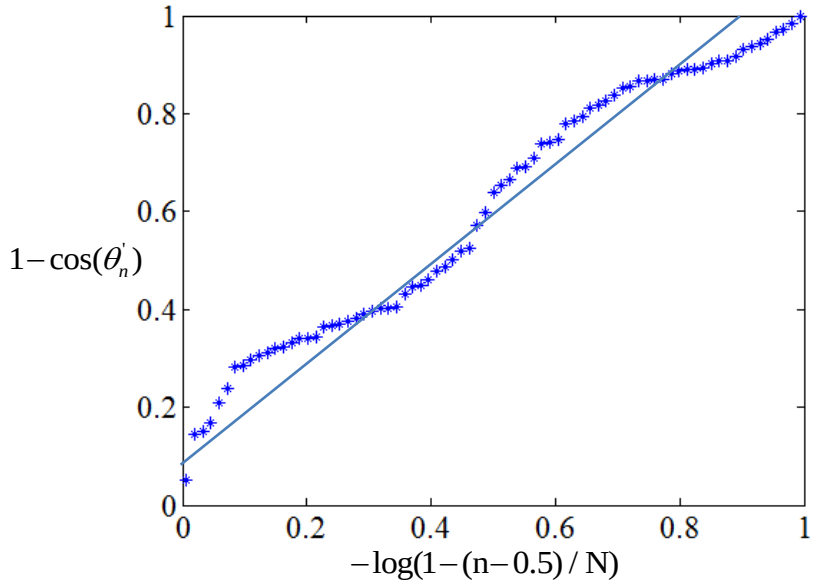

(a) Colatitude plot

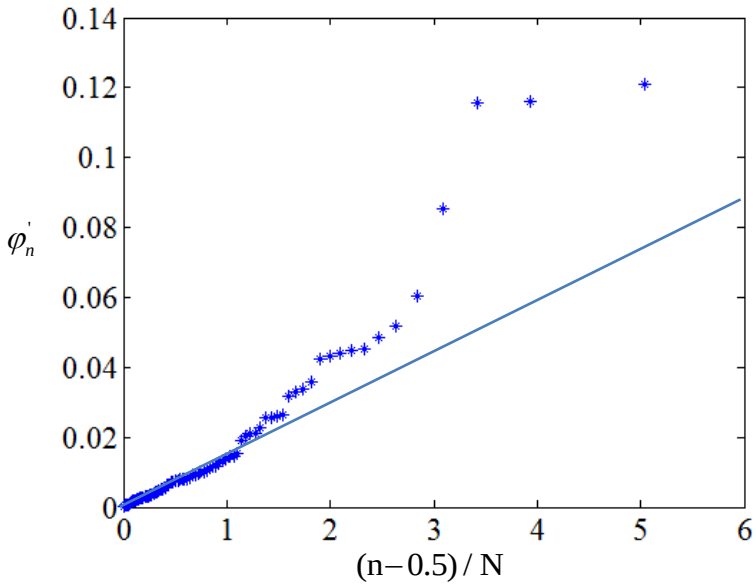

(b) Longitude plot

Figure 3.4 Graphical test for Kent Ridge data set 1

Figure 3.3(a) showed the colatitude plot and the trend of order statistics plot is close to a straight line through the origin with a gradient about 1/120. The dispersion parameter κ is estimated to be 118.4. The longitude plot shows that the trend is close to a straight line through the origin with a unit slope gradient. Therefore, one can conclude that the points of Kent Ridge joint set 2 data follow Fisher distribution with a concentration parameter about 120 from probability plot. Whereas, the graphical test result of set 1 data is shown in Figure 3.4. The colatitude plot tends to curve up and the longitude plot does not start from the origin with unit slope gradient. The probability plots show that set 1 could not follow Fisher distribution. This result is reasonable because the discontinuity data is not of rotational symmetry (as shown in Figure3.2). If data points from set 1 were assumed to fit into a Fisher distribution, errors could occur (Whitaker and Enelder, 2005). As such, Fisher distribution should not be assumed to fit all data set. A more general Kent distribution, which can describe data distribution with an ellipse shape, is investigated in the present study. Although the graphical goodness of fit test using probability plots is convenient to judge by engineers, it involves human judgment and can interrupt simulation process. Therefore, a statistical goodness of fit test should be used.

Mardia and Jupp proposed a test that can be used to compare the goodness of fit of the data for Fisher and Kent distributions (Mardia and Jupp, 2009). To assess the goodness of fit of the Kent model as opposed to the Fisher models, a test statistic was created as follows

$$K_m = n\left(\frac{\kappa_m}{2}\right)^2 \frac{I_{0.5}(\kappa_m)}{I_{2.5}(\kappa_m)}\left(\lambda_{1m} - \lambda_{2m}\right)^2 \tag{3.6}$$

where n denotes the number of samples. $I_{0.5}(\kappa)$ and $I_{2.5}(\kappa)$ represent the modified Bessel function of the first kind and order 0.5 and 2.5 respectively. Von Misesness (hypothesis that the data comes from a Fisher distribution) is rejected at the 100α% significance level if $K > -2\log(\alpha)$. This test statistic assumes that all the clusters are independent. The significance level was usually set to 0.05.

Although the results from probabilistic plots can provide a direct impression on joint orientation distribution, it cannot be quantified and hence is difficult to implement for large data set. Therefore, the statistical goodness of fit test from Mardia and Jupp (2009) can be used. The following example is used to test whether the graphical and statistical approaches can produce the same results. The Mardia and Jupp (2009) method was applied to Kent Ridge data sets 1 and 2 with a significance level of $\alpha = 0.05$. The results of testing with set 1 data show that K=237.035 which is greater than $-2\log(\alpha)$ which is 5.99. This means that the null hypothesis would be rejected and joint set 1 follows Kent distribution. The same test is applied to joint set 2 data. K is found to be 1.52 which is less than 5.99, which means that Fisher distribution is capable to simulate the joint data set. The result is identical to that from probability plot. Another 21 joint sets obtained from 6 discontinuity data from Singapore and other countries were tested using graphical and statistical approaches. Results

are shown in Table 3.2. Except for 6 joint sets originate from Fisher distribution,

Table 3.2 Probability plot result and Goodness of fit test result by Mardia and Jupp (2009)'s method

Data name	Joint set number	K_m	K_o	κ	β	Probability plot	Goodness of fit test
Kent Ridge	1	237.04	5.99	119.04	44.77	Kent	Kent
	2	1.52	5.99	181.66	31	Fisher	Fisher
	3	0.7	5.99	89.17	10.03	Fisher	Fisher
	4	26.36	5.99	229.36	82.17	Kent	Kent
Jurong1A1	1	29.72	5.99	73.28	11.45	Kent	Kent
	2	750.92	5.99	19.23	6.84	Kent	Kent
	3	4.46	5.99	28.72	2.86	Fisher	Fisher
HS	1	24.22	5.99	20.37	3.97	Kent	Kent
	2	11.8	5.99	37.17	9.01	Kent	Kent
	3	117.91	5.99	28.88	9.69	Kent	Kent
Fld	1	445.42	5.99	68.68	30.08	Kent	Kent
	2	52.71	5.99	97.99	32.57	Kent	Kent
	3	97.4	5.99	30.94	10.17	Kent	Kent
	4	4.07	5.99	281.54	64.47	Fisher	Fisher
Dipeg	1	1.93	5.99	81.13	9.41	Fisher	Fisher
	2	23.16	5.99	44.36	11.28	Kent	Kent
	3	6.84	5.99	30.47	4.64	Kent	Kent
	4	0.11	5.99	32.15	0.77	Fisher	Fisher
Jurong1A9	1	155.11	5.99	48.69	16.62	Kent	Kent
	2	159.17	5.99	35.76	9.9	Kent	Kent
	3	28	5.99	37.79	6.42	Kent	Kent

whereas the other 15 joint set are from Kent distribution. In summary, both methods can differentiate Fisher distribution from Kent distribution well. Although the graphical method can show directly the trend of colatitude plots,

human judgment is often required after plotting. On the other hand, Mardia and Jupp (2009)'s method is more quantitative and objective.

3.5 Parameter Estimation of Kent Distribution

For simulation purposes, statistical parameters of a distribution need to be estimated beforehand as inputs. In statistics, point estimation involves the use of sample data to estimate an unknown population parameter of the distribution of interest. One example of the parameter is the concentration parameter κ. The estimation of this unknown population parameter is known as the point estimate. There are various methods for deriving point estimates, for example maximum likelihood estimation and minimum mean squared error. The maximum likelihood estimation is a statistical method used to fit a mathematical model to data. The modeling of actual field data using the maximum likelihood method offers a way to estimate the unknown parameters in the model. It is an optimization technique which continually seeks improvements in the point estimates.

A convenient moment estimator of parameter of Kent distribution is proposed by Kent (1982) for a single Kent distribution from a sample $(\theta_1, \varphi_1)^T$, . . . , $(\theta_n, \varphi_n)^T$. Let $(y_{11}, y_{21}, y_{31})^T$, . . . , $(y_{1n}, y_{2n}, y_{3n})^T$ denote the respective directional cosines. Then the momoment estimates are calculated as follow. First a rotational orthogonal matrix H is formed to rotate the mean direction vector to the North pole (0,0,-1).

$$H = \begin{bmatrix} cos\bar{\theta} & -sin\bar{\theta} & 0 \\ sin\bar{\theta}cos\bar{\varphi} & cos\bar{\theta}cos\bar{\varphi} & -sin\bar{\varphi} \\ sin\bar{\theta}sin\bar{\varphi} & cos\bar{\theta}sin\bar{\varphi} & cos\bar{\varphi} \end{bmatrix} \tag{3.7}$$

where $\bar{\theta}$ and $\bar{\varphi}$ are the polar coordinates of the mean direction. They can be calculated by

$$\bar{\theta} = \sum_{j=1}^{n} \frac{\theta_j}{n}, \bar{\varphi} = \sum_{j=1}^{n} \frac{\varphi_j}{n} \tag{3.8}$$

and

$$R^2 = S_{y1}^2 + S_{y2}^2 + S_{y3}^2 \tag{3.9}$$

where $S_{y1} = \sum_{i=1}^{n} y_{1i}$, $S_{y2} = \sum_{i=1}^{n} y_{2i}$ and $S_{y3} = \sum_{i=1}^{n} y_{3i}$. The mean resultant length $\bar{R}$=R/n and the matrix S, given by

$$S = \begin{bmatrix} \sum y_{1i}^2 & \sum y_{1i}y_{2i} & \sum y_{1i}y_{3i} \\ \sum y_{1i}y_{2i} & \sum y_{2i}^2 & \sum y_{2i}y_{3i} \\ \sum y_{1i}y_{3i} & \sum y_{2i}y_{3i} & \sum y_{3i}^2 \end{bmatrix} \tag{3.10}$$

and then matrix B is given by

$$B = H^T SH \tag{3.11}$$

Then α is defined by

$$\alpha = \frac{1}{2}\tan^{-1}\left\{2b_{23} / \left(b_{22} - b_{33}\right)\right\} \tag{3.12}$$

The matrix K is computed, where

$$K = \begin{bmatrix} 1 & 0 & 0 \\ 0 & cos\alpha & -sin\alpha \\ 0 & sin\alpha & cos\alpha \end{bmatrix} \tag{3.13}$$

The moment estimate of the parameter matrix Γ is

$$\Gamma = HK = (\hat{\xi}_1, \hat{\xi}_2, \hat{\xi}_3) \tag{3.14}$$

where $\hat{\xi}_1, \hat{\xi}_2$ and $\hat{\xi}_3$ are 3×1 column vectors. Then calculate

$$V = \Gamma^T S \Gamma \tag{3.15}$$

and

$$W = v_{22} - v_{33} \tag{3.16}$$

where v_{ij} denotes the element of matrix V in the *i*th row and *j*th column.

When κ is large, the parameter estimates of κ and β are given approximately by

$$\kappa = \left(2 - 2\bar{R} - W\right)^{-1} + \left(2 - 2\bar{R} + W\right)^{-1} \tag{3.17}$$

$$\beta = \frac{1}{2}[(2 - 2\bar{R} - W)^{-1} + (2 - 2\bar{R} + W)^{-1}] \tag{3.18}$$

and the mean direction is denoted by $\hat{\xi}_1$. $\hat{\xi}_2$ and $\hat{\xi}_3$representing the major and minor axis.

Implementing the algorithm proposed by Kent and Hamelryck (2005) for generating pseudo-random samples from Kent distribution, the parameters was estimated. A thousand pseudo-random samples from Kent distribution with parameter κ=100, β=15, and μ=[0 0.7071 0.7071] were generated and using the algorithm, the moment estimates were found to be $\tilde{\kappa} = 101.5, \tilde{\beta}$=12.6 and

$$\tilde{\Gamma} = \begin{bmatrix} 0.00206 & -0.07845 & 0.99692 \\ 0.71063 & 0.70151 & 0.053735 \\ 0.70356 & -0.70833 & -0.057194 \end{bmatrix}$$

respectively. This indicates a very good estimation provided by Kent's algorithm.

A total of 21 joint sets from 6 joint orientation data were tested. Estimated parameter κ is always greater than 2β (Figure 3.5) which means all joint sets are unimodally distributed. Therefore, Equation 2.17 which is $c(\kappa,\beta) \cong 2\pi e^{\kappa}\left[(\kappa-2\beta)(\kappa+2\beta)\right]^{-\frac{1}{2}}$ is suitable for $c(\kappa,\beta)$ estimation.

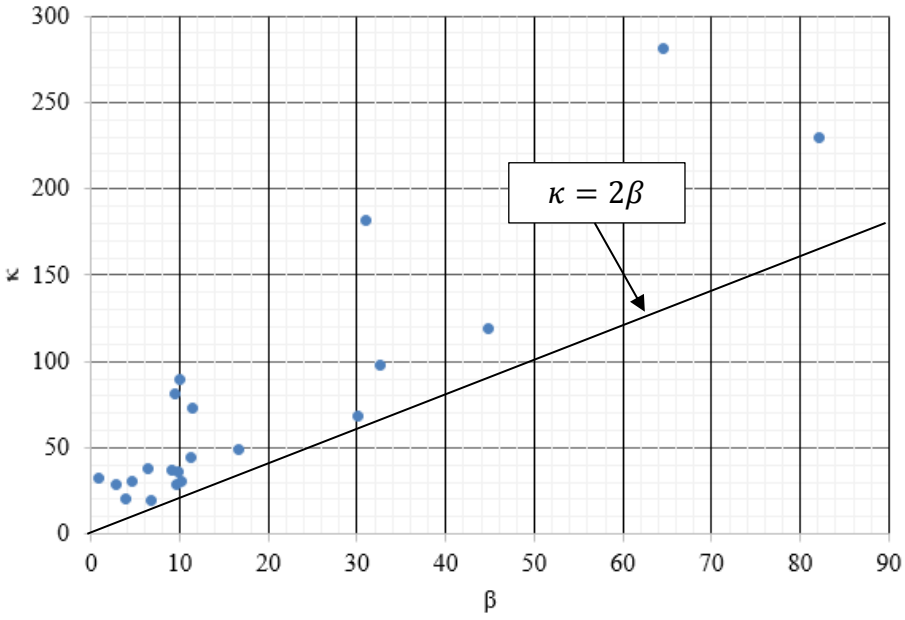

Figure 3.5 Concentration parameter κ vs ovalness β

3.6 Simulation of Kent Distribution

In modern Monte Carlo statistical methods, data point from distributions such as Kent distribution are iterated in a large amount, and efficient algorithms are needed to simulate from such distribution. Kent and Hamelryck (2005)

proposed an exact simulation method with good efficiency properties for the whole range of κ and β values i.e. $0 \leq 2\beta \leq \kappa$.

The Kent distribution, where κ and β are real concentration parameters and Γ is a 3×3 orthogonal matrix representing orientation, was introduced in Kent (1982) and defines a statistical model on the unit sphere in R^3 were defined. Its probability density function in polar coordinates is given by

$$f(\theta,\varphi) \propto \exp\left\{\kappa\cos\theta + \beta\sin^2\theta cos2\varphi\right\} sin\theta \qquad (3.19)$$

where $\theta \in [0,\pi]$ denotes the colatitude and $\varphi \in [0,2\pi)$ denotes the longitude. Euclidean coordinates are defined by

$$u = \begin{bmatrix} u_1 \\ u_2 \\ u_3 \end{bmatrix} = R \begin{bmatrix} sin\theta cos\varphi \\ sin\theta sin\varphi \\ cos\theta \end{bmatrix} \qquad (3.20)$$

One can write $u \sim FB_5(\kappa,\beta,R)$. The concentration parameters are usually required to satisfy

$$\kappa \geq 0, 0 \leq \beta \leq \kappa/2 \qquad (3.21)$$

and we shall restrict attention to this situation in this study. In this setting, the exponent $\{\kappa\cos\theta + \beta sin^2\theta\, cos2\varphi\}$ is a non-increasing function with $\theta \in [0,\pi]$ for each φ (on the other hand, if $\beta \geq \kappa/2$, the pdf increases and then decreases in θ when φ=0). Figure 3.5 shows $\kappa \geq 2\beta$ is valid for all tested joint sets.

The FB_5 distribution was created to provide a spherical analogue for the bivariate normal distribution. The parameter β measures anisotropy. If $\Gamma = I$

in (3.19), the distribution is standardized so that the mode lies in the u_3 direction, and the principal axes are given by the u_1 and u_2 axes, respectively. Under large concentration, the distribution follows an asymptotic bivariate normal distribution when orthogonally projected onto the tangent plane of the sphere.

For simulation purposes, it is helpful to use an equal area projection. Set

$$x_1 = r\cos\theta, x_2 = r\sin\theta, where\, r = \sin(\theta/2) \tag{3.22}$$

where $(2x_1, 2x_2)$ represents an equal-area projection of the sphere.

In (x_1, x_2) coordinates, the Jacobian factor sinθ disappears and the PDF (with respect to $dx_1 dx_2$ in the unit disk $x_1^2 + x_2^2 < 1$) takes the form

$$\begin{aligned} & f(x_1, x_2) \propto \exp\left\{-2\kappa r^2 + 4\beta\left(r^2 - r^4\right)\left(\cos^2\varphi - \sin^2\varphi\right)\right\} \\ & \exp\left\{-2\kappa\left(x_1^2 + x_2^2\right) + 4\beta\left[1 - \left(x_1^2 + x_2^2\right)\right]\left(x_1^2 - x_2^2\right)\right\} \\ & \exp\left\{-\frac{1}{2}\left[\alpha x_1^2 + b x_2^2 + \gamma\left(x_1^4 - x_2^4\right)\right]\right\} \end{aligned} \tag{3.23}$$

where the new parameters

$$\alpha = (4\kappa - 8\beta), b = (4\kappa + 8\beta), \gamma = 8\beta \tag{3.24}$$

satisfy $0 \le \alpha \le b$ and $\gamma \le b/2$. Here we have used the double angle formulas: $\cos\theta = 1 - 2\sin^2(\theta/2)$ and $\sin\theta = 2\sin(\theta/2)\cos(\theta/2)$.

Note that the PDF splits into a product of a function of x_1 alone and x_2 alone. Hence x_1 and x_2 would be independent except for the constraint$x_1^2 + x_2^2 < 1$.

Our method of simulation is to simulate $|x_1|$ and $|x_2|$ separately by acceptance-rejection using a (truncated) exponential envelope, and then additionally to reject any values lying outside the unit disk.

Wood (1987) has also developed a simulation algorithm for the Fisher-Bingham distribution. His method is more general because it includes a wider range of parameter β values and also includes the more general FB_6 distribution (Wood, 1987). However, the Kent distribution proposed by Kent and Hamelryck (2005) is simpler to implement when Equation (3.21) is satisfied (Kent and Hamelryck, 2005).

The starting point for our simulation method is the simple inequality

$$\frac{1}{2}\left(\sigma|w|-\tau\right)^2 \geq 0 \tag{3.25}$$

For any parameters σ, $\tau \geq 0$ and for all w, hence

$$-\frac{1}{2}\sigma^2 w^2 \leq \frac{1}{2}\tau^2 - \sigma\tau|w| \tag{3.26}$$

After exponentiation, this inequality provides the basis for simulating a Gaussian random variable from a double exponential random variable by acceptance-rejection. For x_1 we need to apply Equation (3.26) twice, first with $\sigma = \gamma^{1/2}, \tau = 1$ and $w = x_1^2$, and second with $\sigma = \left(\alpha + 2\gamma^{1/2}\right)^2, \tau = 1$ and $w = x_1$, to get

$$-\frac{1}{2}\left(\alpha x_1^2 + \gamma x_1^4\right) \leq \frac{1}{2} - \frac{1}{2}\left(\alpha + 2\gamma^{1/2}\right)x_1^2 \leq c_1 - \lambda_1|x_1| \tag{3.27}$$

where

$$c_1 = 1, \lambda_1 = \left(\alpha + 2\gamma^{1/2}\right)^{1/2} \tag{3.28}$$

To develop a suitable envelope for x_2, recall that $0 \le 2\gamma \le b$. To begin with suppose b>0. From Equation (3.26) with $\sigma = \left(b-\gamma\right)^{1/2}, \tau = (b/\left(b-\gamma\right))^{1/2}$, and $w = x_2^2$,

$$-\frac{1}{2}\left(bx_2^2 - \gamma x_2^4\right) \le -\frac{1}{2}\left(a-\gamma\right)x_2^2 \le c_2 - \lambda_2 \left|x_2\right| \tag{3.29}$$

where

$$c_2 = b/\left\{2\left(b-\gamma\right)\right\} \le 1, \lambda_2 = b^{1/2} \tag{3.30}$$

If b=0 (and so γ=0), then Equation (3.29) continues to hold with $\lambda_2 = 0$ and $c_2 = 0$

In order to obtain the ellipses in the original position before rotation to the North Pole, the data were first rotated using the Γ matrix, i.e.:

$$\begin{bmatrix} x_i^{'} \\ y_i^{'} \\ z_i^{'} \end{bmatrix} = \Gamma \begin{bmatrix} x_i \\ y_i \\ z_i \end{bmatrix} \tag{3.31}$$

This procedure aligns the principal components of the data with the azimuth and elevation axes, centered about the pole. The standard deviations along the axes are then calculated and an ellipse about the North Pole with major and minor axes one standard deviation in size in computed. The ellipse is then rotated back to the mean position using the Γ matrix to produce the plotting

coordinates of an ellipse centered about the mean direction with major and minor axes in the principal directions of data variance.

The above Kent and Hamlryck method was programed in Matlab, named as *kentgen*, to simulate the behavior of Kent distribution. An example of Kent distribution and it ovalness β effect on data distribution is shown in Figure 3.6. A total of 1000 samples were drawn from the Kent distribution with concentration parameter κ=100, ovalness parameters β=50,30,10,0, and mean direction vector μ=[0 0.7071 0.7071]. It shows clearly that for the same concentration, the simulated points can dissipate more along the major axis when β increases. In short, Kent distribution can provide a more powerful way to model a single rock joint cluster for different shape contours.

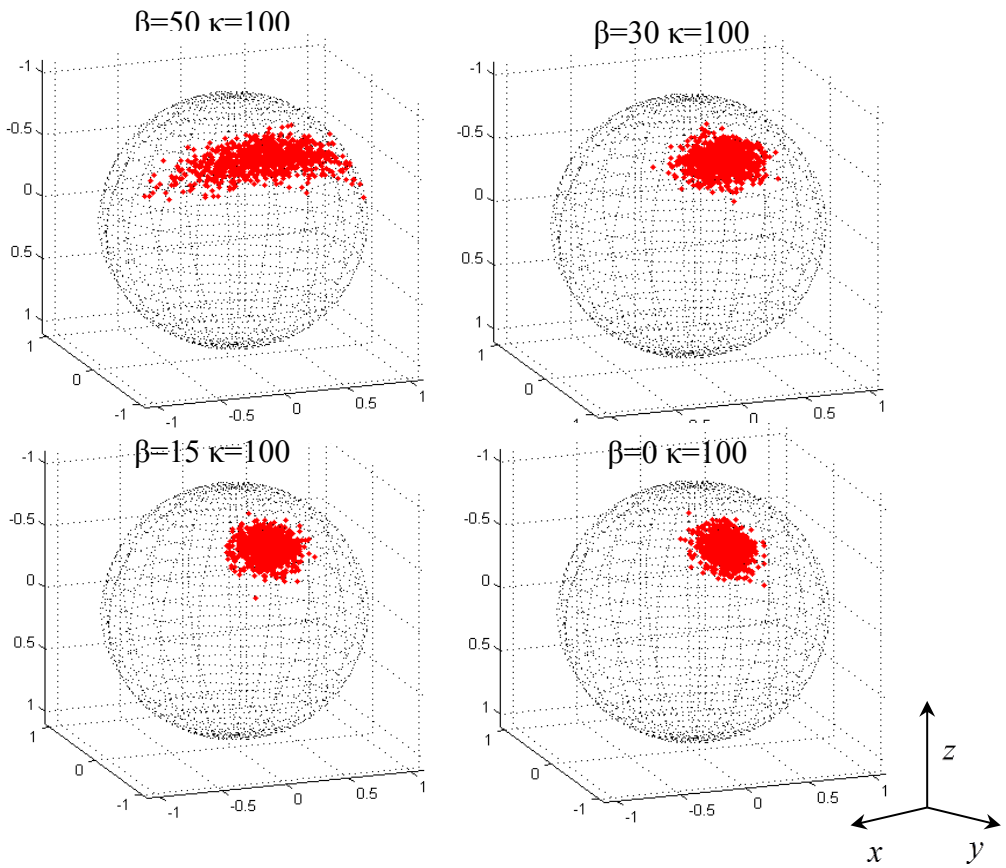

Figure 3.6 Effect of ovalness β

3.7 Rotation Matrix

As mentioned in Section 3.4, data points are generated following Kent distribution around the mean orientation [0,0,-1] with major axis in [0,1,0] direction and minor axis in [1,0,0] direction. In order to rotate the generated data back to the real mean position, a rotation matrix Γ which contains the mean, major and minor axis information is required. Euler equation for 3-dimensional rotations is adopted. The basic rotation matrices rotate vectors about the Cartesian coordinate in three dimensions are as follows:

$$R_x(\theta)=\begin{bmatrix}1 & 0 & 0\\ 0 & cos\theta & -sin\theta\\ 0 & sin\theta & cos\theta\end{bmatrix} R_y(\theta)=\begin{bmatrix}cos\theta & 0 & sin\theta\\ 0 & 1 & 0\\ -sin\theta & 0 & cos\theta\end{bmatrix} R_x(\theta)=\begin{bmatrix}cos\theta & -sin\theta & 0\\ sin\theta & cos\theta & 0\\ 0 & 0 & 1\end{bmatrix} \quad (3.32)$$

For column vectors, each of these basic vector rotations appears counter-clockwise and the coordinate system is right-handed. This matrix can be thought of a sequence of three rotations, one about each principal axis. For general rotations, we can use matrix multiplication for the above three equations. Since matrix multiplication does not commute, the order of axes which one rotates about will affect the result. For this analysis, we will rotate about the x-axis first, then the y-axis and finally the z-axis. Such a sequence of rotations can be represented as the matrix product,

$$R = R_x(\gamma) R_y(\beta) R_z(\alpha) \tag{3.33}$$

α, β and γ represent rotation, yaw, pitch and roll angle respectively. The Euler angles (α, β, γ) are the amplitudes of these elemental rotations. For instance, the target orientation can be reached as follows (also shown in Figure 3.7):

- The *XYZ*-system is rotated by an angle of α about its Z-axis to the new position $X'Y'Z'$
- The *XYZ*-system is rotated about the X' axis by β to the position of $X''Y''Z''$. The Z-axis is now in its final orientation z.
- The XYZ-system is rotated a third time about the new Z'' -axis by γ to the final position of *xyz* system.

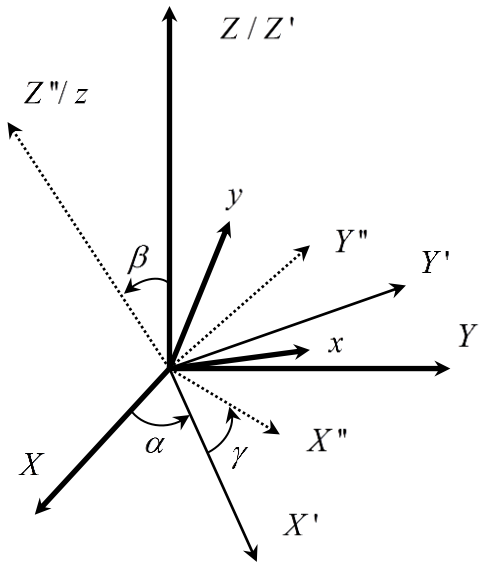

Figure 3.7 Euler angle for 3D rotation

The above-mentioned notation can be summarized as follows: the three elemental rotations of the XYZ-system occur about Z, X' and Z''. Indeed, this sequence is often denoted as $Z-X'-Z''$. It can be represented in right hand Cartesian coordinate as follows:

$$M(\alpha,\beta,\gamma)=R_z(\alpha)R_x(\beta)R_z(\gamma) \tag{3.34}$$

after matrix multiplication:

$$M(\alpha,\beta,\gamma)=\begin{bmatrix} cos\alpha\,cos\gamma-cos\beta\,sin\alpha\,sin\gamma & -cos\beta\,cos\gamma\,sin\alpha-cos\alpha\,sin\gamma & sin\alpha\,sin\beta \\ cos\gamma\,sin\alpha+cos\alpha\,cos\beta\,sin\gamma & cos\alpha\,cos\beta\,cos\gamma-sin\alpha\,sin\gamma & -cos\alpha\,sin\beta \\ sin\beta\,sin\gamma & cos\gamma\,sin\beta & cos\beta \end{bmatrix} \tag{3.35}$$

The above 3 by 3 matrix could be used as rotation matrix Γ for randomized points for data simulation. This rotation matrix is also important for hypothetical case generation.

3.8 Case Study

As discussed in Section 3.3, if the conjugate joint sets occur at the circumference of stereonet, they should be combined and form a complete joint set for goodness of fit test and data simulation. The statistical goodness of fit test from Mardia and Jupp (2009) is used to judge whether the Fisher distribution is suitable for joint orientation simulation. If Fisher distribution cannot be used, Kent distribution will be used instead. The simulation results of the two different distributions are compared.

The joint survey of DIPS program file EXAMPFLD is used as an example. This joint survey was conducted for highway road cut in folded strata in 1992. A total of 175 rock joints were recorded. Lower hemispherical projection is adopted for data plotting. DIPS program from Rocscience is used for this purpose. The joint data is in the Strike (right) and dip format (see Table 3.3). Lower poles are used for data plotting. The contour plot and joint set classification are shown in Figure 3.8. It is evident that the 4 major joint clusters can be identified by visual identification. Joint sets 1 and 2 are simple single sets. Set 3 and set 4 consist of conjugate sets which are separated by circumference of the stereonet. As mentioned earlier, it is necessary to combine two conjugate sets which belong to the same joint set together for data fitting and simulation purposes. Joint set 3 is selected for demonstration. Data points of joint set 3 are shown in Table 3.4. They are in dip angle and dip direction form. The opposite upper pole of conjugate set 3(a) are calculated and combined with conjugate set 3(b) to form the combined joint set 3 for data fitting. The combined procedure has been discussed in Section 3.2. The same procedure is applied to conjugate set 4. Figure 3.9 shows the processed data before and after conjugate sets combination. These 4 joint sets can then be used for data testing. Mardia and Jupp Goodness of fit test and Kent parameter estimation are applied. The results are shown in Table 3.5. Three joint sets are originated from Kent distribution and Joint set 4 is originated from Fisher distribution. Fisher distribution is treated as a special case for Kent distribution; therefore, if a set of data which is originated from Fisher distribution was

simulated by a to Kent distribution, no bias would be resulted. After all parameters are estimated, the simulation could be performed. The Kent and Hamelryck (2005) method is used for data generation. As mentioned in Section 3.5, data are generated on the equal area stereonet and then they will be mapped to 3 D reference sphere. After that, rotation matrix is applied to rotate generated data points to the origin position. Generated points are plotted on stereonet with lower projection method. Simulation results for EXAMPFLD are shown in Figure 3.10 (a).

(a)

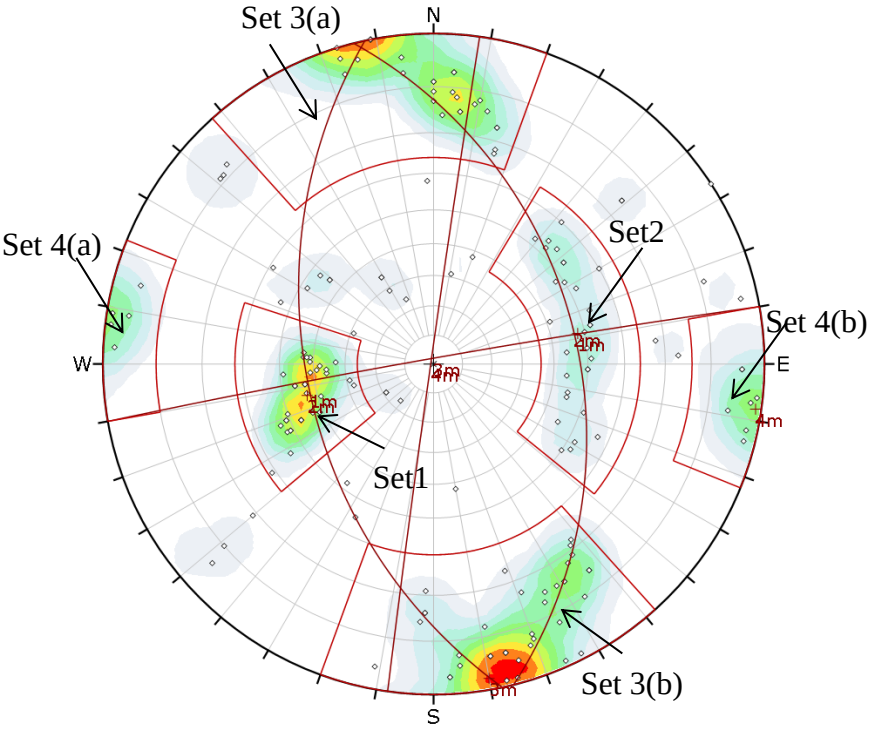

(b)

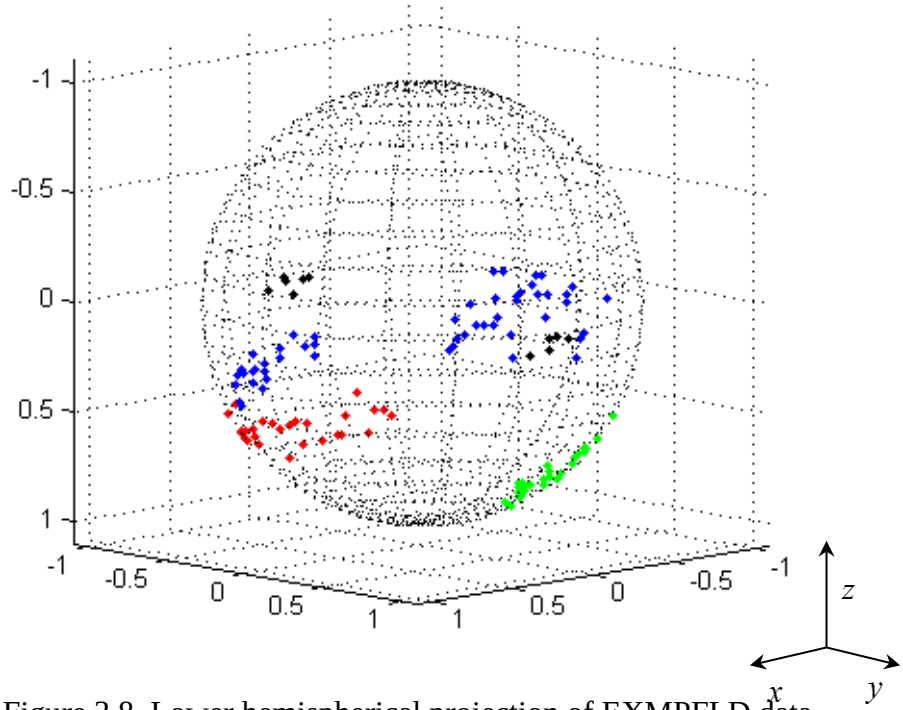

Figure 3.8 Lower hemispherical projection of EXMPFLD data

Table 3.3 Joint orientation of EXAMPFLD

Strike (right) °	Dip angle°	Strike (right) °	Dip angle°	Strike (right) °	Dip angle°	Strike (right) °	Dip angle°	Strike (right) °	Dip angle°
66	29	240	69	221	50	149	53	10	41
253	89	117	38	264	89	333	61	136	52
335	54	272	83	266	78	173	52	280	76
272	85	8	41	83	87	22	85	2	36
48	81	258	84	251	75	101	83	258	67
140	54	257	83	95	58	112	73	250	89
4	39	159	52	243	72	266	84	38	59
86	90	16	86	167	41	240	76	244	80
86	90	241	71	267	42	146	74	10	43
46	44	8	33	239	68	103	75	257	82
274	87	4	36	216	52	185	51	325	84
342	51	251	82	356	29	192	44	261	86
29	53	344	47	345	53	219	52	188	86
246	75	348	50	263	84	189	50	149	53
358	46	358	43	199	45	189	50	199	88
346	51	358	43	175	87	182	44	201	45
66	34	351	39	106	77	51	82	155	50
344	41	6	38	170	81	28	29	342	52
336	19	188	86	91	86	10	42	327	71
175	50	154	90	97	81	86	90	113	68
45	47	252	77	196	84	86	90	113	67
279	69	97	81	352	28	46	44	107	78
3	49	256	73	144	54	274	87	262	89
279	74	173	52	344	47	342	51	157	60
38	48	99	74	80	88	193	89	97	79
12	43	194	88	91	83	246	75	102	78
354	43	10	88	201	88	358	46	101	83
319	17	141	52	205	51	346	51	112	73
16	89	109	76	263	84	66	34	266	84
345	43	304	55	80	85	344	41	240	76
181	68	288	86	344	47	336	19	146	74
3	41	101	79	74	24	211	57	103	75
185	73	139	60	168	53	97	77	212	45
153	48	313	48	49	81	279	74	181	50
80	90	248	75	108	31	14	89	326	80

Table 3.4 Joint orientation of Joint Set 3

Conjugate set 3(a)				Conjugate set 3(b)			
Dip angle°	Dip Direction°	Dip angle°	Dip Direction°	Dip angle°	Dip Direction°	Dip angle°	Dip Direction°
90	169	85	163	89	336	73	339
90	169	79	180	85	355	86	11
81	180	78	185	87	357	86	344
74	182	83	184	75	329	89	347
76	192	73	195	69	2	78	349
79	184	75	186	74	2	75	334
68	196	83	184	76	3	72	326
67	196	73	195	67	341	68	322
87	166	75	186	89	333	84	346
77	189	90	169	80	327	84	346
86	174	90	169	82	340	89	345
81	180	77	180	69	323	84	349
88	163	90	163	83	355	76	323
83	174	78	190	84	341	84	349
				83	340	76	323
				71	324	87	357
				82	334	75	329
				77	335	75	331
				74	2		

Table 3.5 Parameter estimation and Goodness of fit test results

	κ	β	K_m	K_o	Γ	Goodness of fit test
Set 1	68.68	30.09	445.4	5.99	$\begin{bmatrix} 0.9881 & 0.0324 & -0.1503 \\ 0.1323 & -0.6771 & 0.7239 \\ -0.0783 & 0.7352 & 0.6733 \end{bmatrix}$	Kent
Set 2	101.17	31.70	38.4	5.99	$\begin{bmatrix} -0.8657 & 0.4728 & 0.1643 \\ 0.2553 & 0.6994 & -0.6676 \\ -0.4306 & -0.5360 & -0.7262 \end{bmatrix}$	Kent
Set 3	33.73	11.92	106.2	5.99	$\begin{bmatrix} -0.1604 & -0.0657 & 0.9849 \\ 0.7813 & 0.6013 & 0.1674 \\ -0.6023 & 0.7963 & -0.0451 \end{bmatrix}$	Kent
Set 4	281.54	64.47	4.4	5.99	$\begin{bmatrix} -0.9049 & -0.4037 & 0.1348 \\ 0.1183 & 0.0657 & 0.9908 \\ -0.4089 & 0.9125 & -0.0117 \end{bmatrix}$	Fisher

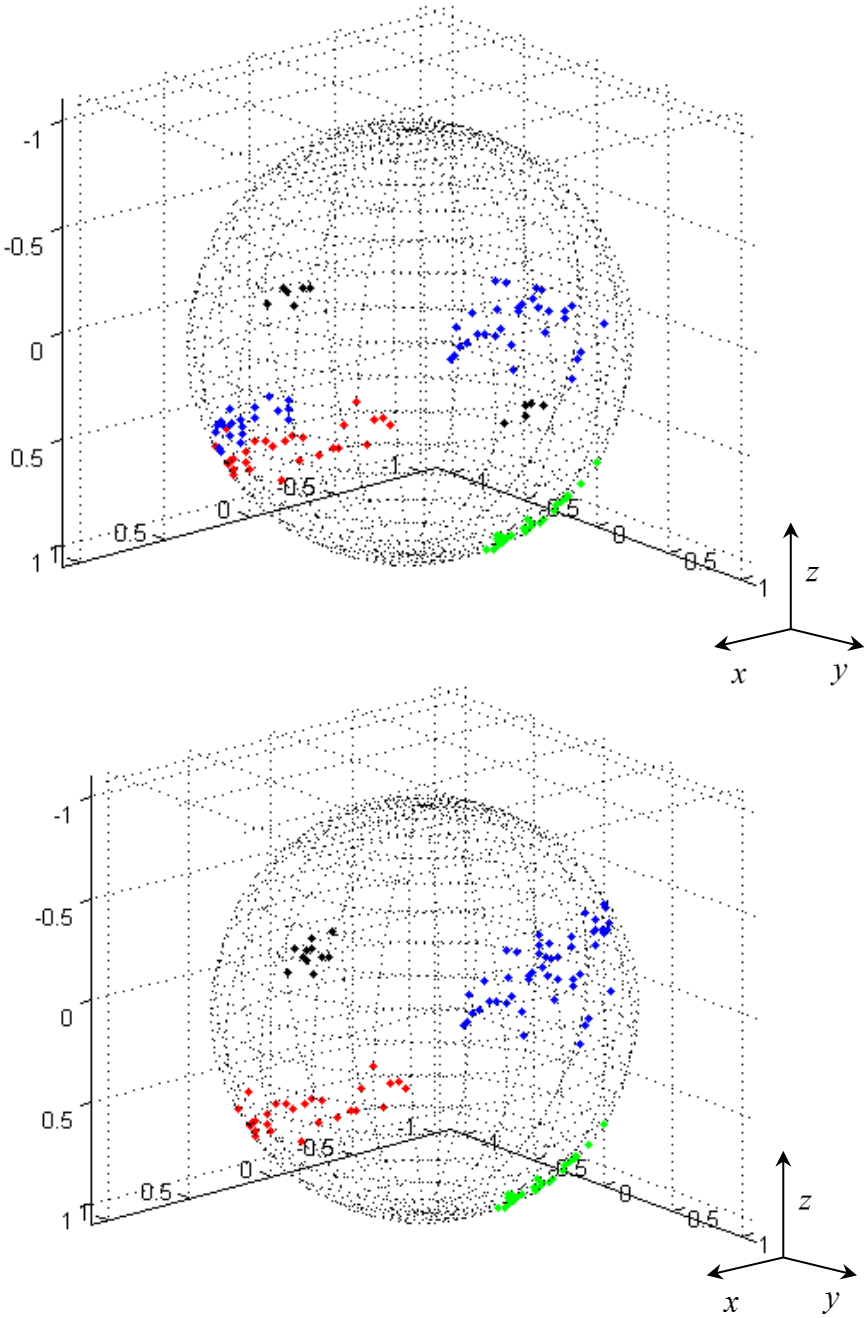

Figure 3.9 Rock joint data before and after conjugate set combination

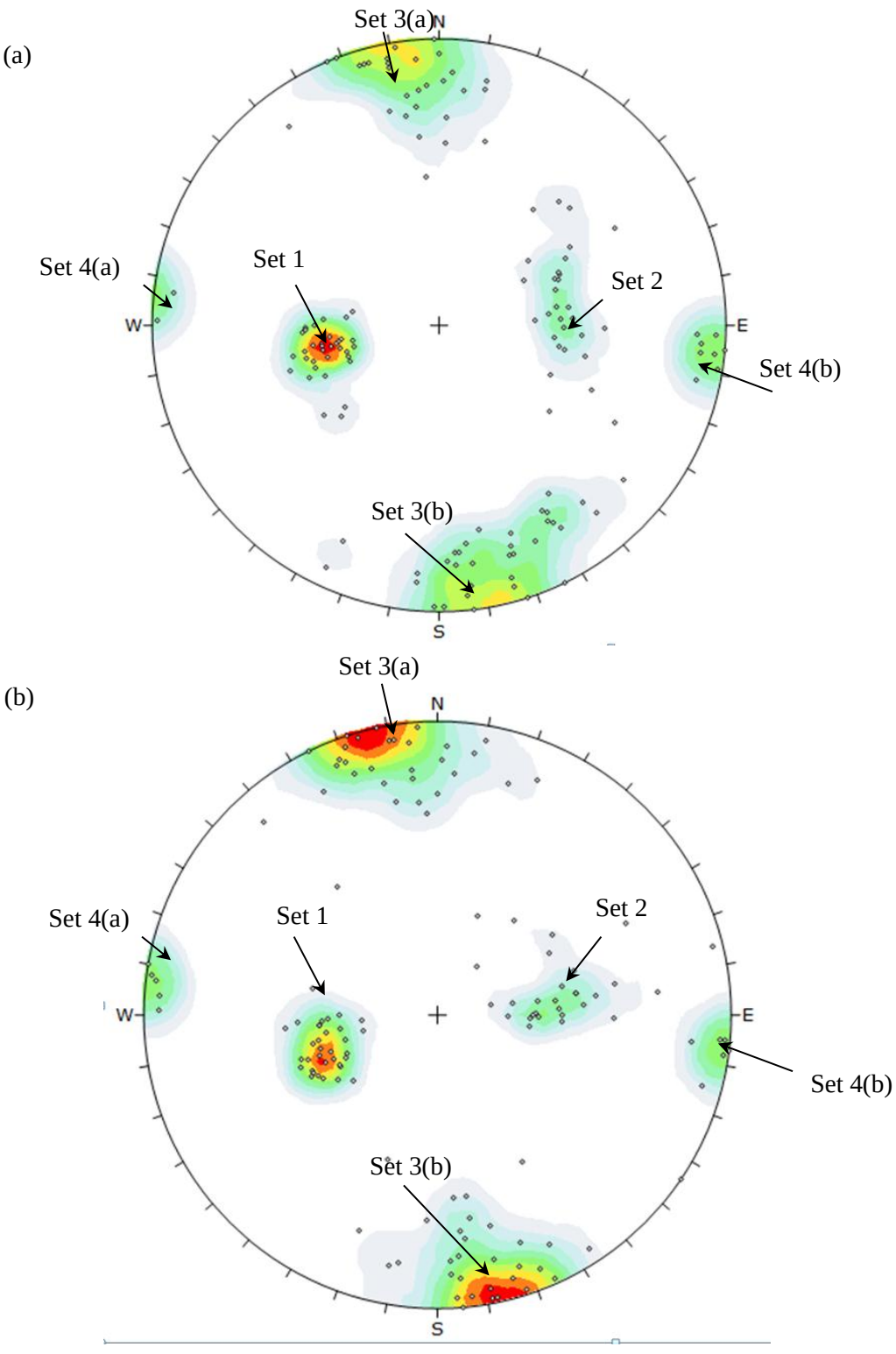

Figure 3.10 Data simulation with Kent distribution (a), Fisher distribution (b)

In order to compare the simulation results between Fisher distribution and Kent distribution, 4 sets of data are assumed to fit a Fisher distribution for this joint orientation simulation. Priest (1985) provided a parameter estimation technique which is used in this study. The data generation method for Fisher distribution can be found in Jung (2009). Their methods are used in this study and the results are shown in Figure 3.9.

Results and Discussion

For the simulation of joint set 4, the results from Fisher distribution and Kent simulation are similar. This is because joint set 4 follows Fisher distribution as confirmed by the goodness of fit test. Fisher distribution is in fact a special case of Kent distribution when the shape factor β is zero. Therefore the Kent distribution is capable to capture the Fisher distribution contour properties well. The result for joint set 1 shows no visual significant difference, although goodness of fit test shows that joint set 1 follows Kent distribution. This is because the contour shape is circular other than elliptical shape. For visual inspection, it is difficult to distinguish Fisher and Kent distribution.

For joint set 2 (single ellipse) and 3 (conjugate ellipse), Fisher distribution cannot generate points with the same properties as well as the original data. In contrast, Kent distribution can handle elliptical data well (compare Figure 3.9(a) with Figure 3.7(a) and it is evident that Kent distribution is better than Fisher distribution for joint orientation simulation, especially when elliptical distributed clusters occur. If joint sets were assumed to follow Fisher

distribution, errors may occur. As Kent distribution is a general form of Fisher distribution it is recommended for joint orientation simulation.

3.9 Summary

In this chapter, Fisher distribution is compared with Kent distribution in joint set data fitting. Precaution should be made when conjugate sets occur. Conjugate sets need to be combined before data analysis. Both graphical probability plot and formal goodness of fit test were conducted on different rock joint orientation data sets from field measurements in Singapore and overseas. The results show that both methods can be used to investigate the validity of Fisher distribution and Kent distribution on evaluating the scatter of joint orientation. Mardia and Jupp method is adopted in the analysis owing to its simplicity and ease of programming. The goodness of fit test results of 21 field joint sets show that most of the tested joint sets (15 out of 21) are non-symmetrical and belong to Kent distribution. As Kent distribution is a general form of Fisher distribution, Kent distribution could be applied for joint set simulation. Descriptive measures of Kent distribution such as sample mean direction vector, sample mean resultant length as well as scatter factors are explained in detail. The results show that concentration parameter κ is always greater than 2β for all the tested cases. Therefore, the Kent and Hamelryck (2005) method for Kent distribution simulation can be adopted. Rotation matrix was introduced which can rotate the generated joint cluster from North Pole of reference sphere to the target position. A case study using example

data from DIPS also shows that Kent distribution is more suitable for joint set data simulation.

Chapter 4 Unstable Block Identification

4.1 Introduction

In order to provide sufficient rock reinforcement to prevent unstable rock block from failure during excavation, unstable block characteristics such as block shape, size and stability need to be carefully investigated. This is because these unstable block characteristics define the rock support required and provide the necessary information for reinforcement design. However, as many rock parameters (such as rock joint orientation, trace length and spacing) are uncertain, the predicted unstable block may vary by a large range. Therefore, the design of rock reinforcement requires a probabilistic solution that takes into account the variation in the rock parameters. This chapter will focus on unstable rock block determination through probabilistic analysis to identify potential instability that may occur during excavation. Monte Carlo simulation is adopted and possible discontinuities combinations are carefully studied. The occurrence of unstable block shape, size and stability of potential rock block are evaluated. The overall simulation steps are shown in Figure 4.1. Besides, Chapter 3 showed that Fisher distribution is not capable to simulated non-symmetrical joint orientation data. If a non-symmetrical joint data is modeled by Fisher distribution, errors might involve in unstable block identification (Whitaker and Enelder, 2005). Therefore, the effect of using different joint orientation models for block size determination should be investigated. A parametric study is performed to study the effect of each

statistical parameter of the joint orientation distribution used on block size determination.

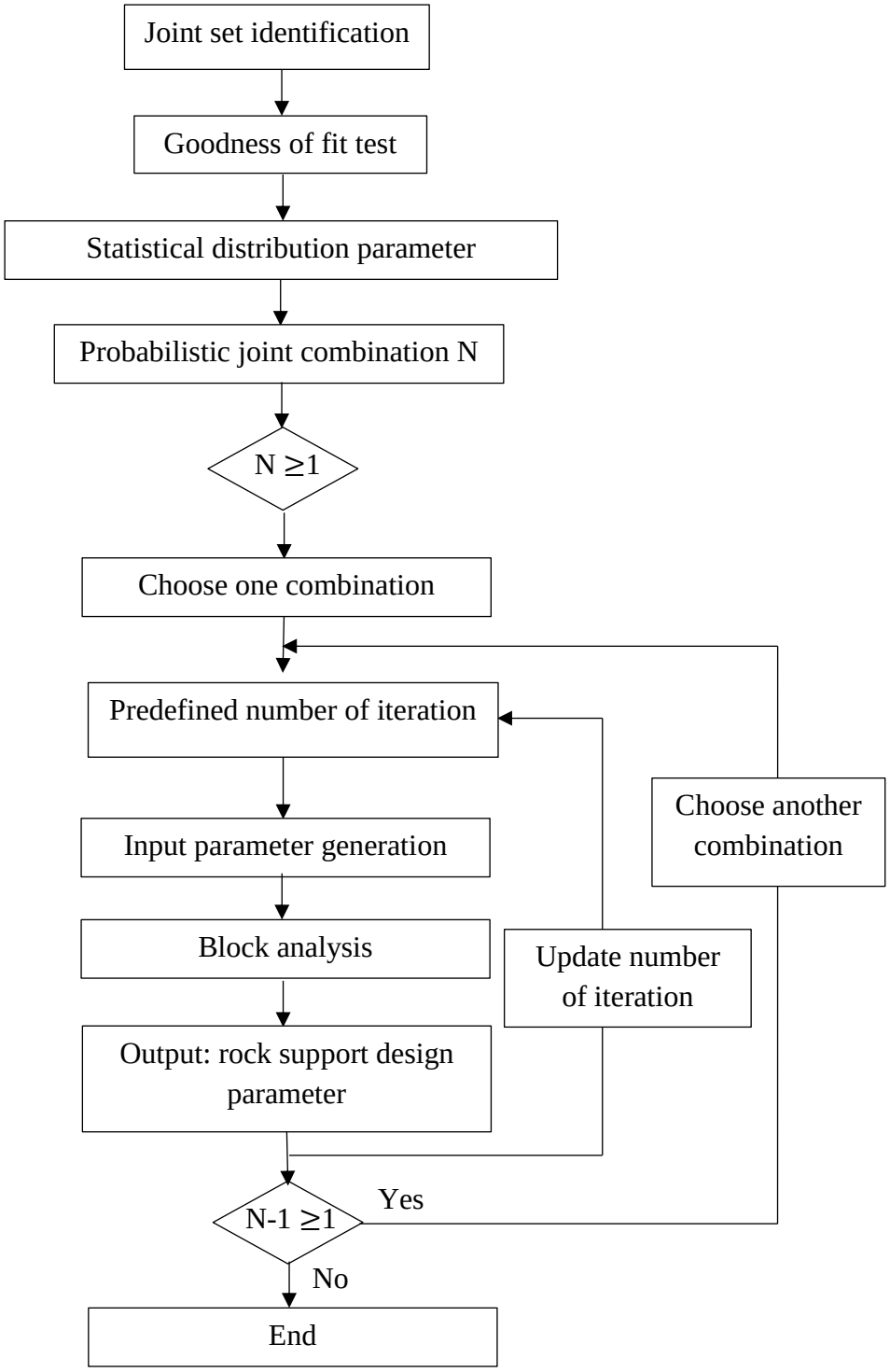

Figure 4.1 Probabilistic simulation steps

4.2 Methodology for Probabilistic Unstable Block Identification

When direct investigation of a failure mechanism is not applicable, Monte Carlo simulation is commonly adopted to evaluate the probability of failure. In Monte Carlo simulation, the value of each variable (such as discontinuity orientation, trace length, spacing) is generated randomly from their measured distributions. All variables are independent of each other and are then combined with fixed input data (such as excavation orientation, excavation dimension) to form a set of input data for deterministic model which is used to determine potential unstable block characteristics (such as block size, apex height and excavation face area). Details are discussed in Section 4.4. After performing a sufficiently large number of iterations, rock block volume, apex height and excavation face area distributions can be derived.

Discontinuity orientation data is plotted on stereonet followed by visual identification of dominant joint sets (discussed in Chapter 3). DIPS6 program from Rocscience is used to aid in contour plot generation. Discontinuity data of each identified joint sets are stalled in separated data files to be used for other programs. As discussed in Chapter 3, three discontinuity planes from three different joints can form a tetrahedral block. However, if the number of joint sets is more than three, probability of combination need to be considered. Leung and Quek (1995) proposed a simple resultant vector approach to calculate the probability of joint orientation combinations. Their method is adopted and will be discussed in details in Section 4.5. Mardia and Jupp (2009) goodness of fit test (discussed in Chapter 3) is adopted to determine the best fit

distribution for joint orientation distribution. Unavailable rock parameters (such as trace length and spacing) need to be reasonable assumed based on existing studies (This will be discussed in Section 4.3). After that, Monte Carlo simulation can be created for probabilistic unstable block identification. After running deterministic model for a sufficient number of times, statistical parameters of unstable block characteristics distribution could be derived. However, large number of iteration means longer computation time which is not effective, whereas, insufficient number of iteration could not achieve the confidence criteria for unstable block prediction. Therefore, the minimum required number of iteration for unstable block simulation needs to be carefully determined. This is discussed in detail in Section 4.6.

4.3 Basic Assumptions and Rock Parameter distributions

If the exact position and size of each discontinuity is known apriori, the location of unstable rock block and corresponding block features (such as size and shape) can be readily determined. Unfortunately, rock parameters (such as trace length and spacing) cannot be collected until excavation has been carried out. Therefore, they need to be reasonably assumed to process probabilistic block analysis in design stage. In addition, the measured values of discontinuity characteristics such as orientation, size, friction, water pressure could be highly variable. They need to be carefully modelled with reasonable distributions which can reflect the same distribution pattern of the origin rock

data. Probability Density Function (PDF) of each rock parameter should be determined carefully.

4.3.1 Ubiquitous Approach

In rock block analysis, the most important concern is the location of each discontinuity and whether unstable blocks could be formed by these discontinuities (Windsor, 1999). The exact location of discontinuities remains unknown prior to the underground excavation. In order to consider all possible discontinuity combinations into consideration, a ubiquitous approach is commonly assumed for rock block analysis (Windsor, 1999). It assumes that rock discontinuities and excavation surface can occur everywhere and anywhere in space. This assumption means that all possible combinations of discontinuities and excavation faces are considered. Hemispherical projection proposed by Priest (1985) and block theory proposed by Goodman and Shi (1985) use ubiquitous approach as the basic assumption. To date, many researchers (Leung and Quek, 1995; Dunn, 2008) adopt this ubiquitous approach for rock block analysis.

4.3.2 Discontinuity Orientation

Discontinuity orientation is considered as the most important parameter for unstable block shape and failure mode determination. As discussed in Chapter 3, discontinuity data are fitted into a more general Kent distribution instead of traditional Fisher distribution and associated statistical parameters (κ, Γ, β) are used for the simulation of rock discontinuity sets.

4.3.3 Trace Length

Trace length and spacing are considered as the size parameters of a rock discontinuity. However, these parameters can only be collected until excavation has been carried out. Therefore, an appropriate trace length distribution needs to be reasonably assumed during design stage. The trace length distribution in the field has been studied by many researchers (Tyler et al., 1991; Song et al., 2001; Park and West, 2001; Hadjigeorgiou et al., 2003; Grenon and Hadjigeorgiou, 2012). A lognormal distribution was found adequate to represent trace length distribution in most cases (Song and Lee, 2001; Hadjigeorgiou and Grenon, 2003). On the other hand, Park and West (2001) stated that trace length distribution follows an exponential distribution. Tyler et al. (1991) observed that different joint sets collected from same borehole may follow different distributions in their case study at the South Crofty tin mine. In their goodness of fit tests with K-S test, 2 out of total 3 joint sets follow lognormal distribution; while the other one follows a negative exponential distribution. In summary, a lognormal distribution or exponential distribution could fit a trace length distribution. In the present probabilistic analysis, a lognormal distribution with appropriate statistical parameters is selected as the Probability Density Function (PDF) for trace length distribution. An average trace length between 1m to 1.7m with a standard deviation from 0.62m to 2m was established by Grenon and Hadjigeorgiou (2003) in their study of an underground mine site in northeastern Canada. Since trace length distribution for Singapore rock formation is not available in the feasibility

study stage, a lognormal distribution with a mean value of 2m and 2m standard deviation is assumed for conservative consideration in the present study.

4.3.4 Discontinuities Spacing

Discontinuity spacing can be used to determine the largest individual block. Thus it should be considered in unstable rock block analysis. However, as mentioned in previous section, spacing data can only be collected after excavation has been constructed. Therefore, discontinuity spacing need to be assumed in design stage for probabilistic unstable block analysis. In the field, exponential, lognormal or more rarely uniform distribution were used for discontinuity spacing simulation (Latham et al., 2006). Table 4.1 shows distributions used by different researchers. Grenon and Hadjigeorgiou (2003) established that a negative exponential distribution with a mean value between 0.34m to 1.2m can fit discontinuity spacing distribution well. Therefore, in this research, an exponential distribution with mean value of 1m is considered as the appropriate PDF for joint spacing distribution simulation.

Table 4.1 Spacing distribution model used in literature

Distribution Name	Research studies on the distribution
Uniform	Windsor, 1999
Lognormal	Tyler et al., 1991 Parker and West,2001
Exponential	Grenon and Hadjigeorgiou, 2003 Hadjigeorgiou et al., 2002

4.3.5 Friction Angle and Cohesion

Discontinuities are formed by tectonic movements. Discontinuity plane roughness and cohesion are not consistent due to different infills in the discontinuity. Friction angle distribution is commonly assumed as a normal distribution based on experimental test by Park (1999). Hoek (1997) suggested a truncated normal distribution should be used for friction angle distribution simulation, because a complete normal distribution can produce unreasonably low or high values. Based on the observation by Park and West (2001), there is very low possibility (about 0.3%) that friction angle would be less than 30° or greater than 50°. A mean (40°) and standard deviation (3.78°) of friction angles for joints were measured in their case study of Highway project in North Carolina, USA. However, a normal distribution with $30 \pm 2.5°$ was determined based on direct shear test on mine sample in northeastern Canada (Grenon and Hadjigeorgiou, 2003). Since friction angle distribution for deep Singapore sedimentary rock is unavailable, a truncated normal distribution with a mean value of 30° and $2.5°$ standard deviation is conservatively assumed in this study. The maximum and minimum of friction angle is set as 35° and 25° accordingly.

Cohesion value of different type of rocks are different. Windsor (1999) assumed a normal distribution with mean values of 0, 2.5, 5, 7.5, 10 kPa for cohesion simulation. However, some researchers assumed cohesion to be zero for conservative consideration (Tyler, et al, 1991; Park and West, 2001). In

this study, cohesion is also neglected for rock stability analysis for the same reason.

4.3.6 Water Pressure

Water pressure is an important parameter in rock stability analysis because water fills rock discontinuity and affects the the resisting forces (Park and West, 2001). Since deep ground water pressure is not easily measured or predicted, water pressure is usually treated as constant for all joint sets in rock stability analysis.

It should be noted that roughness, cohesion and water pressure will only influence the stability of rock block formed, but they will not affect rock block shape or size determination. Therefore, in rock block analysis, the discontinuities can be assumed as persistent, planar and the excavation boundary can be treated as a number of discrete planar faces. In the present analysis, friction angle and water pressure are assumed to follow assigned distribution with reasonable statistical values.

4.4 Deterministic Block Analysis Model

Deterministic block analysis with mean value of each rock parameter is commonly practiced in rock engineering. UNWEDGE program from Rocscience can be used to conduct this deterministic block analysis. The largest block size, apex height and excavation face area could be determined. However, as discussed in Chapter 2, scale factor needs to be applied to derive the representative rock block based on experience and field observations. In

probabilistic block analysis, deterministic model is adopted for unstable block characteristics calculation. This deterministic model needs to be called thousands times to achieve the confidence criteria which will be discussed in detail in Section 4.6. However, UNWEDGE cannot do iterative calculation; therefore, a Matlab program, *Vcal*, is programmed for deterministic block analysis based on Hoek and Brown (1980) which is discussed in Chapter 2. *Vcal* is used here as the deterministic model in probabilistic block analysis. After each rock parameter is generated from their PDFs, *Vcal* could be used to calculate span limited block size and corresponding failure mode. Other rock block characteristics such as apex height and excavation face area are also important for rock reinforcement design (such as rock bolt length relates closely to block apex height) and Hoek and Brown's approach is not capable to determine these two parameters. Therefore, some modification has been done on the original code to include block geometry and provide integration to the *Vcal* program. The analysis outcome of *Vcal* will list the largest possible block volume and corresponding apex height and excavation face area to be used by other programs in the simulation sequence.

4.4.1 Scaling Factor

In deterministic analysis, discontinuity planes are assumed to be persistent and planar. Therefore, only the largest span limited block size will be derived from deterministic analysis. If rock support was designed based on this span limited block size, the design is over conservative. Therefore, size parameters are

essential in predicting the possible unstable rock block. If discontinuity size is not sufficient large, the span limited rock block can only be partially formed or in a smaller scale. That is the reason why scale factor need to be applied in UNWEDGE. Therefore, size parameters (such as trace length and spacing) should be considered for potential unstable block determination.

4.4.1.1 Scaling factor determined by trace length

Trace length is commonly used to determine the possible unstable blocks. This is because trace length related closely with discontinuity size. Discontinuity planes are usually assumed as circular discs in space as discussed in Chapter 2. Trace length determines the diameter of this circular disc. Therefore, trace length can be used to restrain the size of unstable block. A simple calculation method is proposed as follow.

The apex coordinate O of tetrahedral block is assumed as origin (0, 0, 0). Coordinates of the other 3 corners A (ax, ay, az), B (bx, by, bz) and C (cx, cy, cz) can be determined accordingly based on vector approach. Ubiquitous approach assumes all discontinuity planes can occur anywhere in space. This allows the three discontinuities to intersect at their extreme edges to form the largest tetrahedron. This largest block volume is commonly governed by size of the critical discontinuity plane. For example, Figure 4.2(a) show three discontinuity disc plane *i*, *j* and *k* possess the same diameter and intersect with each other by the extreme edges. The largest tetrahedral block OABC can be formed. However, in reality, if discontinuity plane size change, the size of

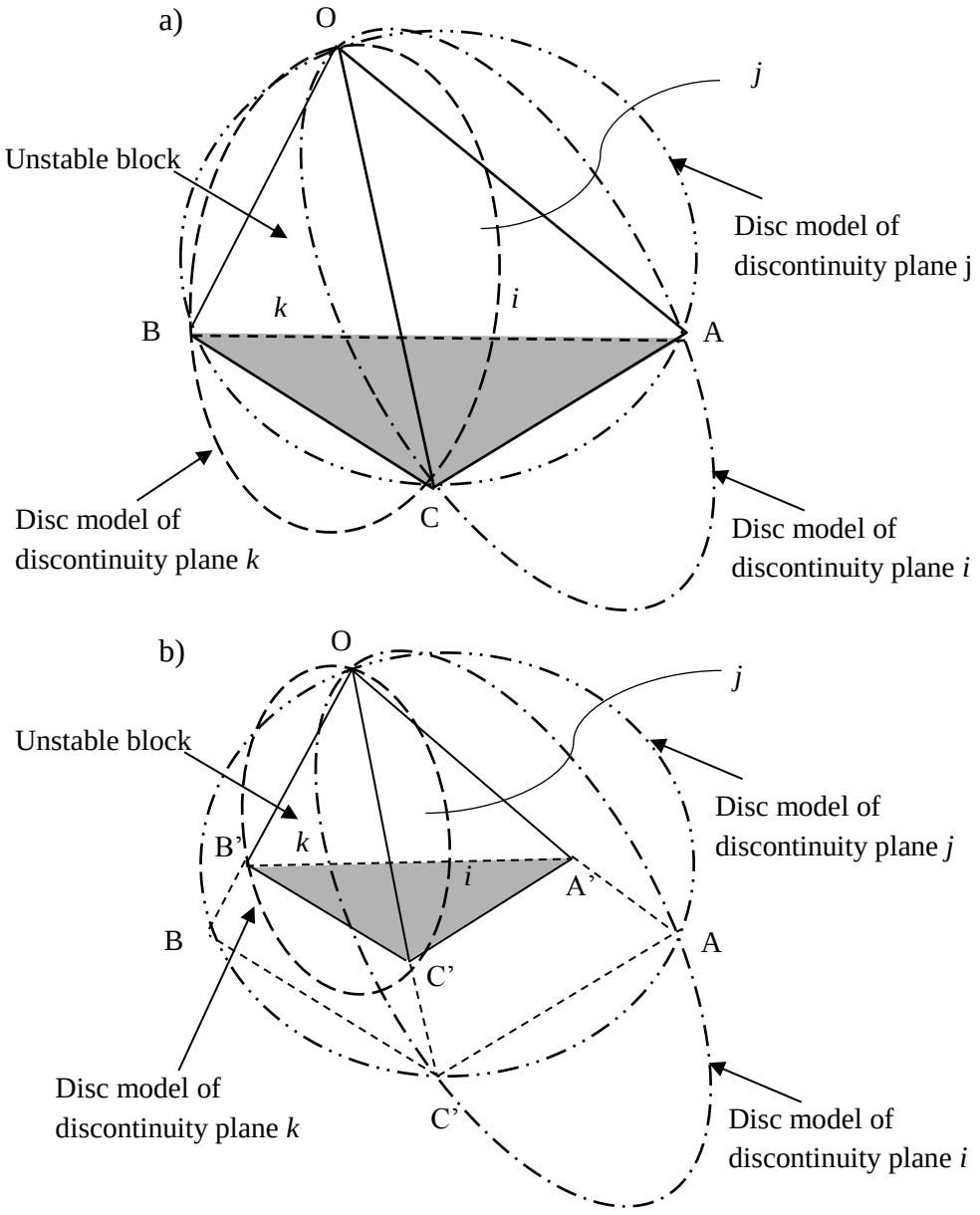

Figure 4.2 Trace length limited block size

block OABC changes accordingly. For example, if disc plane *k* processes a smaller size Figure 4.2(b), the largest triangle shape could be formed within plane *k* will be smaller. Since the block shape only depends on discontinuity

orientations, the block can be scaled to a smaller size with same shape geometry (Block OA'B'C'). Discontinuity disc diameter distribution is assumed to be the same with trace length distribution. Therefore, trace length could be used in unstable rock block size determination. As all vertex coordinates of tetrahedral block can be determined through wedge analysis, the necessary disc diameter of each joint set could be calculated through geometry relationship. A Matlab function *circlefit3d* was used to determine the center and diameter of discontinuity disc (Korsawe, 2013). Then, the i_{th} joint set trace length limit scaling factor γ_{ti} could be calculated as

$$\gamma_{ti} = \frac{t_i}{d_{ti}} \tag{4.1}$$

where i is discontinuity plane number 1,2,3 that form the tetrahedral block. t_i is the simulated or given trace length value of discontinuity plane i. d_{ti} is the disc diameter of discontinuity plane i determined by *circlefit3d* for span limited block. The general trace length limit scaling factor $\gamma_t$is determined as

$$\gamma_t = min\{\gamma_{t1}, \gamma_{t2}, \gamma_{t3}\},\ if\ \gamma_t > 1, \gamma_t = 1 \tag{4.2}$$

Then, scaling factors are applied to the unstable block volume, block free face area and apex height are $(\gamma_t)^3$, $(\gamma_t)^2$ and γ_t accordingly. A Matlab code *scaletl* was programmed for trace length determined scaling factor calculation.

4.3.1.2 Scaling factor determined by spacing

The spacing limited block is the largest individual block that can be formed without it being intersected by additional discontinuities. Therefore, rock

block can only be formed between two adjacent joint discontinuities. As shown in Figure 4.3, the block is scaled such that the vertex (A) opposite the first discontinuity (*i*) lies in the plane of a second discontinuity from the same set. This will produce the largest individual block. Any rock block which is larger than spacing limited block OA'B'C' will be intersected by other discontinuities. The perpendicular distance between the first and second discontinuity is defined as normal joint set spacing. Therefore, spacing value of joint set which discontinuity plane *i* belongs to can be used to restrain the size of rock block formed. Similar events could happen on plane *j* and *k* as well.

The i_{th} joint set spacing limit scaling factor γ_{si} could be determined as:

$$\gamma_{si} = \frac{s_i}{d_{si}} \tag{4.3}$$

where *i* is discontinuity plane number 1,2,3 that form tetrahedral block. s_i is the simulated or given spacing of discontinuity plane *i*. d_{si} is the perpendicular distance between discontinuity plane *i* and the opposite vertex. The general spacing limit scaling factor $\gamma_s$is determined as follow

$$\gamma_s = min\{\gamma_{s1}, \gamma_{s2}, \gamma_{s3}\}\ ,\ if\, \gamma_s > 1, \gamma_s = 1 \tag{4.4}$$

The spacing limit scaling factors are applied to the unstable block volume, block free face area and apex height are $(\gamma_s)^3, (\gamma_s)^2\ and\ \gamma_s$accordingly. A Matlab code *scalesl* was programmed for spacing determined scaling factor calculation.

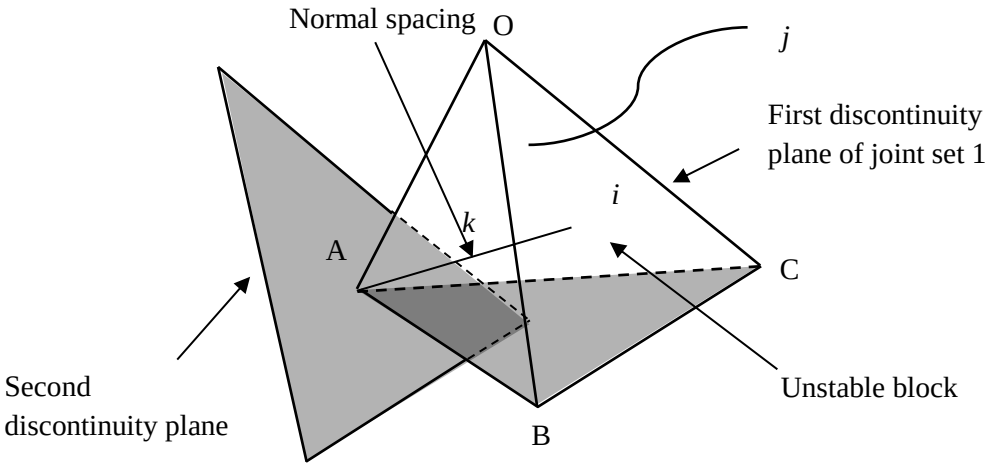

Figure 4.3 Spacing limited block size

4.4.2 Case Study- Louvicourt Mine in Northeastern Canada

The Louvicourt Mine is hard rock mine in Northwestern Quebec, Canada. It is a poly-metallic ore body of copper, zinc, silver and gold. This volcanogenic massive sulfide deposit lies at a depth of 475m from the ground surface, and is part of the Abitibi Greenstone belt within the Precambrian shield of Eastern Canada. The mine uses transverse blasthole open stopes, 50m in length, 15m in width and 30m in height (Grenon and Hadjigeorgiou, 2003).

Scanline mapping was used for rock parameters (such as joint orientation, trace length and spacing) collection. Statistical analyses of three site data were given in Grenon and Hadjigeorgiou (2003). Statistical analysis result of the first site data was used as an example to conduct this deterministic unstable block analysis. There are 4 major joint sets were characterized by visual identification (Figure 4.4), the mean normal spacing, mean trace length and

standard deviation were evaluated for every joint set. The statistical analysis result is shown in Table 4.2.

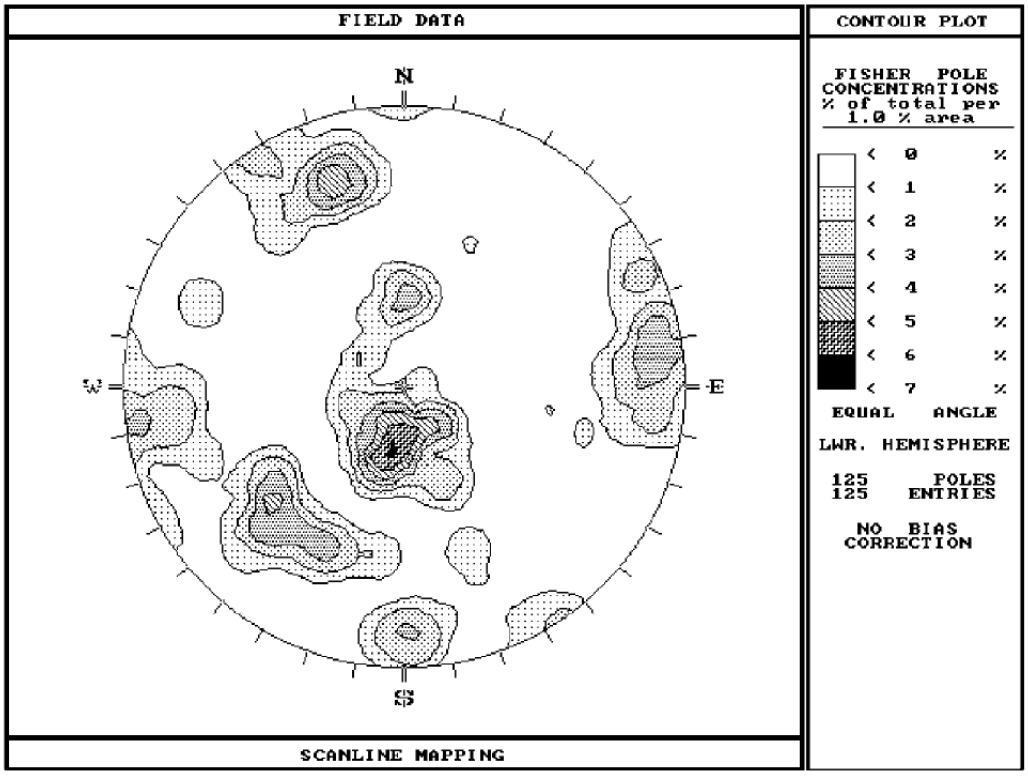

Figure 4.4 Contour plot of Louvicourt mine data (Grenon and Hadjigeorgiou, 2003)

Table 4.2 Statistical analysis result of site #1 of Louvicourt mine

	Orientation (°)	K	Average trace length (m)	Trace length stdev (m)	Normal spacing (m)
Set 1	22/238	26	1.20	1.20	0.34
Set 2	64/009	29	1.00	0.90	0.43
Set 3	76/128	47	1.50	1.20	1.20
Set 4	90/234	26	1.50	1.50	0.56

As discussed in Chapter 2, tetrahedral blocks are more unstable than polyhedral blocks. Therefore, this study only focuses on tetrahedral rock blocks. A tetrahedral block can be formed by 3 discontinuities and an excavation free face. Four dominant joint sets were identified; therefore, a total 4 different combinations of joint sets are possible. The probability of joint set combinations was studied by Leung and Quek (1995) and details will be discussed in Section 4.4. In this example, the first 3 joint sets are selected for deterministic analysis demonstration. A hypothetical 10×10 m horizontal rock tunnel was assumed to be constructed in this area. The excavation axis is 0°/0° (North direction). Friction angle, cohesion and water pressure are neglected for block size analysis.

The Unwedge program from Rocscience is used to verify the result and the result obtained from *Vcal* shows the same result from Unwedge program. The span limited unstable rock block has a volume of 28.53m^3 with apex height of 2.38 m and excavation face area is 36 m^2. The corresponding failure mode is fallout. Stereonet analysis and 3-dimensional plot are shown in Figure 4.5. In

reality, such a large block is unlikely to occur. This is because the actual size of discontinuity planes may not be large enough to form the large block. Therefore, trace length and discontinuity spacing need to be considered for block size prediction. Mean trace length and mean spacing value of each joint set are used for block size determination. Programs *scaletl* and *scalesl* are used to calculate the corresponding scaling factors. The analysis result shown in Table 4.3 reveals that both trace length and spacing will restrain the unstable rock block to a more reasonable smaller size. In addition, apex height and excavation face area will be limited to a smaller size as well. For this case, spacing limited block characteristics are smaller than that of trace length limited block. If mean spacing value of each joint set is larger, the spacing limited block may have a larger volume than deterministic analysis with trace length value. In summary, trace length and spacing have a great effect on unstable rock block size determination.

Table 4.3 Deterministic analysis result with size parameters

	Volume (m^3)	Apex height (m)	Excavation face area (m^2)	Failure mode
Span limited	28.53	2.38	36	Fallout
Trace length limited	0.0263	0.232	0.341	Fallout
Spacing limited	0.0087	0.16	0.163	Fallout

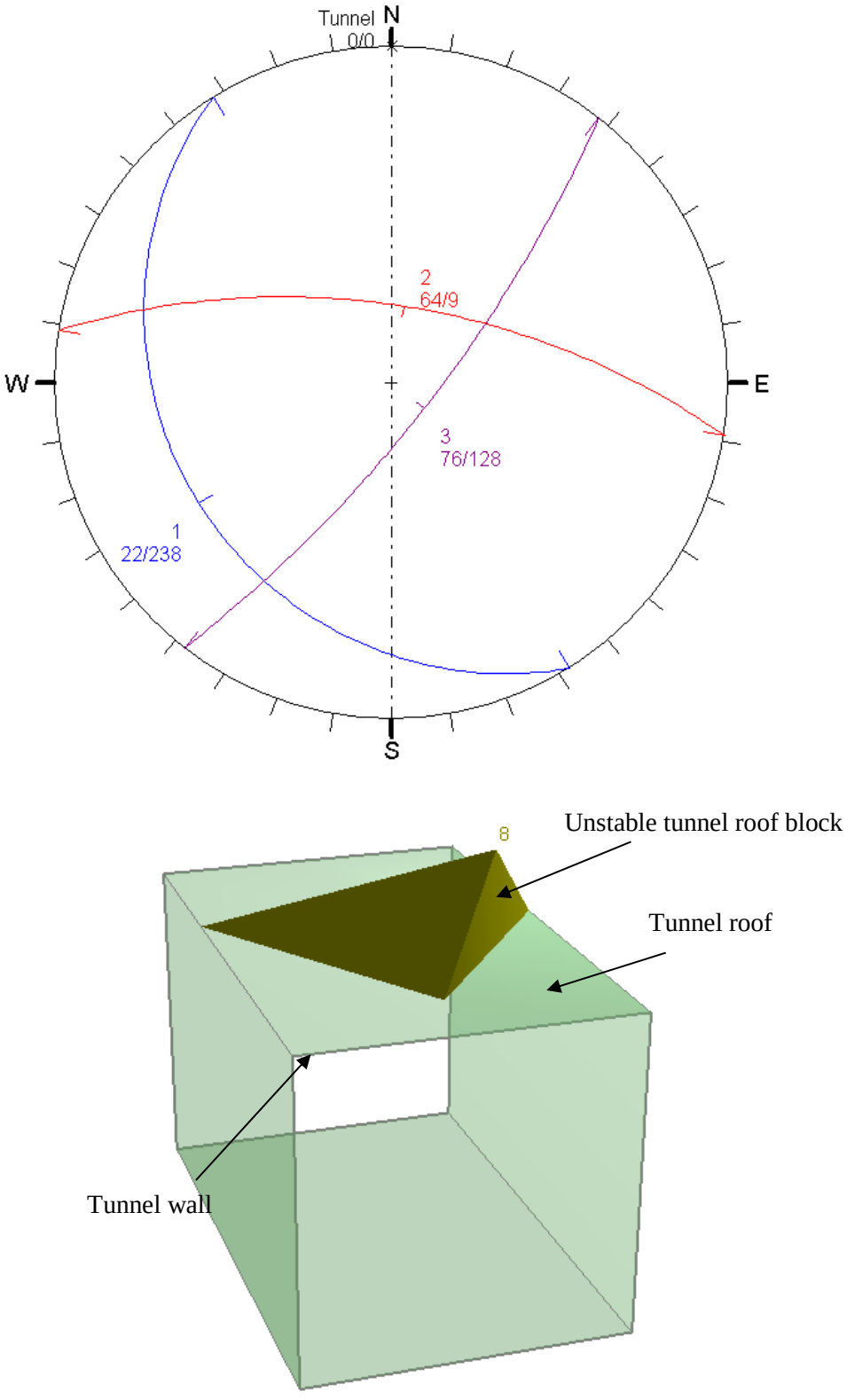

Figure 4.5 Deterministic analysis result

4.5 Probability of Joint Set Combination

Three intersected discontinuity planes from 3 different discontinuity sets combine with excavation free face will form a tetrahedral block. However, if the number of identified joint sets (N) is more than 3, probability of different joint set combinations will be involved. Leung and Quek (1995) proposed a risk model to examine the stability of rock blocks using a probabilistic concept. They assumed that once the orientations of the discontinuities have been identified for a certain location, the characteristics of the rock mass can be well represented solely by the mean discontinuity normal to each of these N clusters. The probability of a rock block b_{123} formed by the excavation free face and discontinuity set 1, 2 and 3 is termed as $P(b_{123})$ and given by the product of the probability of three discontinuity normals

$$P(b_{123}) = \frac{|r_{n1}||r_{n2}||r_{n3}|}{\sum_{i=1}^{N}\sum_{j>1}^{N}\sum_{k>j}^{N}|r_{ni}||r_{nj}||r_{nk}|} \qquad (4.5)$$

where vector r_{ni} is discontinuity normal and its magnitude is $|r_{ni}|$. This probability of joint combination method is adopted in this study.

If a projection satisfied the kinematic conditions of projection for a given face, any spherical triangle on this projection formed by three non-parallel planes of any orientations, will be kinematically congruent with a feasible tetrahedral block at the face. In general, if there are N discontinuity sets, the number of different tetrahedral blocks t is given by

$$t = N!/6((N-3)!) \qquad (4.6)$$

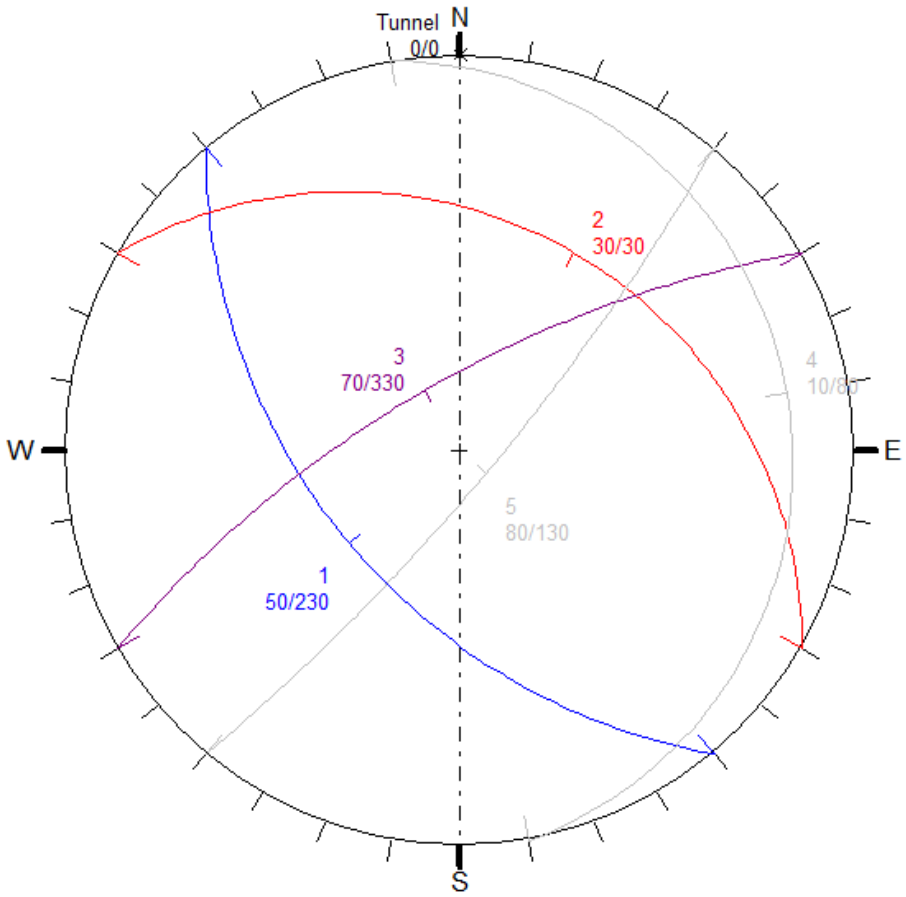

Figure 4.6 Spherical triangles produced by five planes that mutually intersect

Figure 4.6 shows how the great circles of five non-parallel planes intersect to give ten different spherical triangles. In general, N non-parallel planes always intersect to give t spherical triangles, and each of which is associated with a different tetrahedral block. Thus the probability of rock block failing in a certain mode also depends on the probability of occurrence of rock block and the frequency of the rock block failing by this mode. The probability of rock

block containing discontinuities 1, 2 and 3 sliding on any discontinuity is termed as $P(b_{123})_{fallout}$ and defined as

$$P\left(b_{123}\right)_{fallout} = P\left(b_{123}\right)\left(\frac{\text{number of fallout failure}}{\text{number of combinations of rock block}\left(b_{123}\right)\text{generated}}\right) \quad (4.7)$$

The probability of failure in terms of wedge failure involving block sliding on the line of intersection of two discontinuities $P(b_{123})_{intersection}$, and for block slide failure, $P(b_{123})_{slide}$, can be defined in a similar manner. However, in order to determine the probability of a failure mode of one joint set combination, probabilistic analysis is necessary to determine the number of that particular failure mode and the number of combinations of rock block generated.

4.6 Iteration Times for Monte Carlo Simulation

Monte Carlo simulation is usually adopted to simulate the problem when direct investigation is not applicable. The more iterations are performed, the closer the simulation result is to the real case. However, large number of iteration means longer computation time. For example, Figure 4.7 shows the computation time of *Vcal* program with different number of iteration. Quadratic relationship can be observed. In order to perform a cost effective analysis, the minimum required number of iteration which could give a decent simulation result needs to be derived. Confidence limit is usually adopted to determine how close the population is from the sample statistics. Therefore,

confidence limit can be used as a criterion to decide the minimum number of iteration for a particular error percentage. The details are as follow.

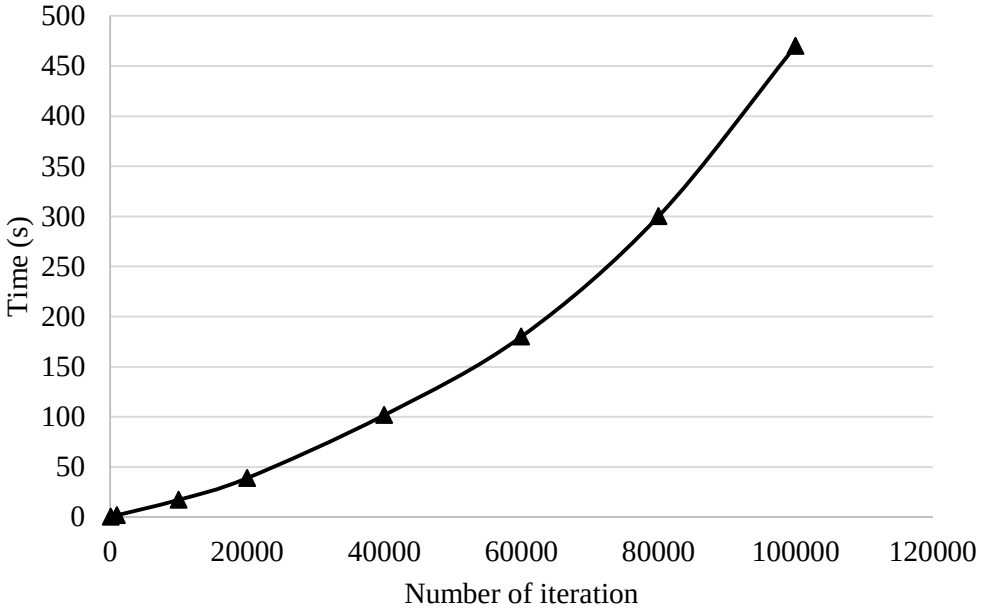

Figure 4.7 Time vs number of iteration

In statistics, mean μ_x and standard deviation σ_x are usually used to describe a distribution. However, in reality, one can only derive the sample mean $\bar{x}$ and the sample standard deviation S_x with limited samples. The mean and variance of a sample with N numbers are defined by

$$\bar{x} = \frac{1}{N}\sum_{i=1}^{N} x_i = \frac{1}{N}\left(x_1 + x_2 + \ldots + x_N\right) \tag{4.8}$$

$$\text{Var} = S_x^{\,2} = \frac{1}{N-1}\left[\left(x_1 - \bar{x}\right)^2 + \left(x_2 - \bar{x}\right)^2 + \ldots + \left(x_N - \bar{x}\right)^2\right] \tag{4.9}$$

The confidence intervals for the mean can be written as

$$\bar{x} \pm z_c \frac{S_x}{\sqrt{N}} \tag{4.10}$$

where z_c is value of confidence coefficient. Table 1 shows z_c values for different confidence levels.

By considering the confidence interval to represent twice this maximum error one can write

$$error_{max} = z_c \frac{S_x}{\sqrt{N}} \tag{4.11}$$

Table 4.4 Values of zc for different confidence levels

Confidence Level %	99.75	99	98	96	95.5	95	90	80	68	50
z_c	3	2.58	2.33	2.05	2	1.96	1.645	1.28	1	0.6745

The percentage error of the mean α becomes

$$\alpha = \frac{z_c S_x}{\bar{x}\sqrt{N}} \tag{4.12}$$

Rewrite for N yields

$$\mathrm{N} = \left[\frac{z_c S_x}{\bar{x}\alpha} \right]^2 \tag{4.13}$$

An example is provided in Driels and Shin (2004) to test the practicability of Equation 4.13. They assume statistical result of a simulation has a mean value ($\bar{x}$) 0.2158 and a standard deviation (S_x) of 0.5216. 95% is set as confidence

limit and the maximum allowable error percentage to the mean value is 5%, the required number of iterations can be calculated as 8977 from Equation 4.13. In other words, if the simulation is run 8977 times, there is 95% confidence to say that the simulated sample mean will not differ more than 5% from the true value.

Figure 4.8 shows the required number of iteration calculated by Equation (4.13) with the statistical parameters ($\bar{x}$ = 0.2158 and S_x = 0.5216) versus n trials. One can observe that the required number of iteration tends to be stabilized around 9000. In order to test whether the minimum number of iteration can achieve the criteria (95% confidence to say sample mean value will not differ more than 5% from the true value), the previous example is simulated 10 times with 8977 times of iteration. The error percentage to the mean value can be determined by Equation 4.11 and they are 4.9227, 4.9473, 5.0112, 5.0274, 4.8880, 4.6608, 4.9525, 4.9098, 4.9899, and 5.0412. Therefore, Equation 4.13 works well to determine the minimum number of iteration.

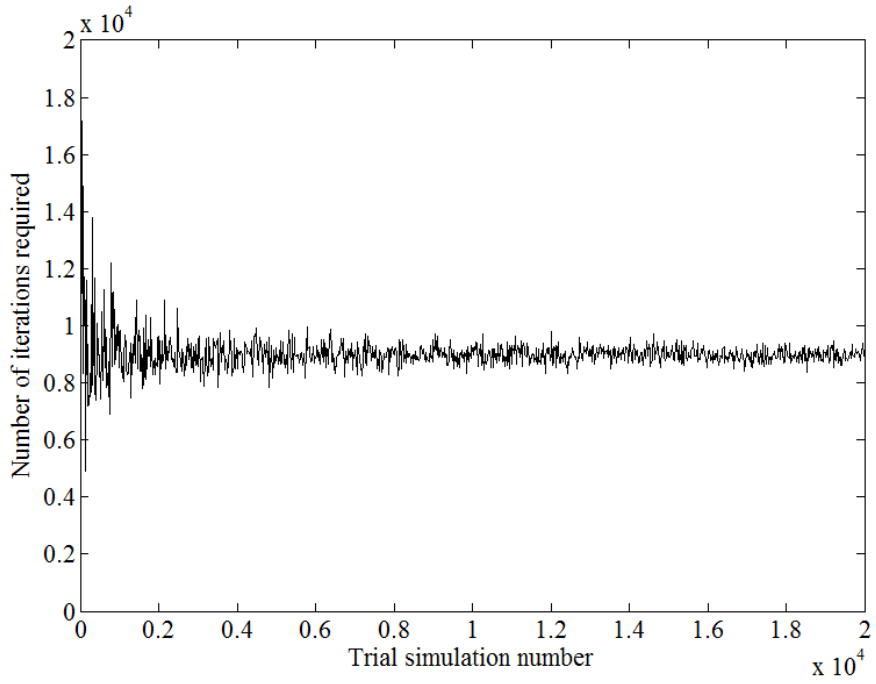

Figure 4.8 Number of iterations required vs. Trial simulation number

4.7 Case Study

The first three case studies with actual field data are used to demonstrate the importance of considering variations of rock parameters in unstable block identification. Results from deterministic analysis with mean value of each rock parameter are compared with results from probabilistic analysis. In addition, Chapter 3 shows that Fisher distribution fails for non-symmetrical data simulation; however, non-symmetrical joint sets often occur in jointed rocks and Fisher distribution is still commonly assumed for joint set simulation. Therefore, case study 4 is used to investigate the effect on unstable block size determination if Fisher distribution is misused for a non-symmetrical joint set simulation. Besides, two parametric studies are

conducted to investigate the effect of statistical parameters of distribution used for joint orientation (concentration κ, ovalness β and rotation matrix Γ) on block size determination.

4.7.1 Louvicourt Mine in Northeastern Canada

The same example for deterministic analysis demonstration (Section 4.4.2) is used again to conduct the probabilistic analysis. The origin rock joint data is not given in Grenon and Hadjigeorgiou (2003). Therefore, the first 3 steps which are shown in Figure 4.1 (joint classification, goodness of fit test and statistical parameter estimation) cannot be performed. However, statistical analysis result of each joint set parameter is provided (Table 4.2) and they are treated as accurate. Fisher distribution is used for joint orientation simulation. Lognormal and negative exponential distributions are used for trace length and spacing distribution accordingly. Four dominant joint sets are classified. There are 4 possible joint combinations by Equation (4.6). However, Equation (4.5) is not applicable without the original discontinuity orientation data, because discontinuity normal and its magnitude are required to perform this calculation. Therefore, only the first 3 joint sets are selected for the probabilistic analysis. Ten thousand times of iteration is used for the first trial unstable block simulation. The statistical analysis result of generated unstable block size shows that the block size distribution has a mean of 132.35 m^3 with a standard deviation 191.19m^3. If the confidence limit is set to be 95% and error

percentage to the mean value is set to be 5%, the required number of iteration can be calculated by Equation (4.13), which is 3207.

Block size analysis that considers trace length distribution and spacing distribution are performed. Size parameters (trace length and spacing) are used to scale the determined block proportionally (discussed in Section4.4.1). The block shape will not change after scale factor is applied. Therefore, the corresponding failure mode of determined unstable block is unchanged as well. Table 4.5 shows probability of occurrence of each failure mode. Due to scatter of joint orientation, fallout failure only consists about 20% of total simulation iterations. The dominant failure mode is sliding along intersection of plane 1 and plane 2 (about 50%). Sliding along intersection of plane 2 and plane 3 (about 17%) and sliding along plane 2 (about 8%) are the minor failure modes. In summary, failure modes other than that from deterministic analysis could occur if variation in joint orientations is considered. Failure mode predicted by deterministic analysis (with mean value of each rock parameter) may not be the dominant failure mode if scatter of joint orientation is taken into consideration.

On the other hand, trace length and spacing can have a significant effect on block size determination. Figure 4.9 shows Cumulative Distribution Functions (CDF) of total block volume distribution by considering size parameters. Span-limited block size varies from several to thousand cubic meters. Large blocks are predicted. This is because the discontinuity plane is assumed to be

persistent. As discussed in Chapter 2, only tunnel span can restrain the largest rock block

Table 4.5 Probability of each failure mode out of total simulation number (%)

Failure mode	Span limited size	Trace length limited size	Spacing limited size
Sliding along plane 1*	3.12	2.89	3.06
Sliding along plane 2	8.65	8.31	7.89
Sliding along plane 3	0.03	0.01	0.05
Sliding along intersection 12*	45.84	50.24	50.80
Sliding along intersection 13	0.23	0.46	0.34
Sliding along intersection 23	16.05	17.89	17.77
Fallout	20.51	20.20	20.00
Total	100	100	100

* Sliding along plane 1 means unstable block will fail by sliding along discontinuity plane from joint set 1.
Sliding along intersection 12 means unstable block will fail by sliding along the intersection of discontinuity planes from joint set 1 and joint set 2.

that could form during excavation. However, large block is seldom fully formed and they are usually intersected by other discontinuities. Therefore, if trace length and spacing are considered, the largest possible rock block size will be limited to a smaller volume. Figure 4.9 shows that after scaling factors are applied, the block size distribution will shift to a smaller range. This is because that if discontinuity size (disc diameter which is determined by trace length) is small, the largest block volume will be restrained by trace length. On the other hand, if joint discontinuity planes are close, the largest individual

rock block can only be formed within spacing. Therefore, rock block size will be smaller if size parameters are taken into consideration. Trace length limited block size is smaller than spacing limited block size; however, this is not necessary for all cases. It depends on block shape and size parameter applied. Apex height and excavation face area will also vary due to change in block size. Figure 4.10 and Figure 4.11 show that span limited block parameters are always larger than that of trace length limited block and spacing limited block.

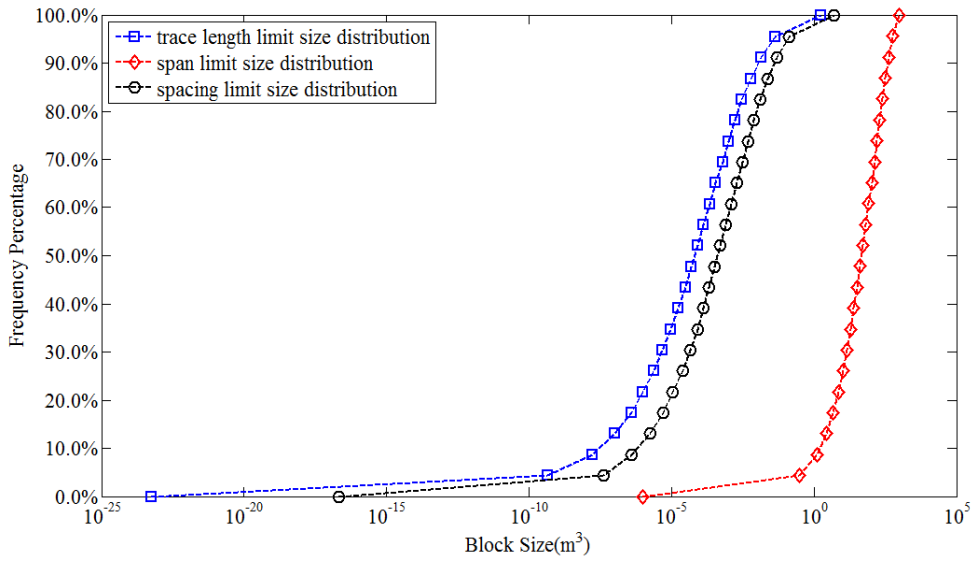

Figure 4.9 CDF of block size considering different size parameters

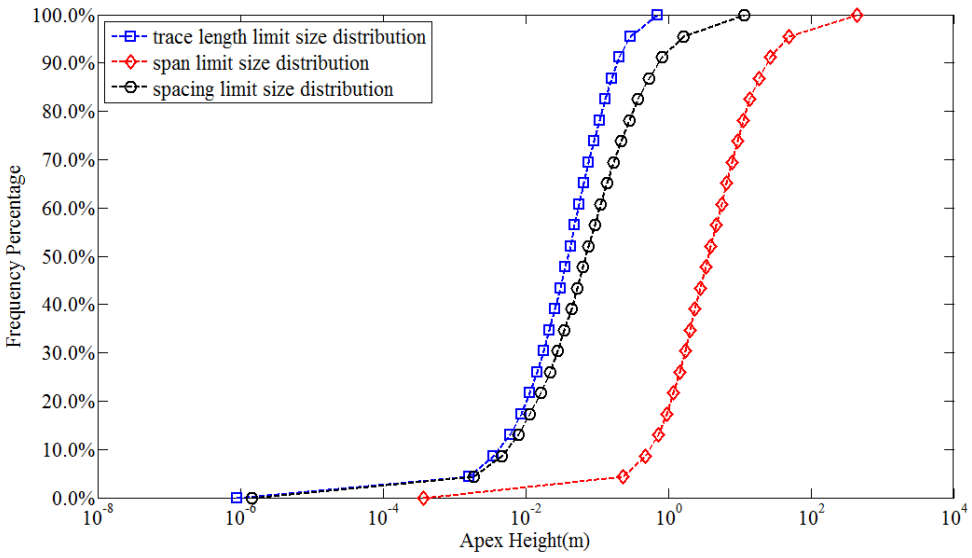

Figure 4.10 CDF of apex height considering different size parameters

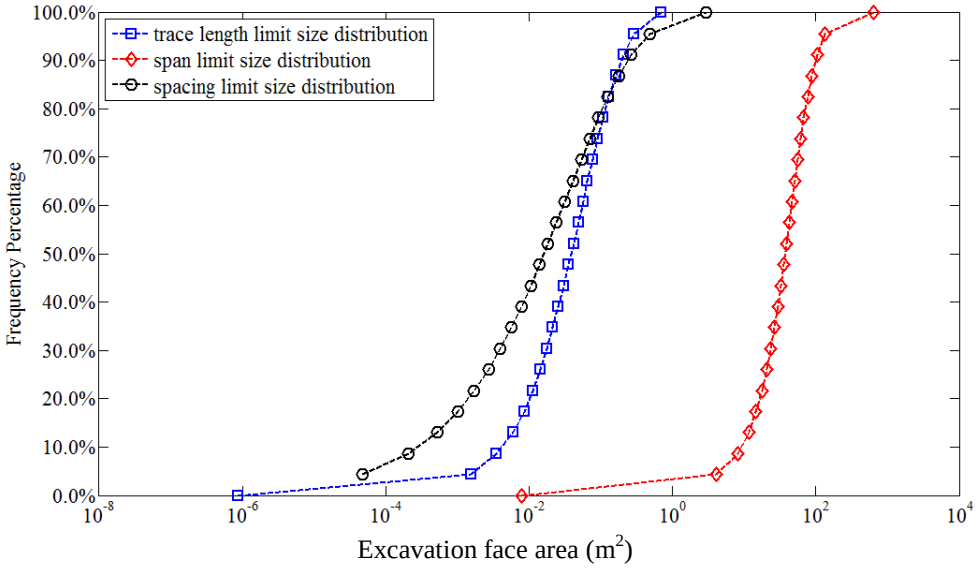

Figure 4.11 CDF of excavation face area considering different size parameters

a)

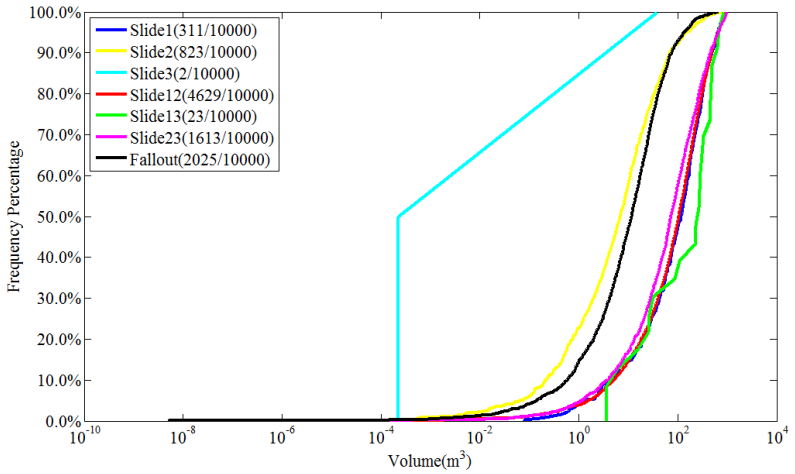

b)

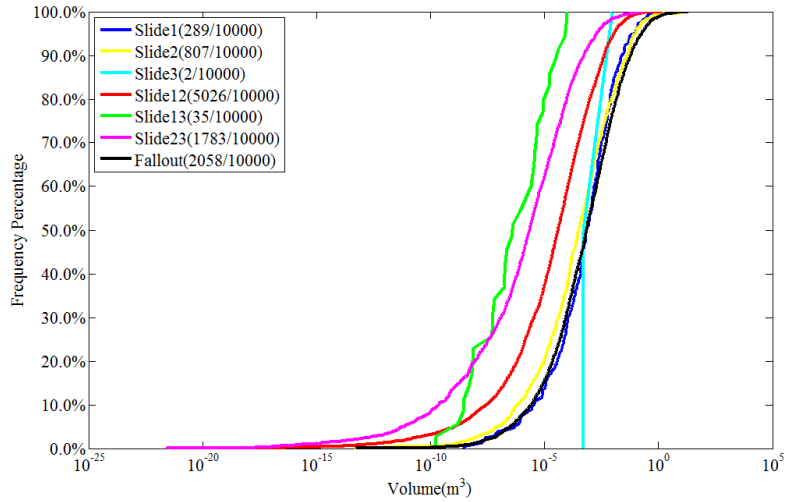

c)

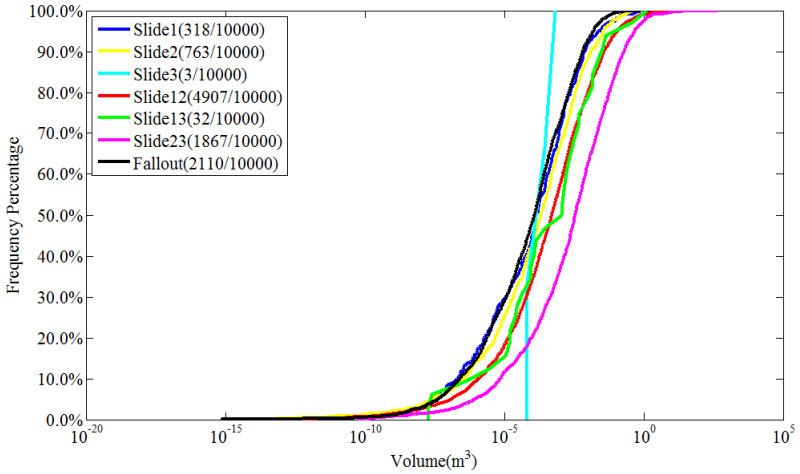

Figure 4.12 Volume distribution CDF according to different failure mode (a) span limited analysis result (b) trace length limited analysis result (c) spacing limited analysis result

Figure 4.12 shows the probability of different failure modes in rock block analysis considering size parameters. It is easy to find that relative position of CDFs of different failure modes change if size parameter is considered. For example, size distribution of slide along intersection of plane 2 and 3 in Figure 4.12(a), has a larger mean value compared with that of fallout failure. However, if trace length is taken into consideration, although the probability of different failure modes is unchanged, the mean value of size distribution of fallout failure is larger than that of sliding along planes 2 and 3 (Figure 4.12(b)). This is because scaling factor is determined by trace length with depends largely on the triangle formed on tetrahedral block face. For example, Figure 4.13 shows two possible unstable blocks with the same block size V, one fallout failure and one sliding failure. In order to form the blocks which are shown in Figure 4.13, a minimum discontinuity disc diameter D_{1i} is required for block1 face *i* and D_{2i} for block 2 face *I* ($D_{2i}>D_{1i}$). If the same trace length D is found on plane *i* for both blocks, scaling factor determined for sliding along intersection will be smaller than that of fallout block ($\frac{D}{D_{1i}} > \frac{D}{D_{2i}}$). Therefore, slide along intersection block after scaling, will have a smaller size than fallout block. The same principles apply to spacing limited block size. If the shape of a potential rock block is elongated, the spacing value of the base plane will have a huge effect on scaling factor determination.

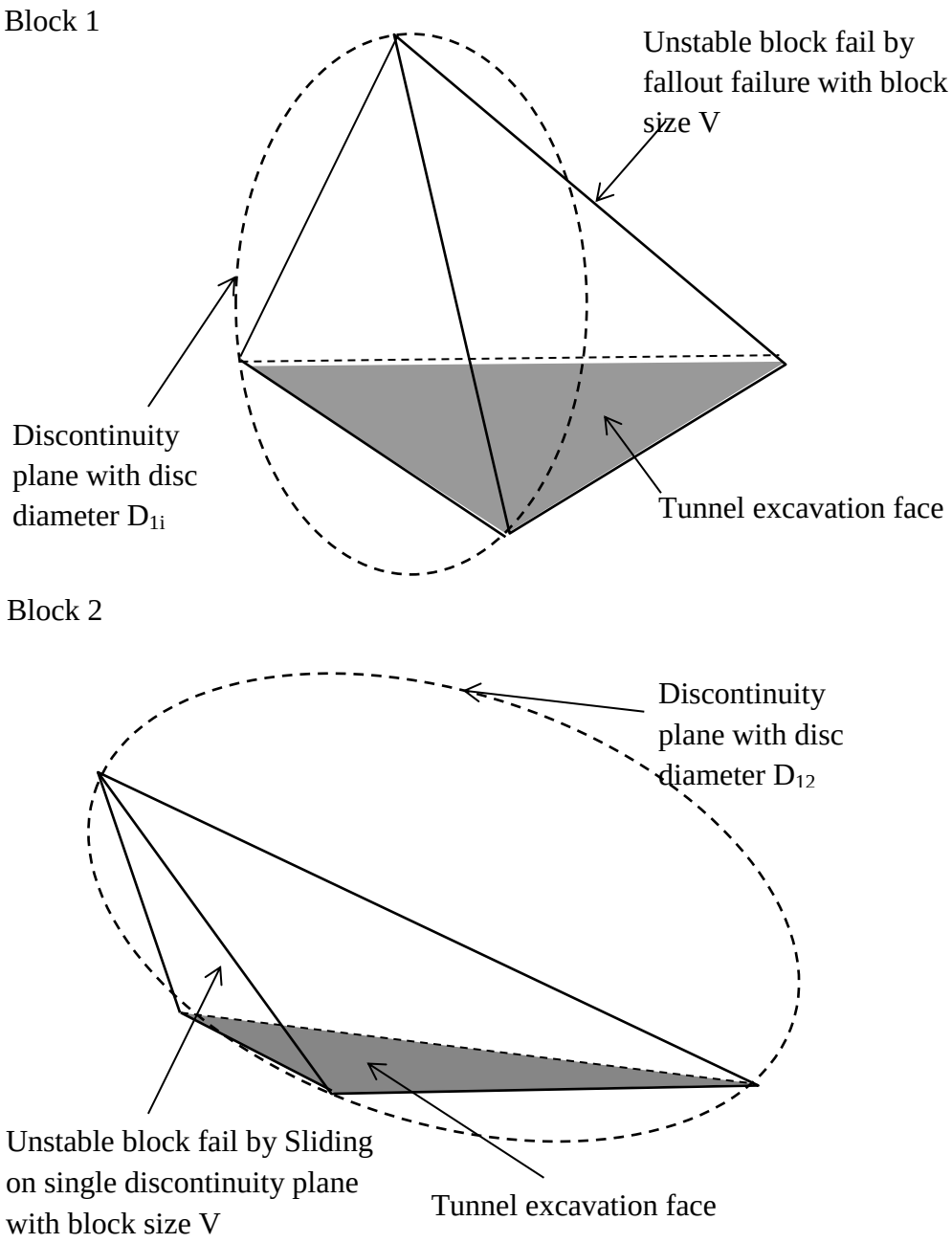

Figure 4.13 Same volume block in different failure modes

4.7.2 Singapore Jurong Formation

Jurong formation covers the west of Singapore with a variety of sharply folded sedimentary rock including sandstone, shale, mudstone and limestone. It was deposited during the late Triassic to early or middle Jurassic. The formation has been severely folded and faulted in the past as a result of tectonic movement (Rahardjo et al., 2004). The feasibility of building underground cavern in this Jurong formation is investigated. Vertical borehole was drilled for site investigation. Borehole was drilled to a depth of 205m from ground surface. The first 48m are soil and fractured rock and rock coring was conducted below this depth. Fracture plane orientation, type, roughness, infilling, alteration and weathering condition were investigated. A total of 952 discontinuity data are recorded through borehole coring. DIPS6 from Rocscience is employed for stereonet plotting (Figure 4.14). Three dominant joint sets can be identified by visual classification (Joint sets 1, 2 and 3 are shown on Figure 4.14). Since tetrahedral blocks could be formed by 3 discontinuities from 3 different joint sets; therefore, only one joint set combination is available. Goodness of fit test is used to test each joint set whether they are from a Fisher distribution or Kent distribution. The result is shown in Table 4.6.

Table 4.6 Goodness of fit test result and statistical parameter estimation

Set	κ	β	K_m	K_O	Γ	Goodness of fit test
1	48.69	16.63	155.1	5.99	$\begin{bmatrix} 0.8286 & -0.1798 & 0.5301 \\ -0.5579 & -0.1877 & 0.8084 \\ -0.0459 & -0.9656 & -0.2559 \end{bmatrix}$	Kent
2	35.76	9.90	159.2	5.99	$\begin{bmatrix} 0.0397 & 0.8142 & 0.5792 \\ -0.9337 & 0.2367 & -0.2688 \\ -0.3560 & -0.5301 & 0.7696 \end{bmatrix}$	Kent
3	37.79	6.42	28.0	5.99	$\begin{bmatrix} 0.0989 & 0.7637 & -0.6380 \\ -0.9773 & -0.0463 & -0.2069 \\ -0.1875 & 0.6440 & 0.7414 \end{bmatrix}$	Kent

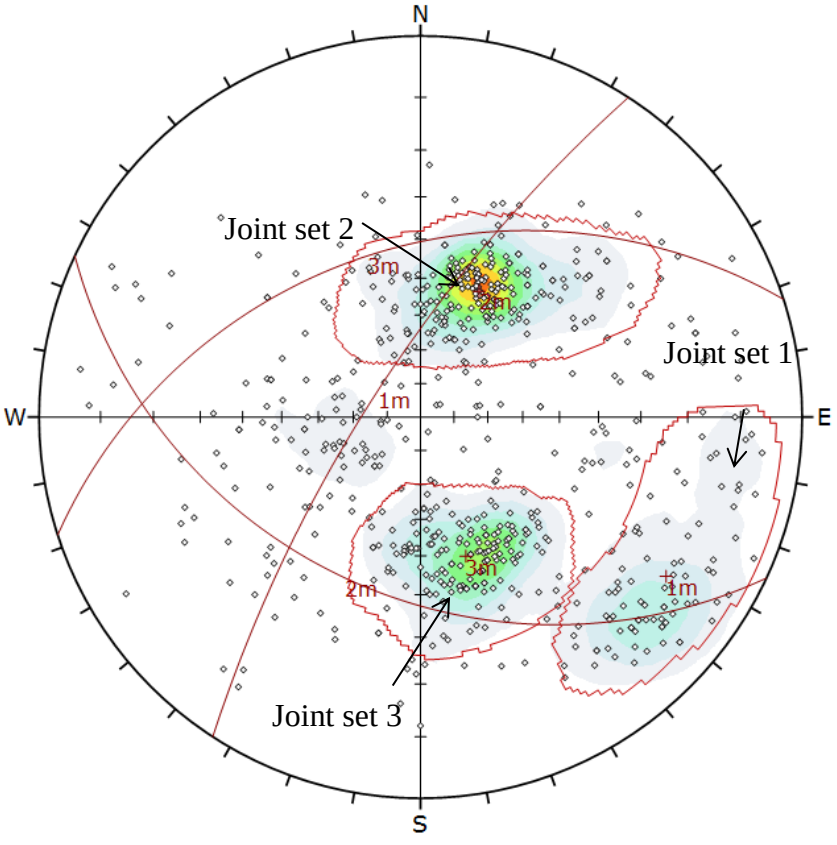

Figure 4.14 Contour plotting and joint set identification (pole plot)

Trace length distribution is not available in borehole sampling and only one set of spacing data can be collected through borehole coring which is insufficient to determine the PDF of spacing distribution. As discussed in Sections 4.2.3 and 4.2.4, trace length distribution and spacing distribution need to be reasonably assumed. A lognormal distribution with mean value 2 m and standard deviation 2m is used for trace length distribution simulation. A negative exponential distribution with mean 1 m is assumed for spacing distribution simulation. A 10 m excavation span is used for span limited block analysis. The deterministic analysis result is shown in Table 4.7.

Table 4.7 Deterministic analysis result

	Block size (m^3)	Apex height (m)	Excavation face area (m^2)
Span limited	21.29	2.68	34.83
Trace length limited	0.0337	0.313	0.473
Spacing limited	0.0825	0.422	0.860

Probabilistic analysis was conducted based on estimated distributions. A total of 10,000 iterations are conducted. The overall block size has a mean value of 25.12 m^3 and a standard deviation of 35.51 m^3. Based on Equation 4.13, the required number of iteration should be 7.5×10^4 to achieve 95% of confidence within 5% error. Therefore, the number of iteration increases to 7.5×10^4 and probabilistic analysis is repeated.

Table 4.8 Probability of each failure mode out of total simulation number (%)

Failure mode	Span limited size	Trace length limited size	Spacing limited size
Slide along plane 1*	88.29	88.03	88.27
Slide along plane 2	0.01	0.02	0.01
Slide along plane 3	0.01	0.03	0.02
Slide along intersection 12*	2.53	2.63	2.58
Slide along intersection 13	0.51	0.46	0.57
Slide along intersection 23	0.01	0.02	0.02
Fallout	9.63	8.82	8.54

* Sliding along plane 1 means unstable block will fail by sliding along discontinuity plane from joint set 1.
Sliding along intersection 12 means unstable block will fail by sliding along the intersection of discontinuity planes from joint set 1 and joint set 2.

Table 4.8 shows that deterministic analysis predicts the dominant failure mode of probabilistic analysis (88%). However, the previous Louvicourt mine example shows that deterministic analysis fails to predict the dominant failure mode in probabilistic analysis. This is because the relative position and concentration of joint sets are different for both case studies. It is difficult to conclude in what conditions failure mode from deterministic analysis will match the dominant failure mode from probabilistic analysis. However, in general, if the concentration parameter of joint set is low and the joint set position is close to stereonet circumference, the deterministic analysis is unlikely to predict the dominant failure mode of probabilistic analysis. Figures 4.15 to 4.18 show the probabilistic analysis results. It is evident that span limited block analysis always predict a larger value for rock bolt design

parameters. If size parameters are taken into consideration, rock blot design parameters distribution will be restrained to a small range.

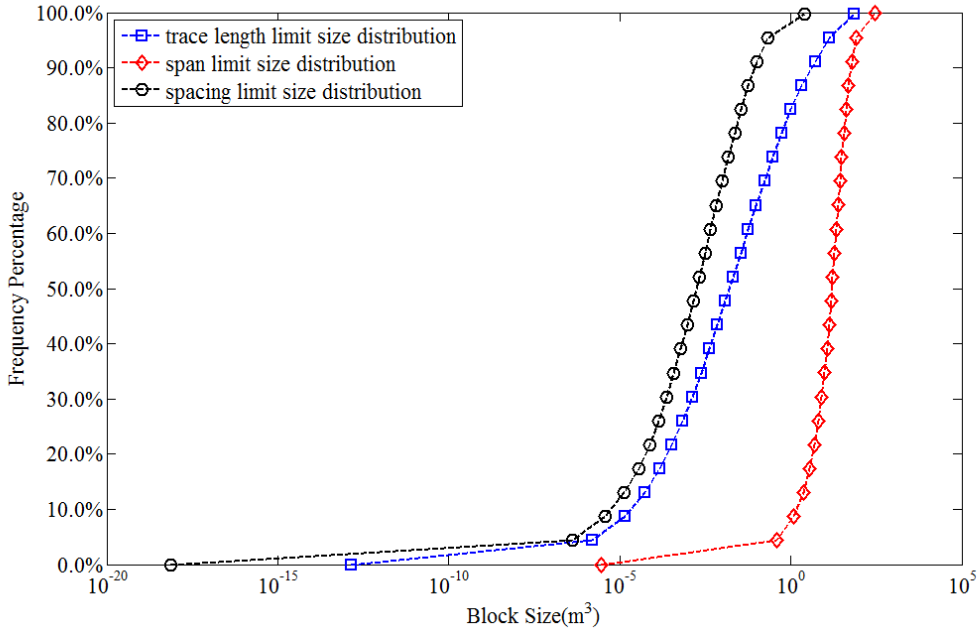

Figure 4.15 CDF of block size considering different size parameters

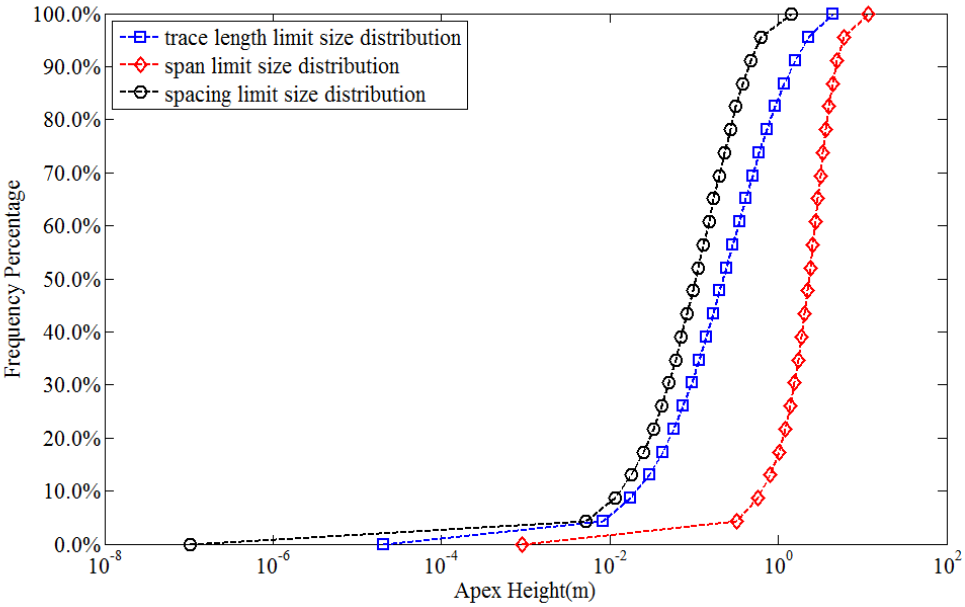

Figure 4.16 CDF of apex height considering different size parameters

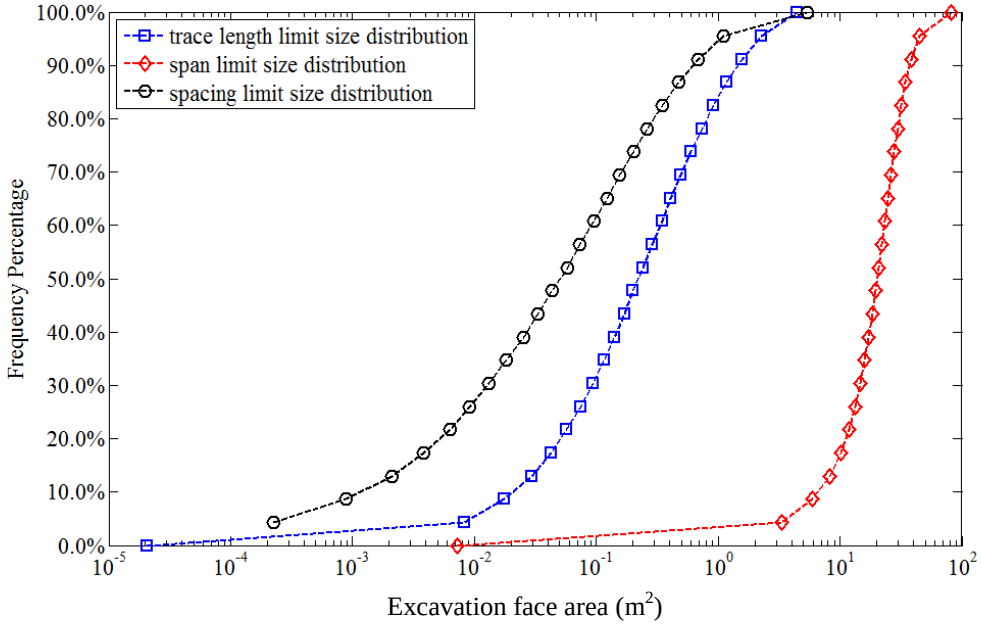

Figure 4.17 CDF of excavation face area considering different size parameters

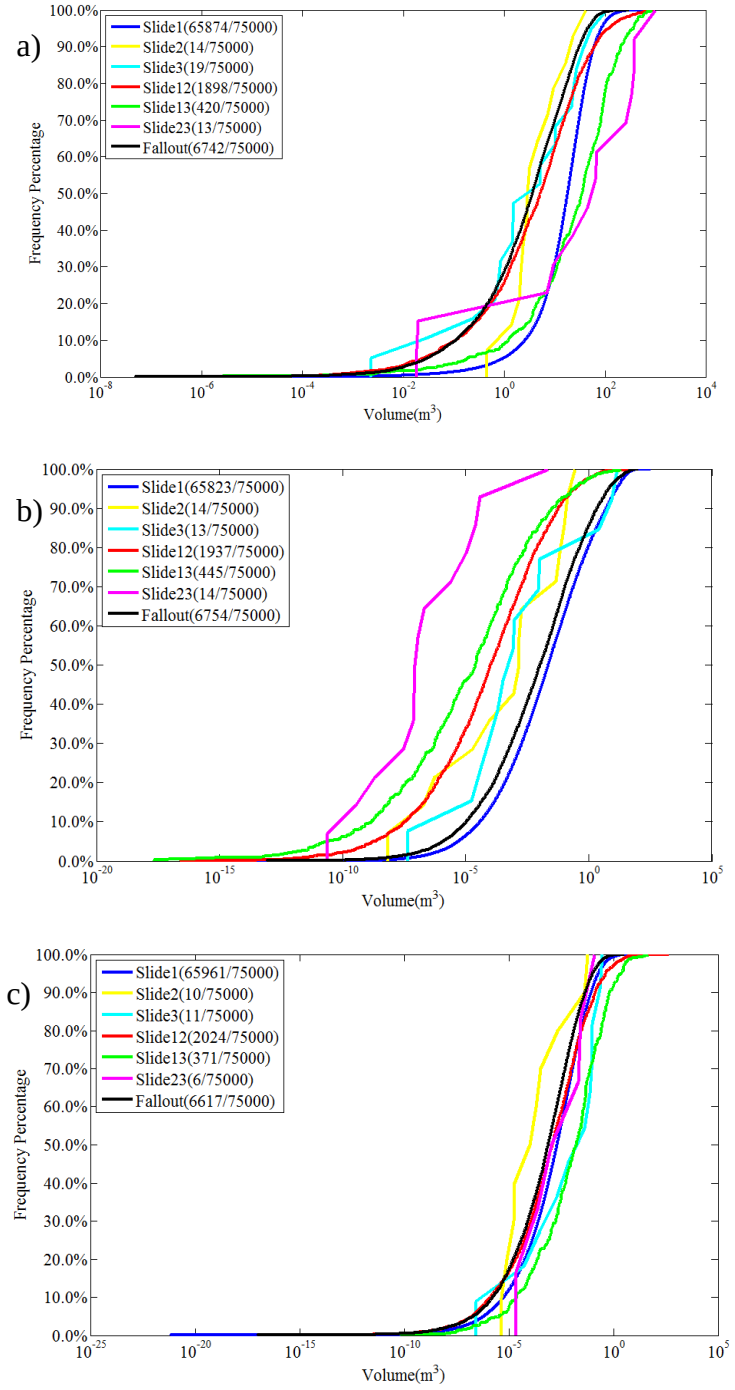

Figure 4.18 Volume distribution CDF according to different failure mode (a) span limited analysis result (b) trace length limited analysis result (c) spacing limited analysis result

4.7.3 Singapore Kent Ridge data

Feasibility study of constructing underground facilities in Singapore Kent Ridge area is conducted in 1980s. The same Jurong formation was found in this area. Jointed limestone and siltstone are the major rock types below 40m from ground surface. Vertical borehole was used for site investigation. Borehole was drilled to a depth of 150m. Altogether 162 discontinuity planes were observed and the 4 dominant joint sets classified by visual identification are shown in Figure 4.19. Goodness of fit test and statistical distribution parameter estimation result are shown in Table 4.9. Set 2 and set 3 are originated from Fisher distribution. As discussed in Chapter 3, Kent distribution is the general form of Fisher distribution. It involves more parameters to describe the shape and location of directional data. Therefore, Kent distribution can still be used instead of Fisher distribution for joint set simulation. As 3 discontinuity planes from 3 different joint sets combining with excavation face can form tetrahedral block; therefore, 4 possible joint set combinations are determined by Equation 4.6. The deterministic results of all combinations are shown in Table 4.10. The probability of each combination can be determined by Equation 4.5. The analysis result is shown in the last column of Table 4.11. Since size parameters do not influence block shape determination, the probability of each failure mode in a certain combination could be derived by Equation 4.7.

Table 4.9 Goodness of fit test result and statistical parameter estimation

Joint set	κ	β	K_m	K_O	Γ	Goodness of fit test
1	119.04	44.77	237.0	5.99	$\begin{bmatrix} 0.6702 & 0.0894 & 0.7368 \\ -0.7417 & 0.1158 & 0.6607 \\ -0.0263 & -0.9892 & 0.1439 \end{bmatrix}$	Kent
2	181.66	31.00	1.5	5.99	$\begin{bmatrix} -0.0031 & 0.1498 & -0.9887 \\ 0.9723 & -0.2307 & -0.0381 \\ -0.2338 & -0.9614 & -0.1450 \end{bmatrix}$	Fisher
3	89.17	10.03	0.7	5.99	$\begin{bmatrix} 0.5854 & 0.3268 & 0.7420 \\ 0.4500 & 0.6303 & -0.6326 \\ -0.6744 & 0.7042 & 0.2219 \end{bmatrix}$	Fisher
4	229.36	82.17	26.4	5.99	$\begin{bmatrix} -0.9643 & -0.0624 & 0.2572 \\ 0.2387 & 0.2149 & 0.9470 \\ -0.1144 & 0.9746 & -0.1923 \end{bmatrix}$	Kent

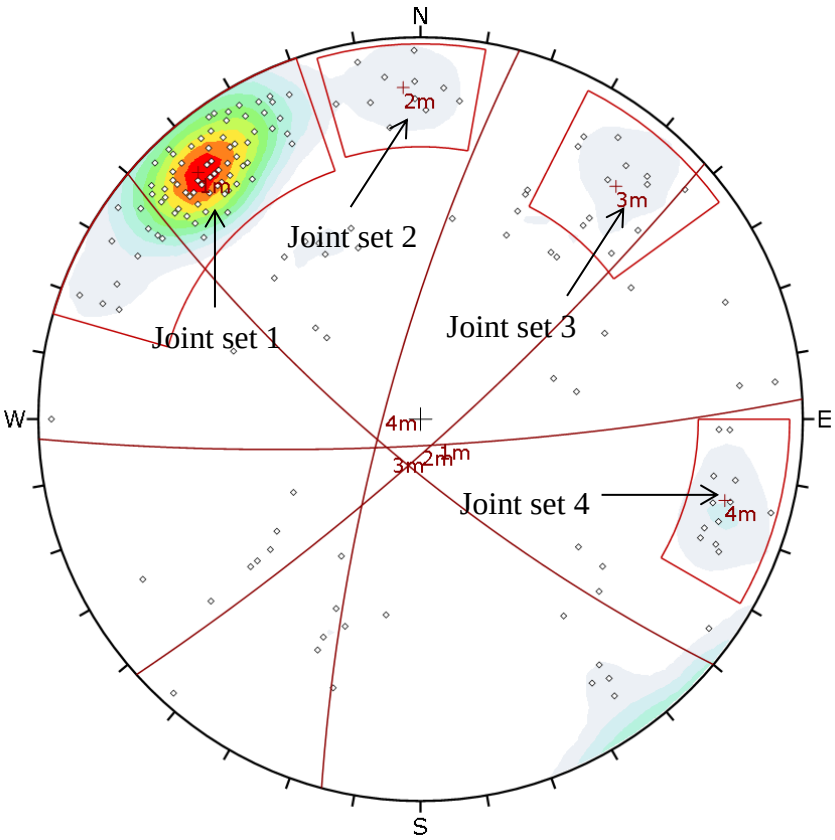

Figure 4.19 Contour plotting and joint set identification

Table 4.10 Deterministic analysis result

Combination	Failure mode	Size parameter	Volume (m^3)	Apex height (m)	Excavation face area (m^2)
123*	Slide along plane 2	Span	319.67	43.87	21.86
		Trace length	1×10^{-5}	0.1386	2.18×10^{-4}
		Spacing	1.1063	6.6368	0.50
124	Slide along plane 2	Span	276.51	25.29	32.80
		Trace length	3.46×10^{-4}	0.2727	0.0038
		Spacing	0.4526	2.9806	0.4556
134	Slide along plane 3	Span	641.03	35.80	53.71
		Trace length	3.39×10^{-8}	0.2896	0.0035
		Spacing	0.2932	2.7586	0.3188
234	Slide along intersection of plane 2 and 3	Span	1605.5	134.56	35.79
		Trace length	8.75×10^{-8}	0.0510	5.14×10^{-6}
		Spacing	1.9508	14.36	0.4076

* Combination 123 means the tetrahedral block which is formed by 3 discontinuity planes comes from joint set 1, 2 and 3 accordingly.

Table 4.11 Probability (%) of rock blocks failure under different joint combinations

Combination	1^{st} &2^{nd}	1^{st} &3^{rd}	2^{nd}&3^{rd}	1^{st}	2^{nd}	3^{rd}	Fallout	Total
123*	6.54	4.47	2.29	1.46	18.14	0.71	0.87	35.09
124	8.08	1.52	0.01	0.03	14.56	0.08	0.68	25.23
134	2.95	2.1	3.22	0.20	24.78	0.08	0.78	35.12
234	0.81	1.59	0.08	0.01	1.75	0.02	0.11	4.56
Total		33.66			61.82		2.44	100

* Combination 123 means the tetrahedral block which is formed by 3 discontinuity planes comes from joint set 1, 2 and 3 accordingly.

Table 4.11 shows that for all different joint set combinations, all the failure modes could happen with different probabilities. Joint set combinations, 123, 124 and 134 will be the major combinations. Block bounded by discontinuity 1, 2 and 3 has a probability of 18.14% of sliding failure along discontinuity plane 2, which is coincident with the result of the deterministic analysis. The same circumstances occurred in combination 124 and combination 134. Major failure mode of each combination is the same with deterministic result. However, for discontinuity combination 234, deterministic analysis shows the failure mode should be sliding along intersection of plane 2 and plane 3. On the other hand, probabilistic analysis shows sliding along discontinuity plane 3 and sliding along intersection of plane 2 and 4 have a major proportion of 1.75% and 1.59% accordingly. However, combination 234 consists only 4.56%. Therefore, in this case, deterministic analysis still can predict the dominant failure mode in probabilistic analysis for this case.

4.7.4 Hypothetical Case

As discussed in Chapter 3, Fisher distribution is not capable to simulate non-symmetrical data. If a non-symmetrical joint set data is modelled by Fisher distribution, errors might involve (Whitaker and Enelder, 2005). Therefore, this case study will study the effect of using different joint orientation distribution models on block size determination. Joint orientation data will be modelled by pure Fisher distribution and pure Kent distribution and then parametric study of statistical distribution parameter will be conducted.

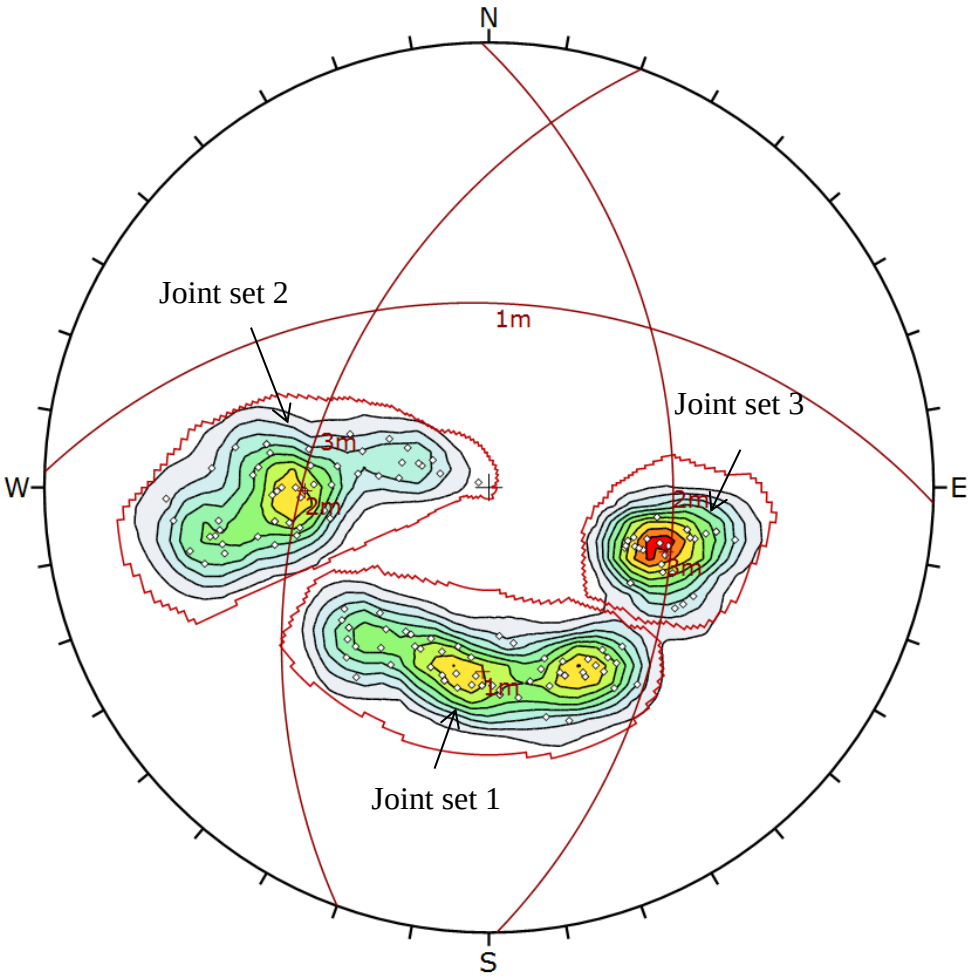

Figure 4.20 Contour plotting and joint set identification

Based on given rock joint orientation data, the joint set classification on contour plot is shown in Figure 4.20. Three dominant joint sets can be identified by visual classification. Table 4.12 shows the goodness of fit test results and statistical parameters estimations. Joint set 1 and joint set 2 follow Kent distribution whereas joint set 3 follows Fisher distribution, a special case of Kent distribution.

Table 4.12 Goodness of fit test result and statistical parameter estimation

Joint set	κ	β	Mean orientation	Γ	Goodness of fit test
1	71.91	31.24	44.61/1.66	$\begin{bmatrix} -0.1248 & -0.7099 & 0.6932 \\ -0.9889 & 0.1457 & -0.0288 \\ -0.0806 & -0.6891 & -0.7202 \end{bmatrix}$	Kent
2	46.77	17.30	45.44/89.27	$\begin{bmatrix} -0.2770 & -0.9608 & -0.0085 \\ 0.6821 & -0.2028 & -0.7025 \\ -0.6768 & 0.1888 & 0.7116 \end{bmatrix}$	Kent
3	106.26	14.73	45.76/289.70	$\begin{bmatrix} 0.2037 & -0.9491 & 0.2403 \\ -0.7477 & 0.0077 & 0.6640 \\ -0.6321 & -0.3149 & -0.7081 \end{bmatrix}$	Fisher

Since trace length distribution and spacing distribution are not available in this case study, the excavation span is used to determine the largest unstable block size. Deterministic analysis shows that the unstable block volume is 277.39m^3 and the corresponding failure mode is sliding along discontinuity plane 1 which is a discontinuity from joint set 1. The probabilistic analysis results with pure Fisher distribution and Kent distribution are shown in Tables 4.13 and 4.14, respectively. Both block size analysis predict the same dominant failure mode which is sliding along plane 1. While probabilistic block analysis with pure Fisher distribution shows a dominant failure mode is 70.42%; 82.36% is shown for the simulation with pure Kent distribution. Besides, the minor failure modes fallout failure and sliding along intersection of planes 1 and 2 drop from 6.18% to 1.41% and 17.12 to 12.60% accordingly. Model with Fisher distribution also predicts sliding along plane 3 (0.2%) and sliding along intersection of planes 1 and 3 (2.43%); however, the model with Kent

distribution shows that these two failure modes have no chance to occur. The span limited block size distributions derived from two simulations are shown in Figure 4.21. In this case, it is evident that the model with Kent distribution generally predicts a larger block size than that with Fisher distribution. If rock bolts with maximum capacity 5400kN ($27kN/m^3 \times 200\ m^3$) and with sufficient length and rock bolt spacing are assumed to be used to stabilize the unstable block, the probability of failure (PoF) would reduce to about 10% (Figure 4.21). This is due to the assumption of an inappropriate distribution (Fisher distribution) in joint orientation simulation. As such, distributions used do have an impact on block size determination and rock bolt design. It is hence be worthwhile to conduct a parametric study for statistical parameters used in joint orientation simulation.

Table 4.13 Probabilistic block analysis with pure Fisher distribution

Failure mode	Mean	Median	Stdev	Percentage (%)
Sliding along plane1	170.36	150.54	135.15	70.42
Sliding along plane2	0.00	0.00	0.00	0.00
Sliding along plane3	4.17	4.17	2.59	0.20
Sliding along plane12	420.26	406.50	205.93	3.65
Sliding along plane13	235.54	211.12	206.87	6.18
Sliding along plane23	299.11	231.96	254.92	2.43
Fallout	37.08	22.88	67.27	17.12

*Sliding along plane 1 means unstable block will fail by sliding along discontinuity plane from joint set 1.
Sliding along intersection 12 means unstable block will fail by sliding along the intersection of discontinuity planes from joint set 1 and joint set 2.

Table 4.14 Probabilistic block analysis with pure Kent distribution

Failure mode	Mean	Median	Stdev	Percentage (%)
Sliding along plane1	198.60	169.36	148.09	82.36
Sliding along plane2	0.00	0.00	0.00	0.00
Sliding along plane3	0.00	0.00	0.00	0.00
Sliding along plane12	482.16	454.68	208.23	3.63
Sliding along plane13	184.11	107.39	209.83	1.41
Sliding along plane23	0.00	0.00	0.00	0.00
Fallout	51.35	13.74	117.51	12.60

*Sliding along plane 1 means unstable block will fail by sliding along discontinuity plane from joint set 1.

Sliding along intersection 12 means unstable block will fail by sliding along the intersection of discontinuity planes from joint set 1 and joint set 2.

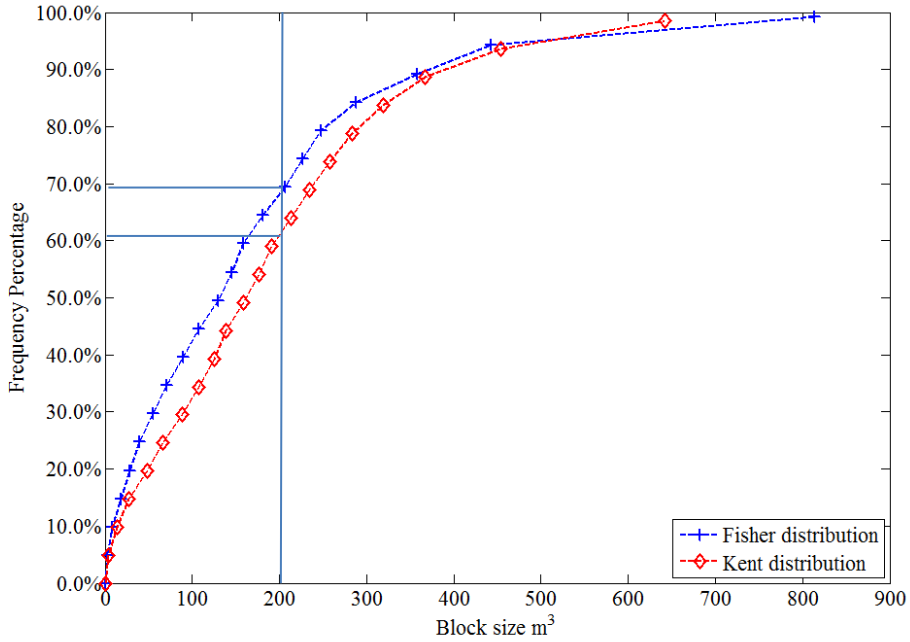

Figure 4.21 Comparison of unstable block size (span limited) generated by simulation with pure Fisher distribution and simulation with pure Kent distribution

4.7.4 (a) Parametric Study of Statistical Distribution Parameters on one Joint Set

Fisher distribution only has two statistical parameters: mean orientation and concentration factor, whereas more parameters are needed to describe Kent distribution. Besides mean and concentration, Kent distribution needs to consider ovalness of distribution contour and rotation matrix which comprise the major axis and minor axis of an elliptical distributed contour. In order to perform a case study on the effect of each statistical parameters, only one joint set (joint set 1) is assumed as distribution, whereas the other two joint sets (joint set 2 and 3) are assumed to possess extremely high concentration which can be assumed as fixed points. Therefore, 3 statistical parameters (such as concentration κ, ovalness β and rotation matrix Γ) are investigated in this parametric study. Γ_i means the rotation matrix which can rotate the origin data points anti-clockwise i° around its corresponding mean orientation. The results are shown in Figures 4.22 to 4.24.

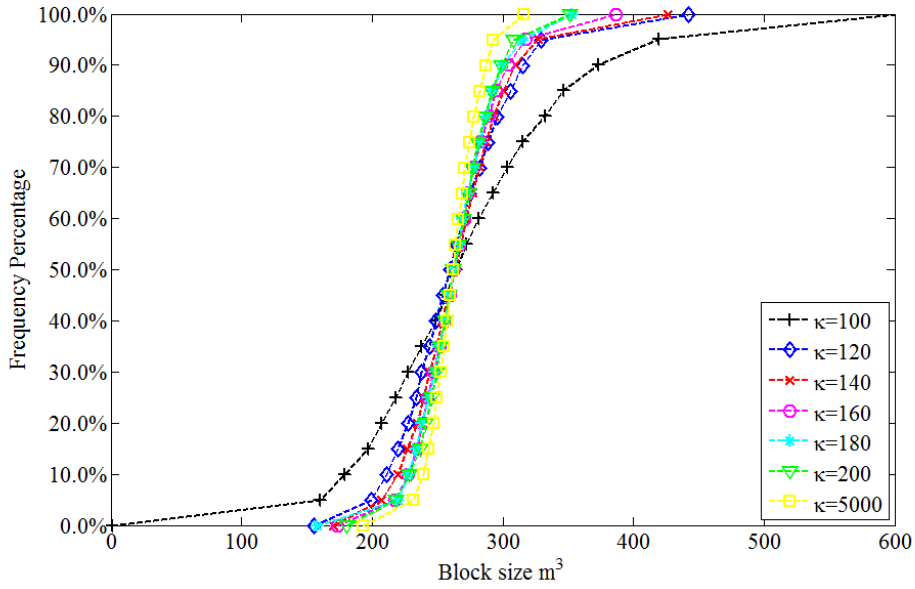

Figure 4.22 Block size distributions β = 50 and with different κ values

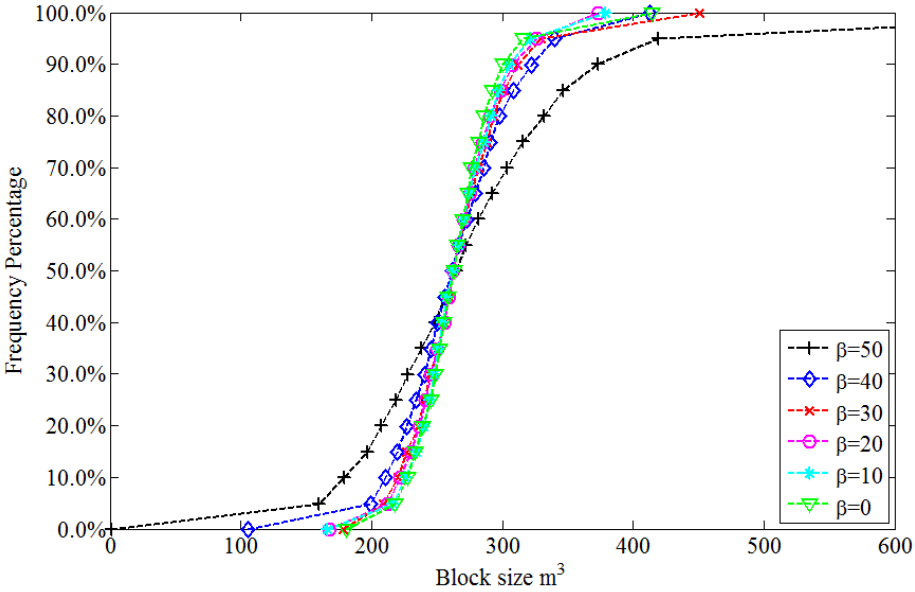

Figure 4.23 Block size distribution κ = 100 and with different β values

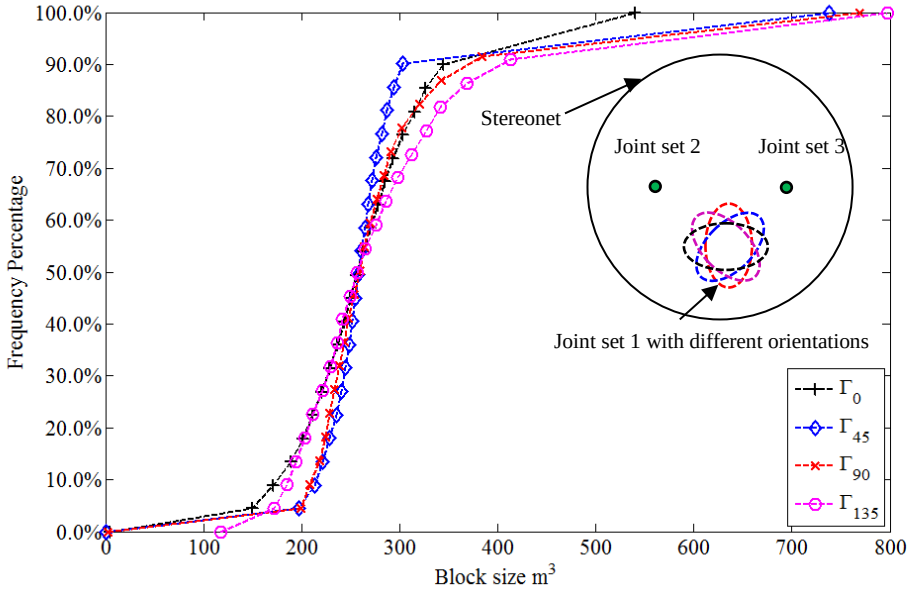

Figure 4.24 Block size distribution κ = 100 β =50 with different Γ

Figure 4.22 shows the effect of concentration parameter κ on block size determination with the value of the other two parameters (β= 50 and Γ_0) unchanged. As discussed in Chapter 3, κ value is never less than 2β in unimodal Kent distribution. Therefore, κ is increased to beyond a value of 100. When κ value increases from 100 to 200, the joint set data are more concentrated around its mean value. Unstable block size distributes around the deterministic analysis result (277.39m^3). If κ is very large (such as κ=5000), the block size will distribute very closely to its deterministic answer. This result makes sense that high concentrated parameters will produce a less scatter result. Besides, it is clearly to see that when κ increases from 100 to 120, the scatter of block size distribution reduces significantly. After that,

although the block size distribution becomes more concentrated, the trend is not significant.

Figure 4.23 shows the effect of ovalness factor β on block size determination with the other two parameters (κ=100 and Γ_0) unchanged. As β value decreases from 50 to 0, which implies that the joint set distribution contour shape changes from ellipse to circle, the block size is distributed more towards its deterministic result. When β reduces from 50 to 40, the dispersion of block size distribution reduces significantly. However, when β reduces further from 40 to 0, the increase in block size distribution concentration is not obvious.

Figure 4.24 shows the effect of rotation matrix Γ on block size determination with the fixed concentration (κ=100) and ovalness (β=50) values. Four rotation angles ($0°, 45°, 90°, 135°$) are used to rotate origin joint set 1 anti-clockwise around its mean orientation. The results show that $45°$ anti-clockwise rotation of joint set 1 is the most favorable joint set orientation, which produces the most concentrated rock block size distribution. A rotation of 135° will result in the most dispersed block size distribution.

In summary, statistical parameters (κ, β, Γ) play important roles in joint orientation simulation of this case study. Increase in joint orientation concentration (κ increases) can result in a less distributed block size distribution. Decrease in ovalness β value will lead to a more concentrated block size distribution. When β=0, Kent distribution will be simplified to Fisher distribution. Therefore, if a non-symmetrical joint orientation is modelled by a Fisher distribution (β value is assumed as zero), block size

would be more concentrated than that modelled with Kent distribution. Thus, uncertainty in block size determination will be reduced. If reinforcement design is proposed based on this result, high risk could be involved. Besides, rotation matrix also has an impact on block size distribution. If a joint set has an unfavorable orientation, the block size can distribute further in a larger range. Therefore, the scatter of joint orientation should be appropriately modelled in rock block analysis.

Owing to time limit of this study, parametric study of varying two joint sets and three joint set statistical parameters is not included. Nevertheless, the parametric study of these single joint set statistical parameters has demonstrated the importance of joint orientation simulation. Further studies are clearly needed on this subject matter.

4.7.4 (b) Parametric Study of Concentration Parameter κ on three Joint Sets

The parametric study in Section 4.7.4 (a) shows the importance of joint orientation simulation by varying statistical parameters of single joint set. This section will focus on parametric study of the concentration parameter κ and study the effect on unstable block size determination when more than 1 joint set concentration change while the other two statistical parameters (ovalness β and rotation matrix Γ) remain constant. Eight possible combinations can be determined by varying determined concentration parameter κ (shown in Table

4.12) with very high concentration (κ=5000). They are listed in Table 4.15 and corresponding analysis results are shown in Appendix Figures 1 to 8.

Table 4.15 Combinations of varying concentration parameter κ

Case number	κ_1	κ_2	κ_3	Results
1	71.91	46.77	106.26	Appendix 1 Figure 1
2	5000	5000	106.26	Appendix 1 Figure 2
3	5000	46.77	5000	Appendix 1 Figure 3
4	71.91	5000	5000	Appendix 1 Figure 4
5	71.91	46.77	5000	Appendix 1 Figure 5
6	5000	46.77	106.26	Appendix 1 Figure 6
7	71.91	5000	106.26	Appendix 1 Figure 7
8	5000	5000	5000	Appendix 1 Figure 8

*κ_1 is the concentration parameter of joint set 1; κ_2 is the concentration parameter of joint set 2 and κ_3 is the concentration parameter of joint set 3

Figure 4.25 compares block size distribution with different κ values for each joint set. Case 8 assumes joint concentration parameter (κ) of 3 joint sets is 5000 which means the joint set is very concentrated with small variation (simulation result is shown in Appendix). Probabilistic analysis shows that block size distributes in a narrow range around its deterministic analysis result which is 277.39 m^3. However, block size still can differ from 180 m^3 to 320 m^3. The normal concentration parameter κ in nature rock is only 5 to 300 (Leung and Quek, 1995). Therefore, larger variation in block size is expected

if determined concentration parameters (shown in Table. 4.12) are used for rock block

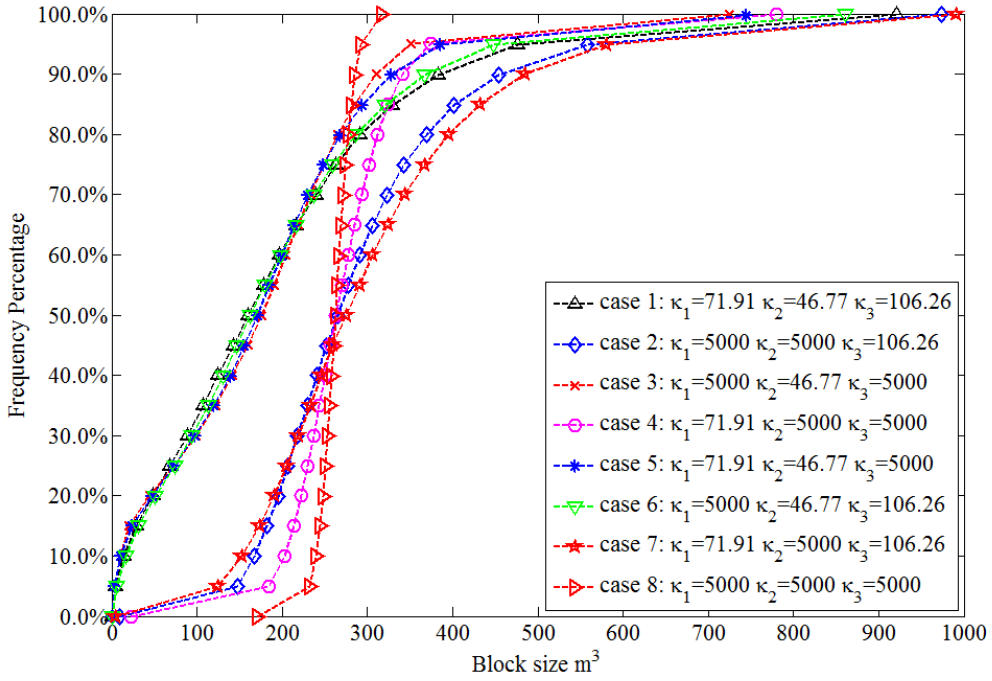

* κ_1 is the concentration parameter of joint set 1; κ_2 is the concentration parameter of joint set 2 and κ_3 is the concentration parameter of joint set 3

Figure 4.25 Block size distribution by vary concentration parameter κ of each joint set

determination. Block size of case 2, 4, 7 also distribute around the deterministic analysis result but in a larger range. Applying determined κ_3 in block analysis (Case 2) leads to a larger variation in block size than applying determined κ_1 in block analysis (Case 4). In the meanwhile, applying both κ_2 and κ_3 in block analysis (Case 7) will result in the largest variation as shown in Table 4.16. In these cases, κ_2 value keeps unchanged as 5000. Varying of κ_1 and κ_3 value can cause dispersion of block size around its deterministic

analysis block size. However, case 1, 3, 5 and 6 predicts similar block size distribution, but they are much different from case 2, 4, 7 and 8. One can observe that case 1, 3, 5 and 6

Table 4.16 Percentage of each failure mode and statistical parameter of different case

	Statistical parameter		Failure mode (%)							
	Mean block size (m^3)	Standard deviation (m^3)	Sliding along plane 1	Sliding along plane 2	Sliding along plane 3	Sliding along plane 12	Sliding along plane 13	Sliding along plane 23	Fallout	Total
Case 1	187.16	155.28	83.10	0	0.03	3.93	2.04	0.05	10.86	100
Case 2	295.46	134.74	99.6	0	0	0	0.03	0	0.37	100
Case 3	169.57	113.16	90.53	0	0.05	1.14	0	0	8.27	100
Case 4	269.45	60.71	99.07	0	0	0.23	0.70	0	0	100
Case 5	174.07	125.17	86.74	0	0.05	4.6	0.74	0.02	7.84	100
Case 6	184.75	145.34	88.14	0	0.05	0.90	0.04	0	10.87	100
Case 7	302.85	145.36	97.10	0	0	0.34	2.12	0.01	0.43	100
Case 8	262.29	18	100	0	0	0	0	0	0	100
Deterministic analysis	277.39	-	100	-	-	-	-	-	-	100

adopt the determined κ_2 value. No matter how κ_1 and κ_3 vary, the determined block size distributions are very similar. Therefore, one can conclude that variation in joint orientation concentration of joint set 2 has a greater influance on block size identification for this case.

4.8 Summary

In this chapter, probabilistic analysis for unstable block identification is presented. Ubiquitous approach is assumed to consider all possible unstable blocks which may be formed during excavation. Monte Carlo simulation was created with reasonable rock parameter distributions. After sufficient number of iterations, unstable block characteristics can then be determined. Case studies are provided for probabilistic analysis. The probabilistic analysis results show that more failure modes with different probabilities are predicted compared to deterministic analysis as shown in Section 4.7. Besides, deterministic analysis predicts failure mode that may not be the dominant failure mode in probabilistic analysis. This depends on relative position and concentration of each joint set. Although the probability of different failure modes remains unchanged with/without considering size parameters, size parameters have a great significant on rock block size determination. Rock block size would be significantly smaller if size parameters are taken into consideration.

If Fisher distribution is misused for non-symmetrical data simulation, unstable rock block size distribution and probability of each failure mode will change.

Parametric studies are used to investigate the effect of joint orientation simulation with different distributions on bock size determination. Statistical parameters (κ, β, Γ) play important roles in joint orientation simulation and variation of each of these statistical parameters can lead to changes in unstable block volume. Small variation in joint orientation can result in block size varying in a large range. As shown in case study presented in Section 4.7.4, the statistical parameters of a particular joint set (joint set 2) may have greater impact on block size determination compared with that of other joint sets.

Chapter 5 Rock Support Design

5.1 Introduction

Safety is a prime concern in rock engineering. An adequate reinforcement system that supports unstable rock blocks has to be carefully designed. A successful design of rock support depends on the proper identification of potential unstable rock block (discussed in Chapter 4) and the installation of sufficient rock bolts to counter any form of instability (Tyler et al, 1991). Rock bolt design parameters such as bolt length, capacity and installation spacing are the major considerations in rock reinforcement design. As shown in Figure 5.1, these parameters are closely related to the predicted rock block characteristics. However, variation in rock parameters can have tremendous impact on rock block identification. Thus, designer may not be able to provide a set of reliable reinforcement parameters using deterministic analysis. In addition, rock reinforcement design criteria need to be established to check whether a design is acceptable. A factor of safety (FS) is commonly used to ensure that the design is safe. Despite conventional belief, a design with a higher FS does not necessarily mean that the design has lower risk. The probability of failure (PoF) might in fact be higher due to the large variability and uncertainty associated with loading conditions (Dunn, 2013). Therefore, the reliability-based design is investigated in this chapter and a parametric study on rock reinforcement design is performed.

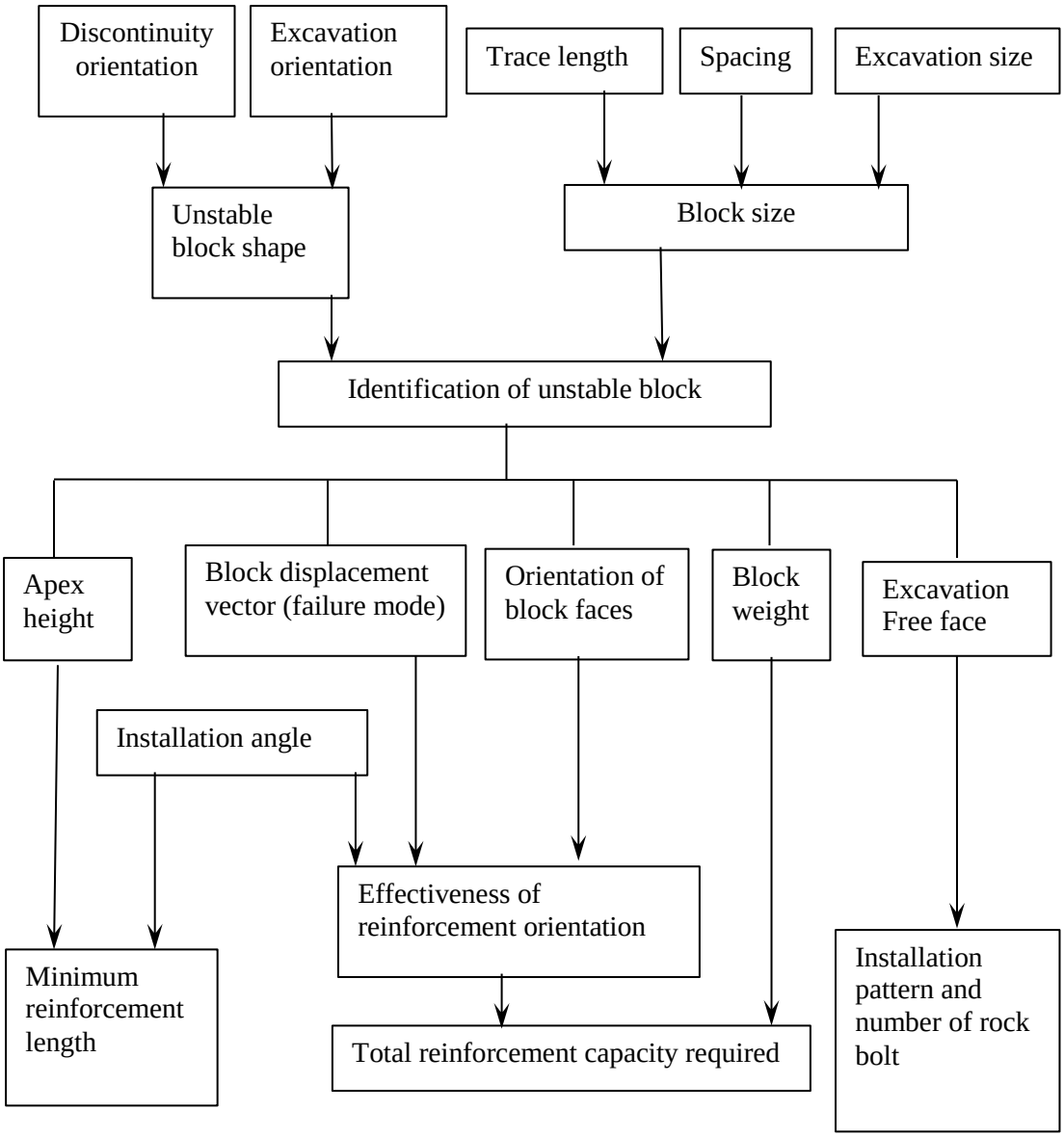

Figure 5.1 Procedure for reinforcement design of single blocks

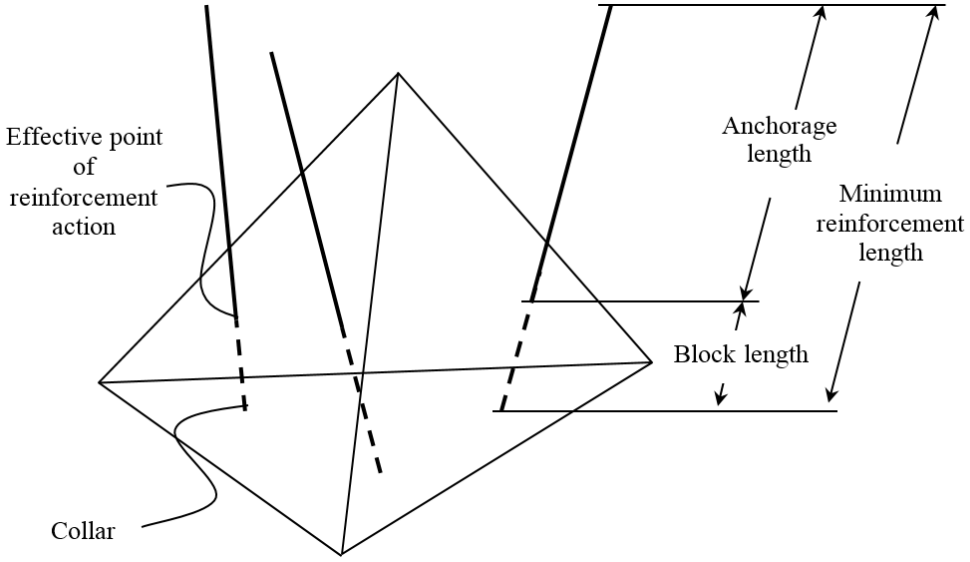

Figure 5.2 A tetrahedral block with its associate reinforcement (after Windsor and Thompson, 1992)

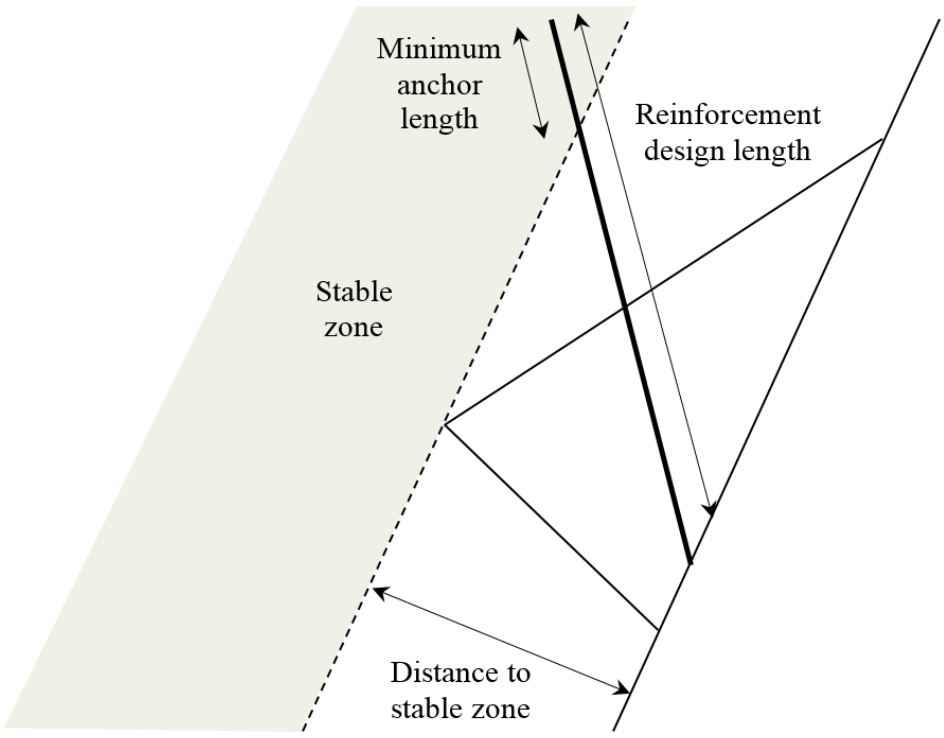

Figure 5.3 The reinforcement design length relative to block size (after Windsor and Thompson, 1992)

5.2 Reinforcement Design

5.2.1 Rock Bolt Length

Bolt length plays an important role in tunnel roof reinforcement design. Rock bolt is installed into adjacent stable strata to hold the unstable block. Rock bolt length is determined based on the total thickness of unstable strata. A minimum reinforcement length is required to achieve target bolt capacity (Figure 5.2). However, the portion of rock bolt within the unstable zone may not be sufficient to contribute sufficient bolt capacity. Therefore, minimum anchorage length in stable zone is required to ensure that adequate bolt force could be generated (Figure 5.3).

The minimum anchor length, L_1, can be calculated by (Hanna, 1982)

$$L_1 = \frac{P_A}{\pi d \tau_{bond}} \tag{5.1}$$

where P_A is the bolt load; τ_{bond} is the average working bond stress between grout and borehole wall or grout and bolt; d is the diameter of borehole if τ_{bond} is the average working bond stress between grout and borehole; or the diameter of bolt if τ_{bond} is the average working bond stress between grout and bolt.

The total rock bolt length can be calculated by

$$B_l = L_1 + L_2 \tag{5.2}$$

where B_l is the length of bolt; L_1 is the length of anchor; L_2 is the length in zone to be stabilized. The apex height of the unstable block H_w is usually chosen as the depth of the stable zone (as shown in Figure 5.4). However, the results from probabilistic analysis in Chapter 4 show that H_w varies with a large range due to the uncertainty of rock parameters. Therefore, the rock bolt length has to be carefully designed. Tyler et al. (1991) proposed a regression analysis of apex height with different levels of risk. The minimum rock bolt length can be calculated from the factored risk based on the best fit equation. Details are given in Tyler et al. (1991).

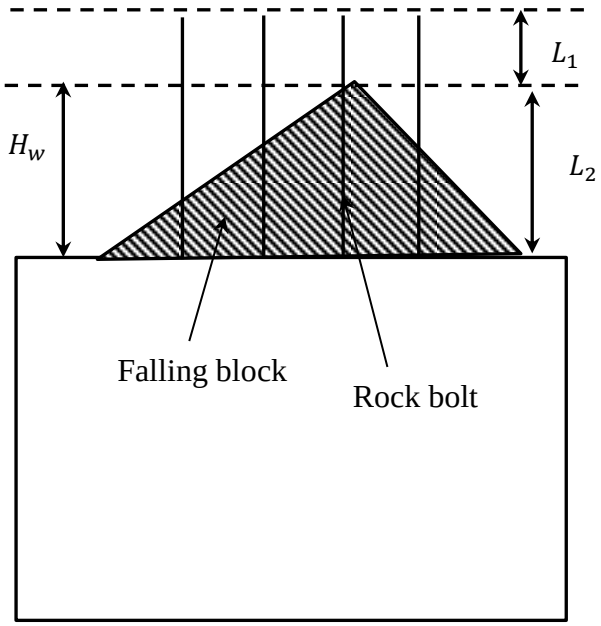

Figure 5.4 Design of length of rock support (after Chen, 1994)

5.2.2 Number of Bolts

A sufficient number of rock bolt should be applied to stabilize the target block. The total resistance force required to stabilize the unstable block can be calculated using block force equilibrium. Then the required number of bolts, N_b can be calculated using

$$N_b = \frac{F_s F_t}{\sigma A_b} \tag{5.3}$$

where F_s is factor of safety; F_t is the resultant force; A_b is the cross section of a single bolt; σ is the tensile strength of bolts if support is required to prevent a wedge falling directly from the roof; σ is the shear strength of bolts if support is required to prevent sliding from the roof or the walls on one or two joint planes.

In rock tunnel construction, the position of rock bolts has to be specifically defined. Reinforcement are usually designed for tunnel segment and the reinforcing elements are installed at constant spacing over a designed section. However, the number of active reinforcing element per block can vary. As shown in Figure 5.5, the number of active rock bolt on the block may reduce from 4 to 2 because of different rock bolt positions relative to the given shape. In addition, the block excavation face can also change with variation in rock parameters. The number of reinforcing element per block and the excavation face area of the block will govern the spacing for rock bolt design (Windsor and Thompson, 1992). Besides, the number of rock bolt on each block is important for stability assessment of a reinforced rock block. Hence, it should

be carefully determined. Windsor and Thompson (1992) and Windsor (1999) emphasized the importance of considering variation of number of rock bolt on each block, but they did not mention how to tackle the problem. Therefore, a simple method to determine active rock bolt number on each block is proposed and it will be discussed in detail in Section 5.5.

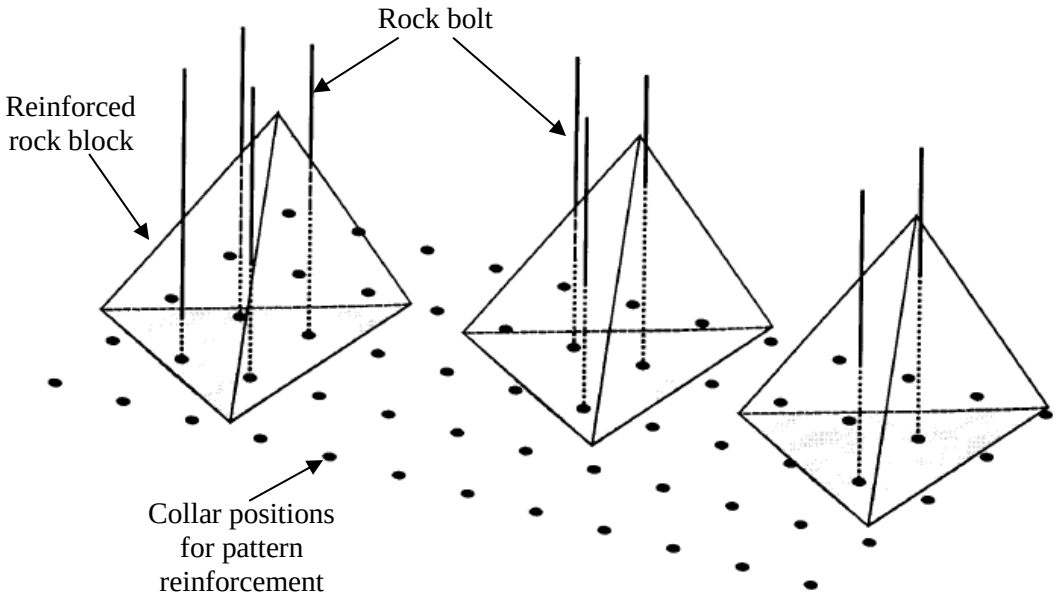

Figure 5.5 Varying the relative position of the block with in a reinforcement array (after Windsor, 1999)

5.2.3 Resultant Force

The resultant force is important for determining reinforcement capacity and number of bolts. It is defined as the sum of all forces acting on the unstable block. The resultant force is mainly caused by self-weight of the unstable block and is closely related to block failure mode. The probabilistic analysis presented in Chapter 4 had shown that more failure modes would be

encountered if variation in rock parameters is considered. Therefore, the resultant force has to be carefully considered using block failure mode on the basis.

5.2.3.1 Resultant force of a fallout failure

If an unstable block has the tendency to fail by fallout, the resultant disturbing force (F_t) is its self-weight as shown in Figure 5.6.

$$F_t = W \tag{5.4}$$

where W is the dead weight of block. The displacement vector is vertically downward and separation will occur on all discontinuities. Frictional force and cohesion do not need to be considered in the computation of resultant force acting on rock block.

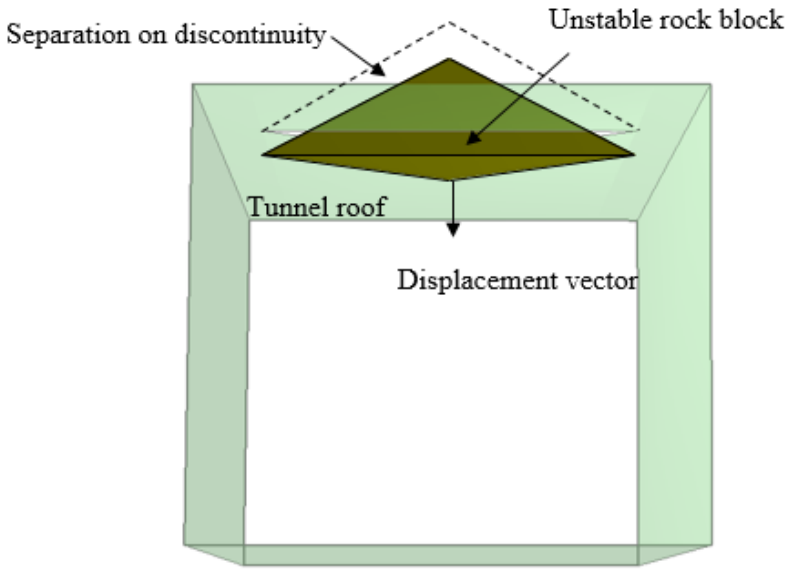

Figure 5.6 Fallout failure

5.2.3.2 Sliding along a single discontinuity

If an unstable block has the tendency to fail by sliding along one discontinuity planes, the forces acting on the block are its self-weight, friction and cohesion. The resultant force comprising of normal compression and sliding are shown in Figure 5.7.

The total resultant disturbing force can be calculated by

$$F_t = W\left(sin\alpha_i - cos\alpha_i tan\Phi_i\right) - C_i A_{ri} \tag{5.5}$$

where F_t is the resultant force in the sliding direction; W is the weight of the wedge; α_i is the dip of the i_{th} plane; Φ_i is the friction angle of the i-th plane; C_i and A_{ri} are the cohesion coefficient and area of the i-th plane, respectively.

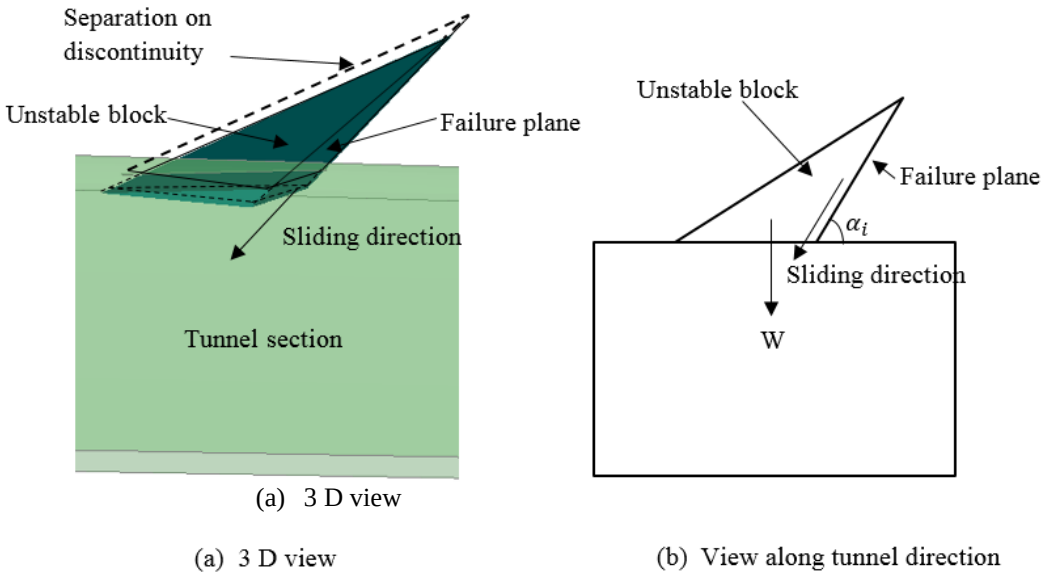

(a) 3 D view

(a) 3 D view (b) View along tunnel direction

Figure 5.7 Sliding along a single discontinuity

5.2.3.3 Sliding along intersection of two discontinuities

If an unstable block fails by sliding along the intersection of two discontinuities as shown in Figure 5.8, the resultant force is acting along this intersection. In order to find R_i and R_j, the equilibrium equation is established horizontally and vertically as

$$R_i cos\psi_i = R_j cos\psi_j \tag{5.6}$$

$$R_i sin\psi_i + R_j sin\psi_j = W cos\gamma_{ij} \tag{5.7}$$

where R_i and R_j are the normal reactions provided by planes i and j; ψ_i and ψ_j are the angle between planes i and j and the vertical plane passing through the intersection of planes i and j respectively; and γ_{ij} is the dip angle of the intersection along which the wedge slides.

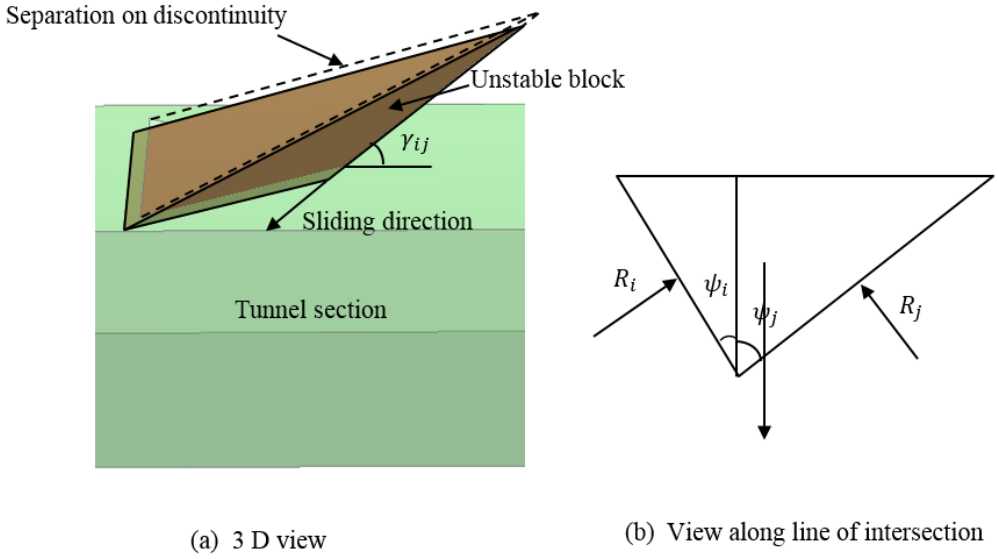

Figure 5.8 Sliding along intersection of two discontinuities (after Hoek and Bray, 1979)

Solving Equations (5.6) and (5.7) and let $\psi_{ij} = \psi_i + \psi_j$, Equations (5.8) and (5.9) obtains

$$R_i = W\cos\gamma_{ij}\cos\psi_i / \sin\psi_{ij} \tag{5.8}$$

$$R_j = W\cos\gamma_{ij}\cos\psi_j / \sin\psi_{ij} \tag{5.9}$$

The resultant force, F_t, can be found using

$$F_t = W\sin\gamma_{ij} - \left[\frac{W\cos\gamma_{ij}}{\sin\psi_{ij}} \left(\cos\psi_i \tan\Phi_i + \cos\psi_j \tan\Phi_j \right) + C_i A_i + C_i A_j \right] \tag{5.10}$$

where Φ_i and Φ_j are the friction angles of planes *i* and *j* respectively; C_i and C_j are the cohesion of plane *i* and *j* respectively ; and A_i and A_j are the areas of planes *i* and *j* respectively.

5.2.4 Rock Bolt Capacity

The single rock bolt capacity depends on bolt diameter and steel strength. Once the number of rock bolt applied on each unstable block is determined, the diameter of bolt can be estimated (Biron and Arioglu, 1983)

$$d = 2\sqrt{\frac{R \times F_s}{\pi\sigma_a}} \tag{5.11}$$

where F_s = Factor of Safety; R = allowable axial force in bolt; and σ_a = yield strength of steel

Equation (5.11) determines the maximum capacity of a single rock bolt. However, as discussed in Section 5.2.1, the bolt carrying capacity is determined by not only the bolt diameter and steel strength but also by the

anchorage capacity. Hence, the bearing capacity of a rock bolt is the minimum of single bolt capacity and bolt anchorage capacity.

5.2.5 Bolt Angle

Bolt installation angle has a significant effect on bolt bearing capacity. Rock bolts should be installed in the direction that the maximum bolt capacity can be reached (such as tension bolts achieve their maximum capacity in the direction of displacement vector and shear bolts achieve their maximum capacity in the direction normal to the sliding plane). However, as mentioned in Section 5.2.2, rock bolt are installed uniformly along a tunnel section. The bolt installation angle varies due to variation in rock block failure modes (discussed in Chapter 4). If a rock bolt is not installed in the optimal direction, the effective rock bolt capacity has to be reduced from its nominal capacity. The block displacement vector and the orientations of the block faces are commonly used to assess the effectiveness of reinforcement installed at different orientations (Figure 5.9). The reinforcement effectiveness factor *E* can be determined by

$$E = \frac{\delta_t}{|\delta_s|} \tag{5.12}$$

where δ_t is axial tension of reinforcement; δ_B is block displacement resolved onto the discontinuity; and $|\delta_s|$ is block displacement vector resolved onto the discontinuity.

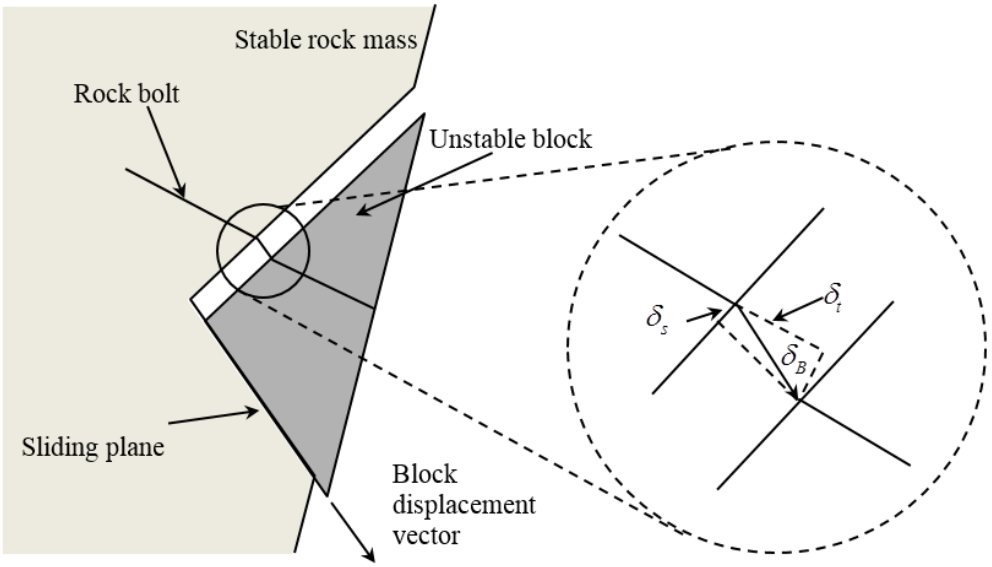

Figure 5.9 Rock bolt deformation with unfavorable bolt angle (after Windsor and Thompson, 1992)

5.2.6 Rock Bolt Spacing

Beside bolt length, bolt spacing is another important parameter in rock support design. If the bolt spacing is too small, more rock bolts are required to be installed and cost of design will increase. On the other hand, if spacing is too wide, the unstable block cannot be effectively stabilized. Thus, a reasonable bolt spacing has to be determined. In general, ground condition such as strata thickness, bolt characteristics can affect bolt spacing. Therefore, past research studies had attempted to relate spacing design with rock or tunnel characteristics. Many empirical approaches were proposed. Stillborg (1986) proposed that bolt spacing, B_s, should be designed as $B_s < 3S_p$ (where S_p is joint spacing) in a jointed rock mass and half the bolt length in other rock

conditions. Coates and Cochrane (1970) related bolt length and roof span to rock bolt spacing design:

$$B_s = \frac{2}{3}l \quad \text{or} \quad b = \frac{2}{9}L \tag{5.13}$$

where b = Bolt spacing; l =Bolt length; and L =Roof span.

A general rule to obtain the maximum bolt spacing is that the maximum spacing is the least of one half of the bolt length; one and one-half the width of the critical and potentially unstable rock blocks; and 6 feet (1.83m). The minimum bolt spacing should not be less than 3 feet (0.914m) (Luo, 1999).

5.4 Design Criteria

5.4.1 Introduction

As discussed in Chapter 4, parameter uncertainty is inevitable in rock support design. Besides, conceptual uncertainty in failure mechanism may also be involved. Therefore, it is necessary to establish some criteria to decide whether a design is acceptable. A reasonable acceptance criterion should be applied to capture the various uncertainties associated with a particular design. In geotechnical engineering, the factor of safety (FS) is commonly used. FS is a deterministic measure of the ratio between the resisting forces (capacity) and driving forces (demand) of a failure mechanism (Wesseloo and Tead, 2009). The key block from deterministic analysis is commonly used for reinforcement design. However, deterministic analysis might predict the major failure mode wrongly as shown in Chapter 4. As a result, the FS used in reinforcement design may not guarantee that the design is 100% safe.

Therefore, probability of Failure (PoF) is increasingly used in engineering design to consider variations in capacity and demand (Dunn, 2013). The degree of confidence in the capacity depends on the variability in the material properties; testing errors; installation practices; quality control procedures and others. Similarly, the degree of confidence in demand depends on removable block size; loading conditions; etc. (Dunn, 2013). Figure 5.10 shows the basic concept of PoF. Failure occurs only when the capacity function curve is less than the demand function curve shown as shade area. FS can be used as an indicator to evaluate the system failure rate. If FS is less than 1, the system is considered unstable. The PoF (FS<1) is shown by the shaded area in Figure 5.11.

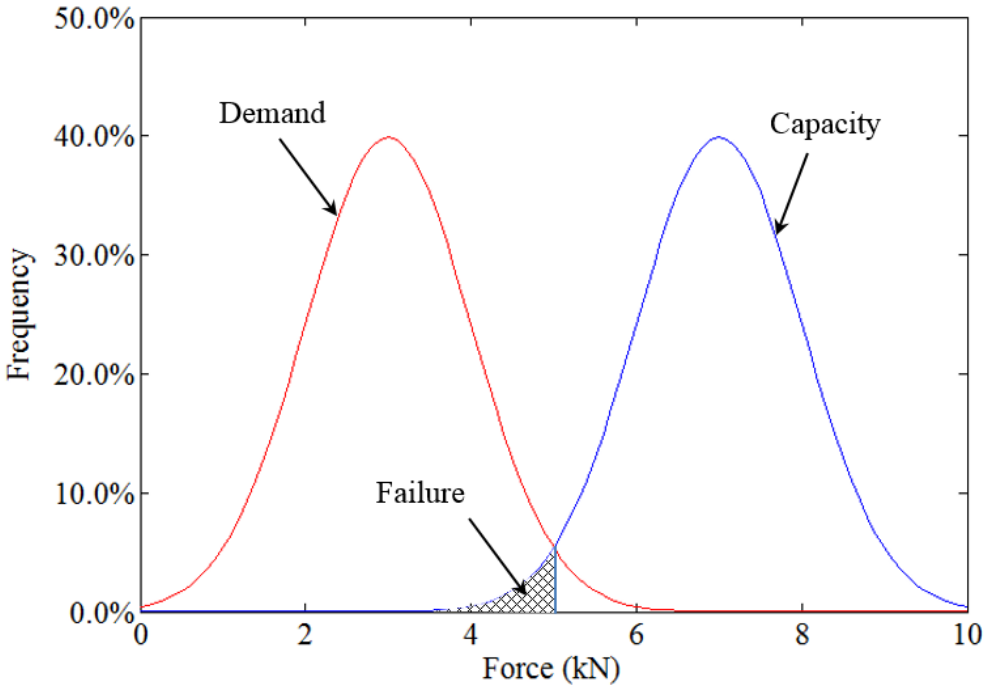

Figure 5.10 Probability of Failure concept

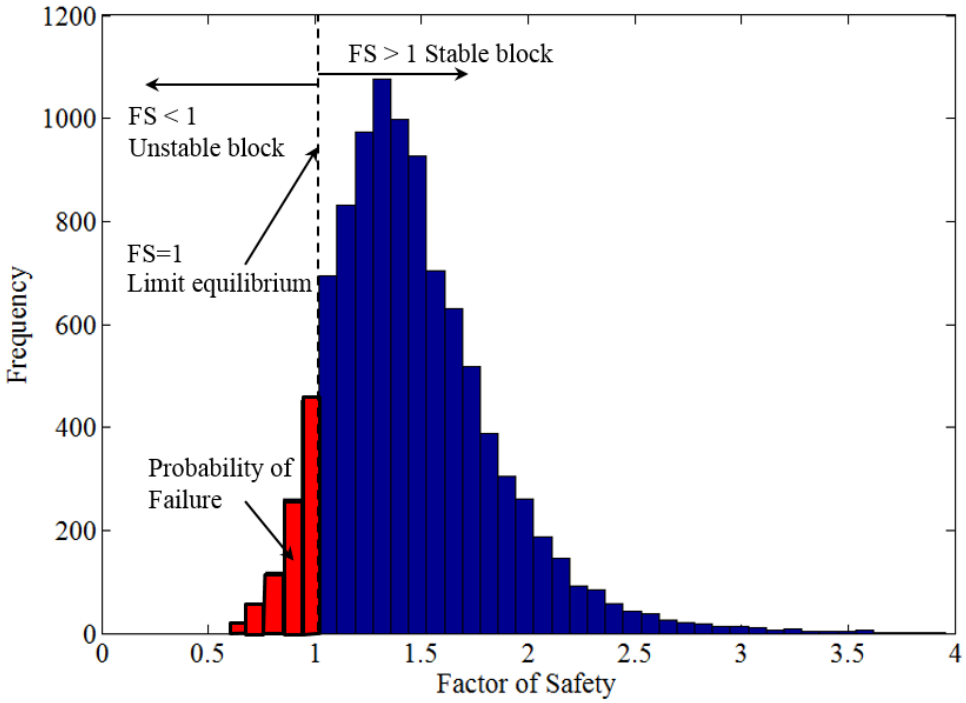

Figure 5.11 PDF of FS distribution

5.4.2 Factor of Safety vs. Probability of Failure

A large FS indicates a larger difference between demand and capacity. This means that design is safer. However, if the FS used is small as shown in Figure 5.12, the failure area will be large. The choice of a suitable FS value for design indicates the risk tolerance that a design engineer is prepared to bear. Currently, the selection of an appropriate design FS value is empirical. Hoek *et al.,* (1995) suggested a FS value of 1.3 for temporary openings and 1.5 to 2.0 should for permanent excavations. It is to be noted that a design with a large FS value may not mean that there is a lower risk. Using a slope design example, Dunn (2013) showed that the PoF for a design with FS value of 1.5

can be higher than that of the design with a FS value of 1.35 (Figure 5.13). It was also found that it is equally applicable to rock excavation design.

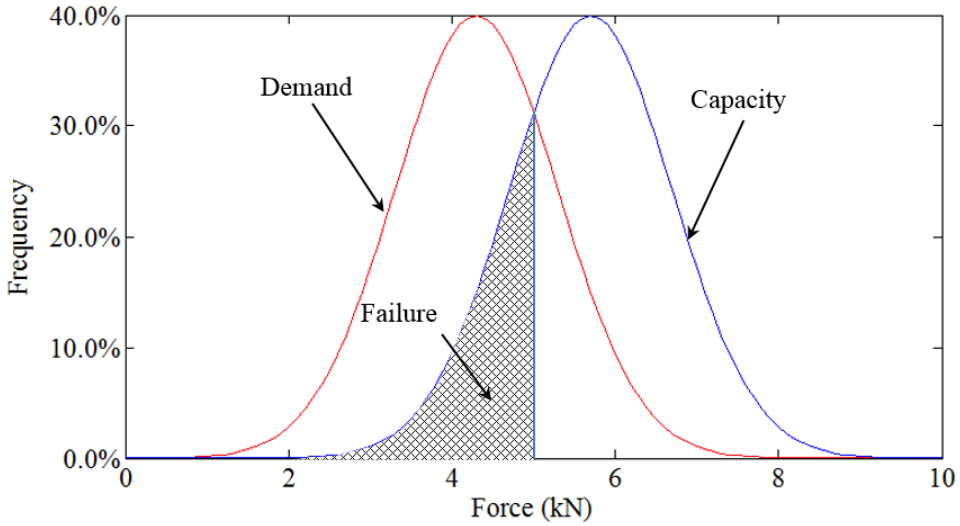

Figure 5.12 High probability of failure

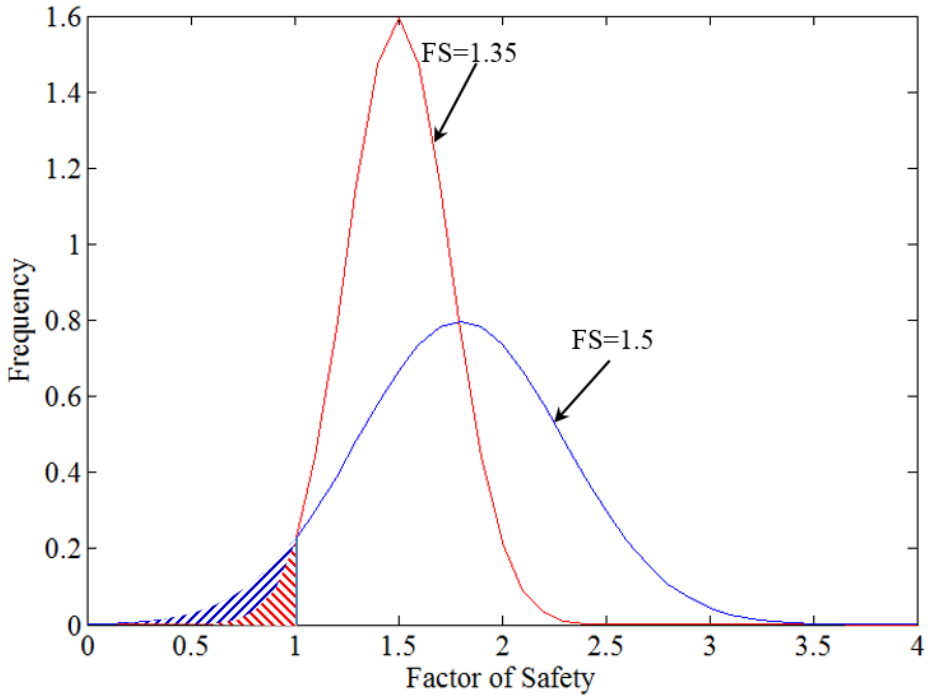

Figure 5.13 Variation effect on PoF with different FS

Although the use of PoF is increasing (Fenton, 1997; Phoon, 2004), the most widely used acceptance criterion is still FS in engineering practice (Priest and Brown, 1983; Lunder, 1994; Carter and Miller, 1995). PoF is not commonly used in ground support design in underground mining (Dunn, 2013), because more detail rock information is required for PoF analysis. However, designing with PoF is more reliable. Therefore, a reliability-based design is studied in Section 5.6 through case study.

5.5 Model for Reliability Assessment

The proposed reinforcement design should be assessed for reliability. Monte Carlo simulation is commonly adopted for this reinforced block assessment (Dunn, 2013). Three types of rock block distributions (span limited block distribution, trace length limited block distribution and spacing limited block distribution) can be produced by probabilistic block analysis (shown in Chapter 4). The range of block size defer tremendously. Excavation span can determine the largest possible rock block during excavation; although, it is unlikely to occur. This is because the size of rock discontinuities is finite. Size parameters such as trace length and spacing can restrain the rock block size (discussed in Chapter 4). Thus, either trace length limited block size or spacing limited block size should be used for reliability assessment has to be carefully chosen.

Spacing limited block might be larger than trace length limited block as shown in Figure 5.14(a). This condition could only occur when discontinuity size is

large enough to form the spacing-limited block. However, if the size of each discontinuity is insufficient, the spacing-limited block can only be partially formed (such as block 1 shown in Figure 5.14(a)). Partially-formed blocks are treated as stable in the stability analysis. Joint discontinuities can intersect with each other to form the largest possible block, trace length limited block, in the ubiquitous approach. Therefore, trace length limited block should be used for reinforcement reliability assessment, if spacing-limited block is larger than trace length limited block.

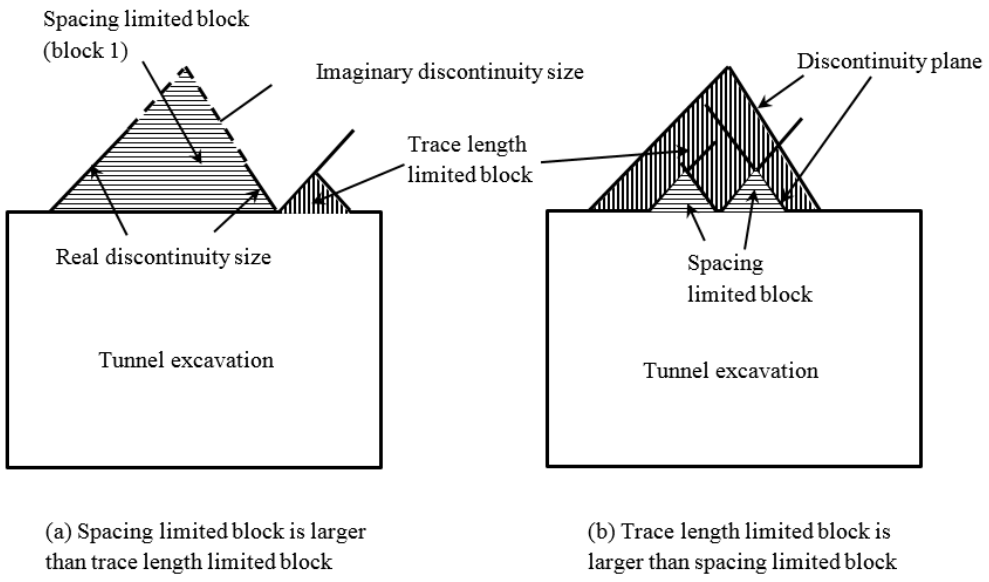

Figure 5.14 Size parameter limited blocks

On the other hand, rock discontinuity spacing defines the largest individual rock block (Windsor, 1999). It could be smaller than trace length limited block (such as case study shown in Section 4.7.2). This means the trace length

limited block can be intersected by other discontinuities to form smaller individual blocks as shown in Figure 5.14(b). In other words, the trace length limited block may consist of several individual spacing limited blocks. However, trace length limited block is still the largest block that could form during excavation. Therefore, trace length limited block should be used for reliability assessment, even though spacing-limited block is smaller than trace length limited block.

Monte Carlo simulation is commonly used to investigate the reliability of the proposed design (Tyler et al., 1991; Windsor, 1999). Rock reinforcement is applied to all simulated blocks. The demand of each block can be derived by considering block dead weight, friction and failure modes. The capacity of active rock bolts can be determined based on the number of active rock bolts installed and effectiveness of each rock bolt. FS is evaluated to determine block stability. If FS is less than 1, the reinforced block is considered to be unstable. After a sufficient number of calculation is performed, the PoF can be derived. *Reinassess* is programed in Matlab for this stability assessment. The overall analysis process is shown in Figure 5.15 for the stability reliability computations. Preliminary reinforcement design parameters such as single bolt capacity, installation spacing, and installation angle are required as inputs to initiate the reliability assessment. The design needs to be revised until the design criteria are achieved. In addition, design optimization is performed to determine the most economical design.

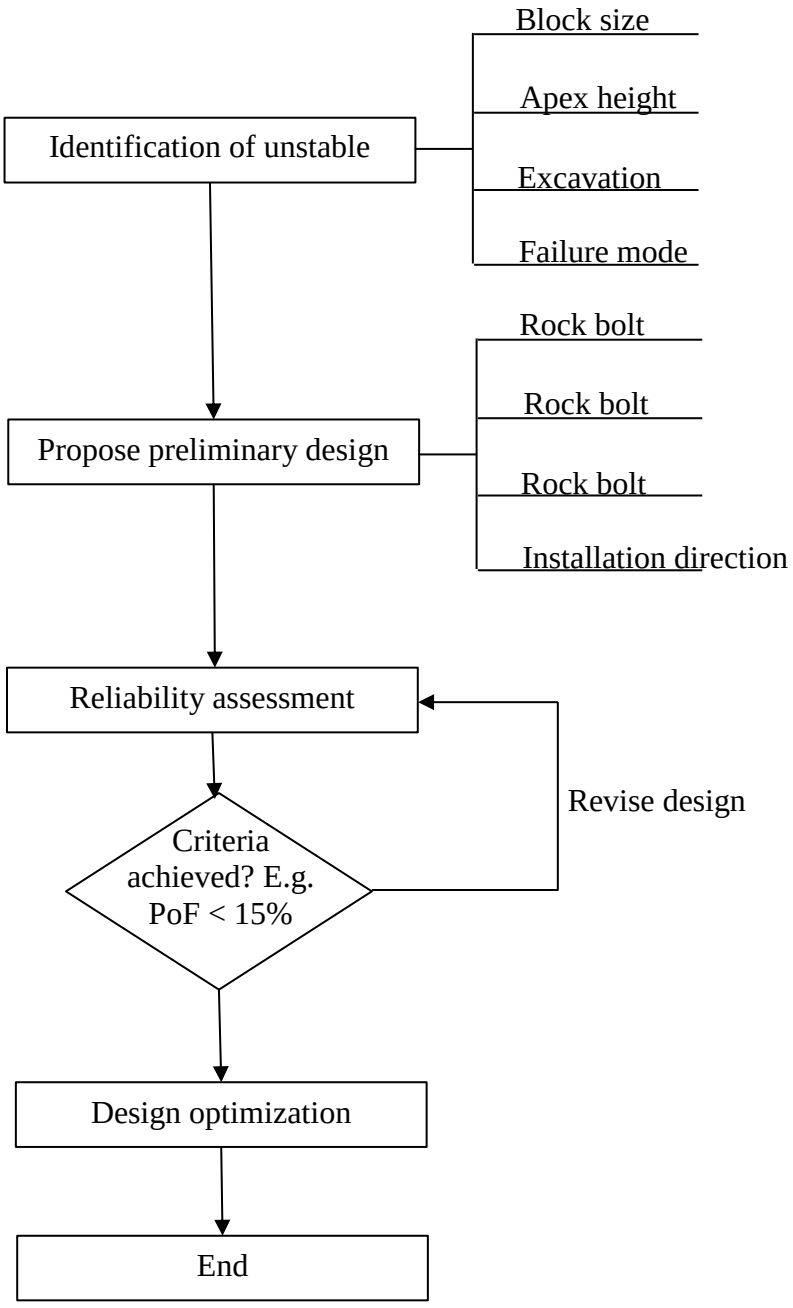

Figure 5.15 Rock design procedure

As discussed in Section 5.2.2, the number of active reinforcing elements for each unstable block is important for reinforced block assessment. This number may vary depending on the bolt position relative to the block face as shown in Figure 5.5. Thus, specific rock bolt position relative to a rock block should be considered. Rock reinforcement element matrix should start with a random position to simulate the real installation. Figure 5.16 illustrates a simple approach to determine the number of active reinforcing elements in the stability analysis. The computation steps are:

Step 1: Move ABC to $A'B'C'$ along vector $\overrightarrow{AA'}$, where A' is the origin

Step 2: Rock bolts are placed with constant spacing in quadrants with positive x.

Step 3: A random movement vector $\overrightarrow{AA''}$ (x'', y'') is generated, where $x'' \in (0, l]$ and $y'' \in (0, l]$

Step 4: Move $A'B'C'$ to $A''B''C''$ along vector $\overrightarrow{A'A''}$.

Step 5: The active number of rock bolts could be determined by counting the number of rock bolts bounded by triangle $A''B''C''$.

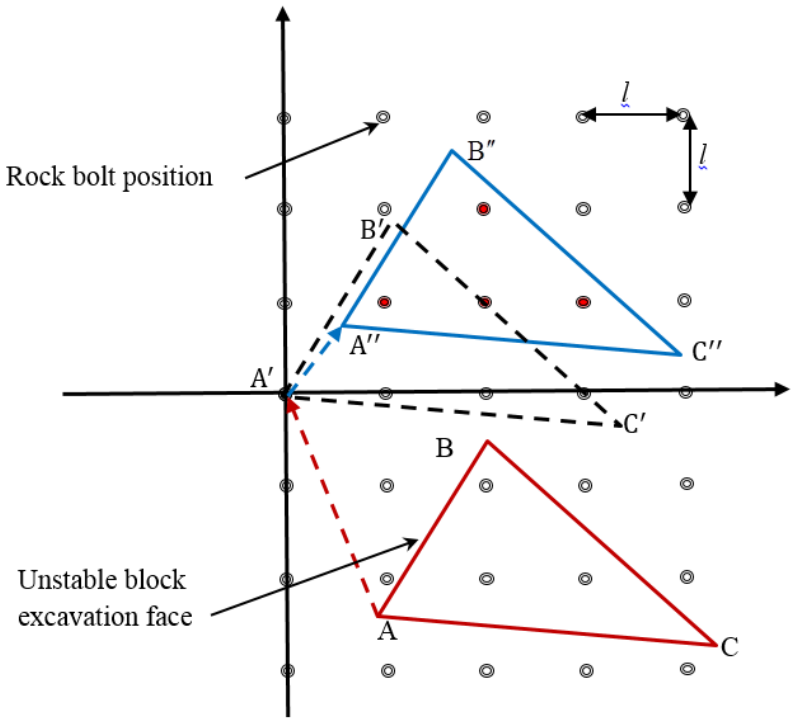

Figure 5.16 Number of active rock bolt determination

This approach generates a set of random rock bolt position relative to the unstable block. The number of active rock bolts can then be derived. A Matlab fuction *checknum* is programmed for this purpose. The capacity of rock bolts installed on a block could be determined by

$$Capacity = \sum_{i=1}^{N} C_i E_i \tag{5.14}$$

where N is the number of effective rock bolts; C_i is tension capacity of i_{th} rock bolt, if rock bolt is used for taking axial load. C_i is shear capacity of i_{th} rock bolt, if rock bolt is used for taking shear load; E_i is the effectiveness of the i_{th} rock bolt determined using Equation 5.12. The demand can be

determined from calculating the resultant force as discussed in Section 5.2.3. Then, the FS of each rock block can be determined. After a sufficient number of iterations is performed, the PoF of the proposed design can be derived.

5.5.1 Model setup Assumptions

Uncertainty in ground condition and different quality of installations often make it difficult to assess the stability of reinforced blocks. As such, simplifications and assumptions are necessary to simplify the complicated problem at hand. They are:

- The rock bolt is assumed to be loaded uniformly in each block. Small relatively rotation is ignored.
- If the minimum rock bolt length does not meet the minimum reinforcement length (apex height + minimum anchor length), the effectiveness of this rock bolt is assumed to be zero.
- Load-displacement response of the rock bolt is not considered in this study.
- The diameter of rock bolt is assumed be very small
- All rock bolts are assumed to have good quality control
- Rock mass is assumed to be a rigid body. Stress reduction during excavation is not considered.

5.6 Case study

A factor of safety (FS) is commonly used to ensure that the design is safe. However, a design with a higher FS does not necessarily mean that the design has lower risk (Dunn, 2013). Therefore, rock reinforcement design based on deterministic block analysis with FS is assessed for reliability. Parametric study is performed to investigate the effect of rock block parameters (bolt length, capacity and spacing) variations on design reliability.

5.6.1 Singapore Jurong formation (1)

Block analysis is performed as part of a feasibility study for tunneling in the Jurong Formation as presented in Section 4.7.2. Small size parameters are chosen based on Grenon and Hadjigeorgiou (2003). The block analysis result shows that small rock blocks are likely to form during excavation. Since rock bolt is hardly applicable for highly fractured rocks, other reinforcements such as concrete lining or meshing with shotcrete need to be considered. However, large discontinuity size is also possible in cavern construction. Rock bolts are needed to stabilize the unstable rock block. The rock joint data in Section 4.7.2 are analyzed again with larger size parameters. A lognormal distribution with a mean length of 3m and a 1m standard deviation is assumed as trace length distribution. An exponential distribution with a mean 2m spacing is assumed as joint spacing distribution. The deterministic results are shown in Table 5.1 and the probabilistic analysis results are presented in Figures 5.17 to 5.19.

Table 5.1 Deterministic analysis result

	Volume (m^3)	Apex height (m)	Excavation face area (m^2)	Failure mode
Span limited	21.292	2.683	34.831	Sliding along plane 1
Trace length limited	0.114	0.469	1.063	Sliding along plane 1
Spacing limited	0.012	0.220	0.235	Sliding along plane 1

* Sliding along plane 1 means unstable block will fail by sliding along discontinuity plane from joint set 1.

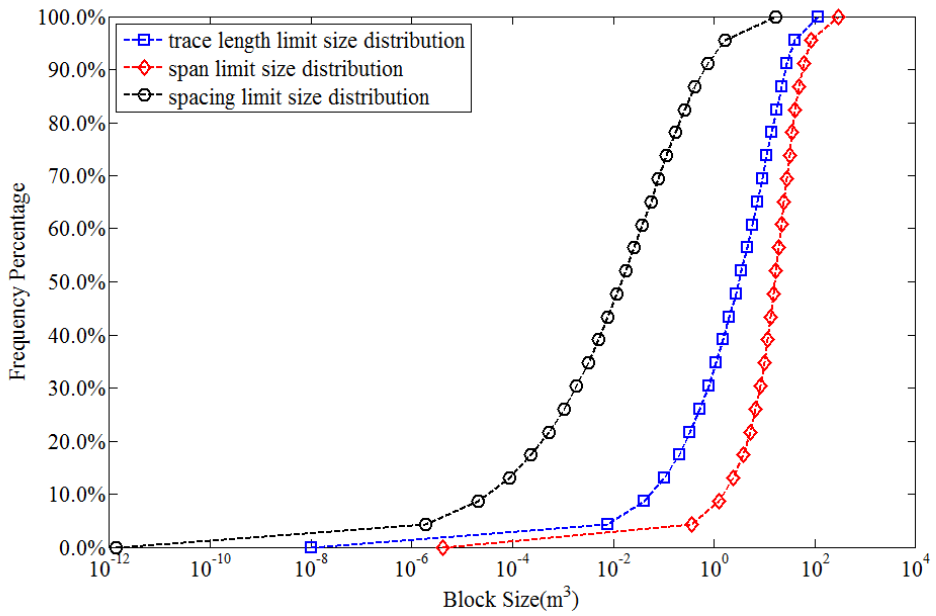

Figure 5.17 CDF of block size considering different size parameters

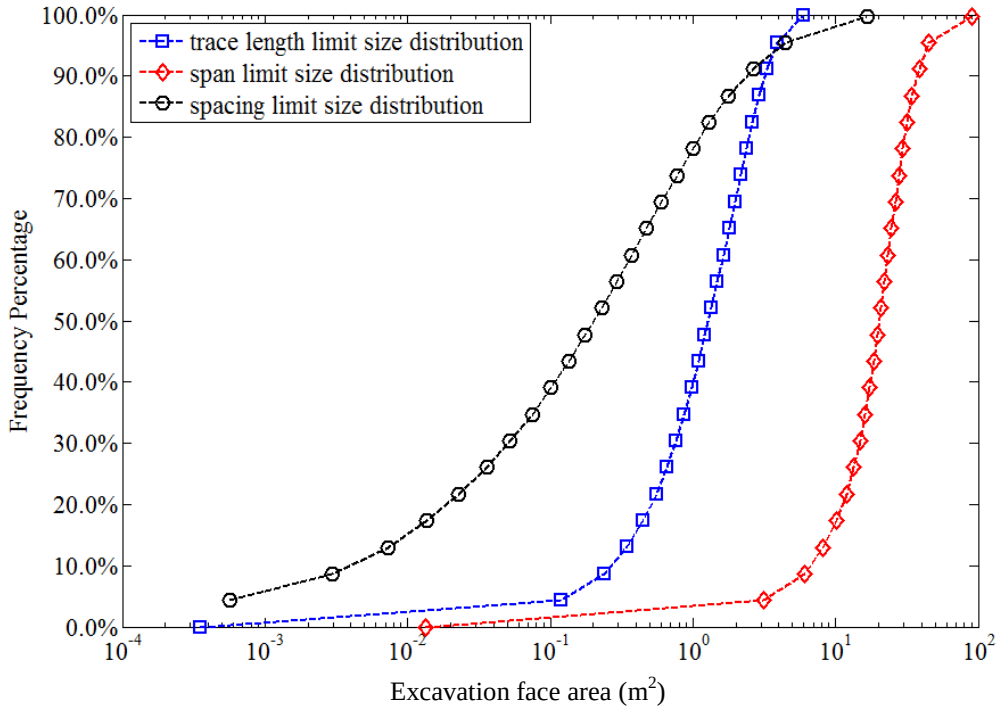

Figure 5.18 CDF of excavation face area considering different size parameters

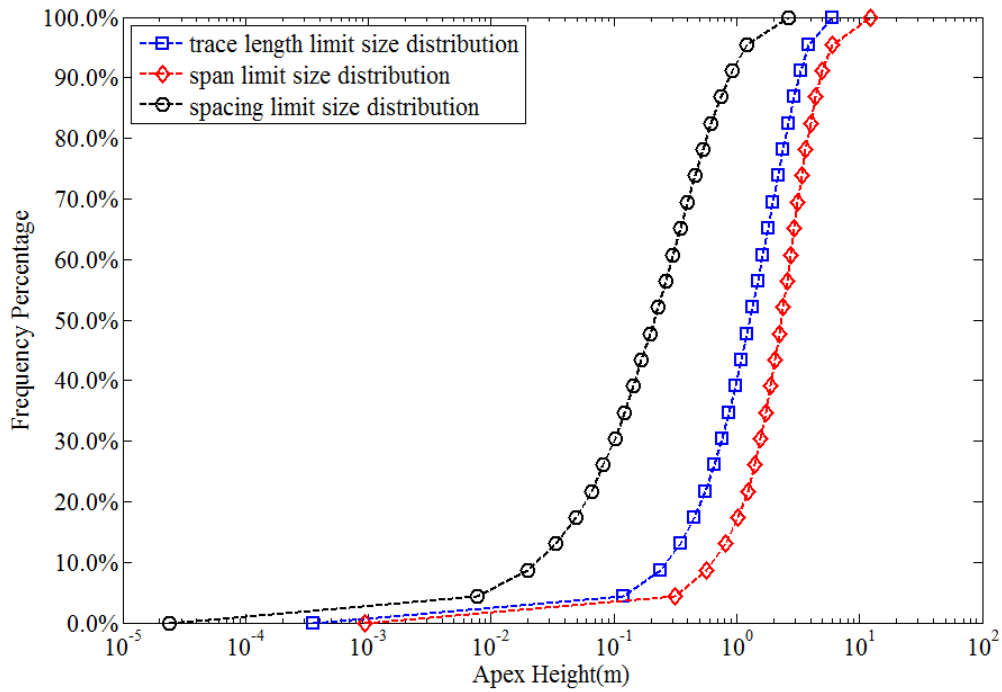

Figure 5.19 CDF of apex height considering different size parameters

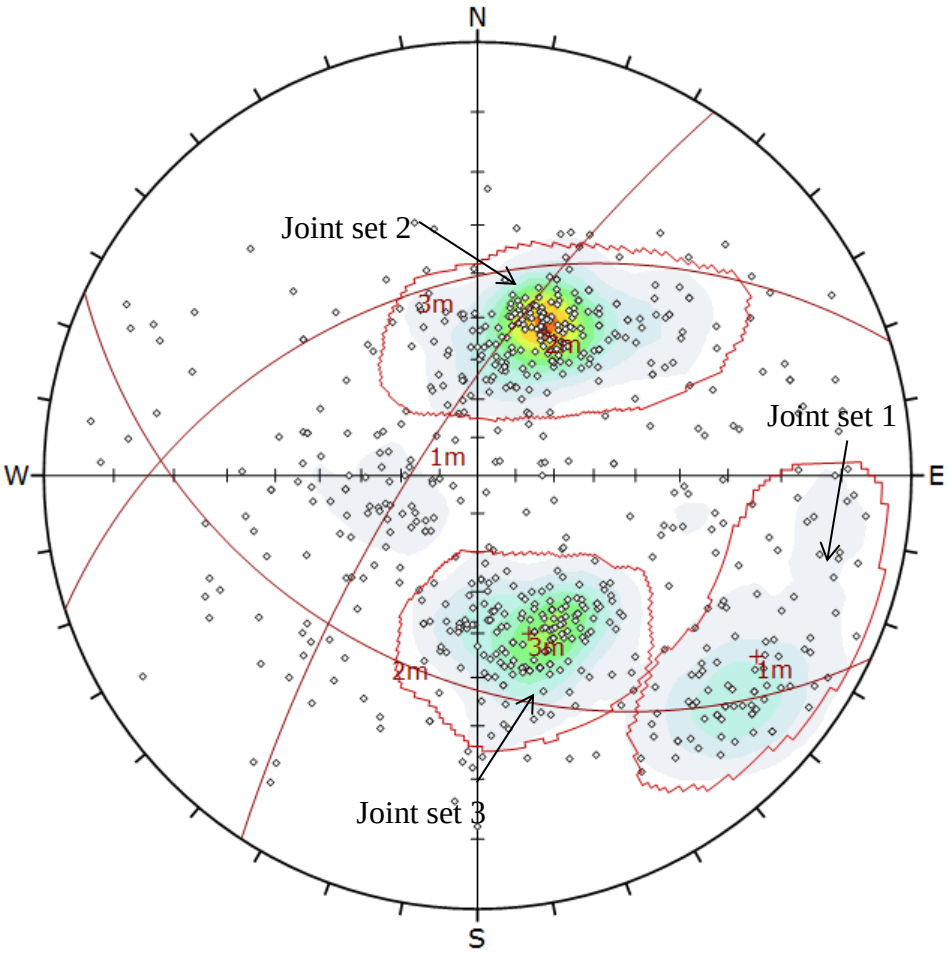

Figure 5.20 Contour plotting and joint set identification (pole plot)

Conventional reinforcement design based on deterministic analysis with FS=2 is proposed as a preliminary design. The span-limited block size is adopted to be conservative. Since the predicted failure mode is sliding along discontinuity plane from joint set 1 and joint set 1 has deep dip angles (70° to 84° as shown in Figure 5.20), the normal force on sliding plane is small. Thus, the total resistance contributed by friction is negligible. Therefore, the vertical tension

rock bolt is proposed. Using the equations listed in Section 5.2, the proposed design is presented in Table 5.2.

Reinassess is used to assess the reliability of the proposed design. PoF (FS<1) of reinforced block is calculated after 10,000 iterations. The PoF of the preliminary design is presented in Figure 5.21. Although the largest span limited block with FS of 2 is used for rock bolt design, 62% of reinforced blocks are still classified as unstable. Therefore, the preliminary design needs to be revised. Parameters such as rock bolt length, capacity and installation spacing will affect the stability of reinforced block (Windsor, 1999). Therefore, a parametric study is performed using a case study to investigate the effect of each rock bolt parameter on the reinforced block stability. The results are shown in Figures 5.22 to 5.24.

Table 5.2 Preliminary design parameters

Rock bolt design parameters	**Design value**
Bolt length	3m
Capacity	50kN
Installation angle	Vertical
Installation pattern	2m by 2m square pattern

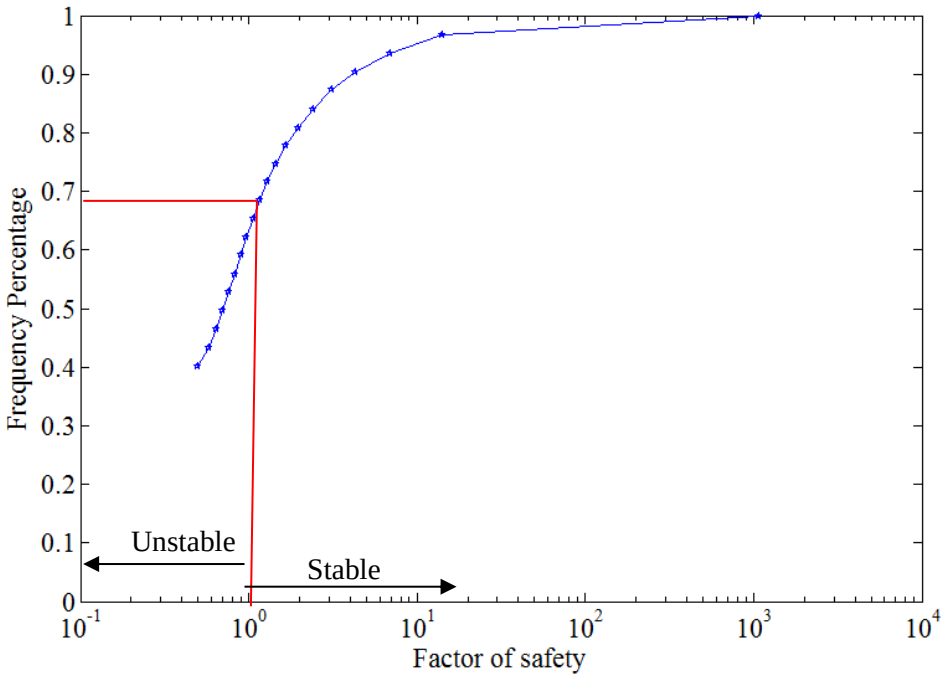

Figure 5.21 PoF of deterministic design with span limited block

The PoF decreases with increasing bolt length until the maximum bolt capacity is achieved. As shown in Figure 5.22, PoF remains at around 10% for bolt length greater than 5m. It was pointed out at Section 5.2.4 that the overall bolt bearing capacity should be the minimum of the single bolt capacity and bolt anchorage capacity. Bolt anchorage capacity is closely related to the bond force developed by rock bolt portion in the stable zone. If bolt anchorage capacity is less than single bolt capacity, the overall bolt bearing capacity increases with bolt length until bolt anchorage capacity equals to single bolt capacity. However, if the bolt anchorage capacity is larger than the maximum single bolt capacity, the rock bolt properties (such as rock bolt diameter and steel strength) will govern the maximum capacity. The overall rock bolt

bearing capacity will not change with increase in bolt length. Therefore, if rock bolt design with sufficient anchorage length is used to stabilize the unstable block and this reinforced block is still classified as unstable, thus increase in rock bolt length will not enhance the stability of the block.

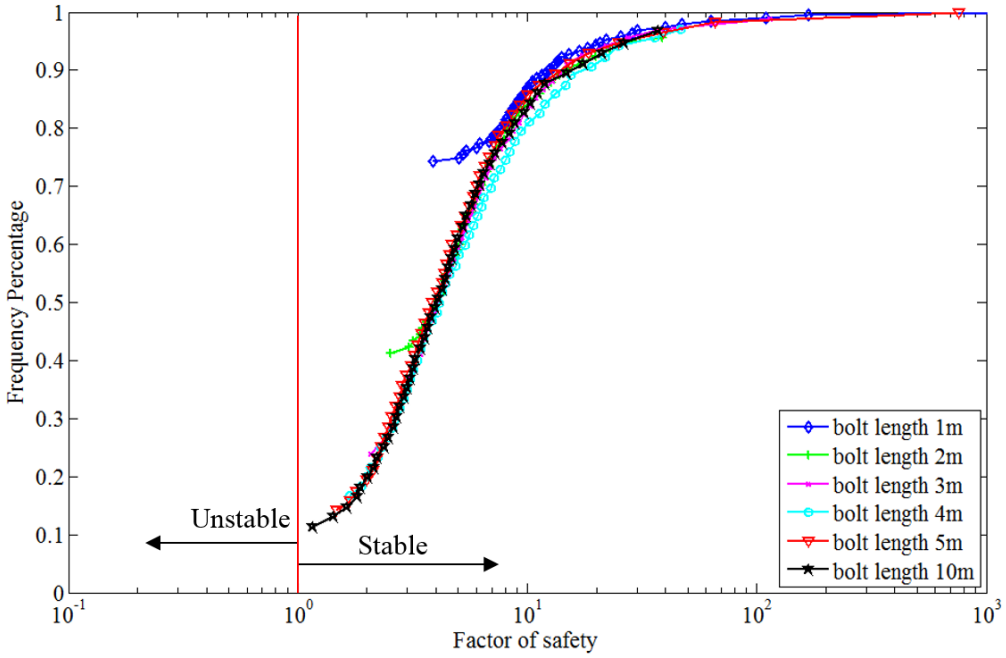

Figure 5.22 FS distribution of 30kN rock bolt installed with 1m by 1m square pattern and various bolt length

PoF decreases with an increase in single bolt capacity. As shown in Figure 5.23, PoF decreases from 65% to 14% as the rock bolt capacity increases from 10 kN to 30 kN. This observation is attributed to the fact that the total resistance on each reinforced block increases as bolt capacity increases. As a result, number of stabilized rock block increases. However, the PoF remains at around 15% when bolt capacity increases from 30 kN to 50kN. This is because the effectiveness of rock bolt (which is related to bolt length) governs the total

resistance on a reinforced block. For example, if a rock bolt is shorter than the minimum required anchorage length, the rock bolt cannot reach the stable zone and the effectiveness of this rock bolt is assumed as zero (basic assumption in Section 5.5.1). Therefore, the number of stabilized block does not increase with increase of rock bolt capacity. That is why PoF remains at about 15%. In addition, small blocks in between rock bolts are still possible to form. Rock bolt cannot stabilize them because the minimum spacing of rock bolt is 3 feet (0.914m). Therefore, in this case, rock bolt length and rock bolt spacing will limit the upper limit of a design. However, FS of single reinforced block still can increase with bolt capacity. As shown in Figure 5.23, PoF curve shifts to the right. This is because the overall capacity of a reinforced stable block increases as rock bolt capacity increases, given the same demand.

Rock bolt spacing has a significant effect on the PoF of a design. A small bolt spacing means that there is a higher chance for rock bolts to intersect the unstable block. The increase potential of having more active rock bolt on each block leads to an increase in total resistance capacity of reinforced block. The number of stabilized block out of total simulation will increase. As shown in Figure 5.24, PoF decreases from 75% to 17% when rock bolt spacing decrease from 2.5m to 1m. Therefore, PoF will drop with decrease in rock bolt spacing. However, caution should be taken. In practice, the minimum rock bolt spacing should not be less than 1m for installation (Luo, 1999).

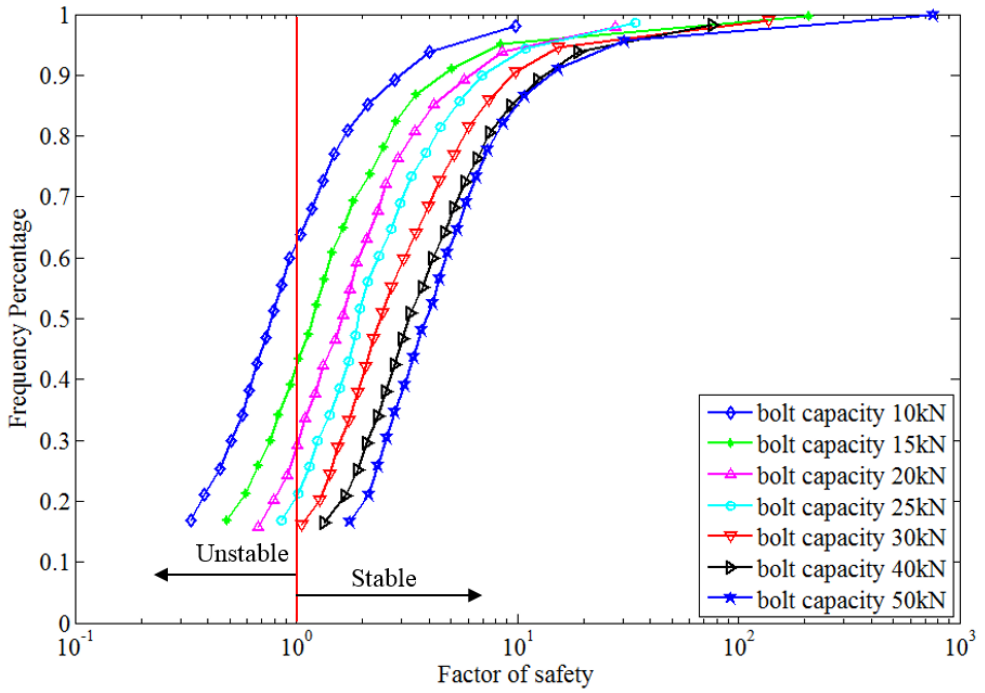

Figure 5.23 FS distribution of 5 m rock bolt installed with 1m by 1m square installation pattern and various bolt capacity

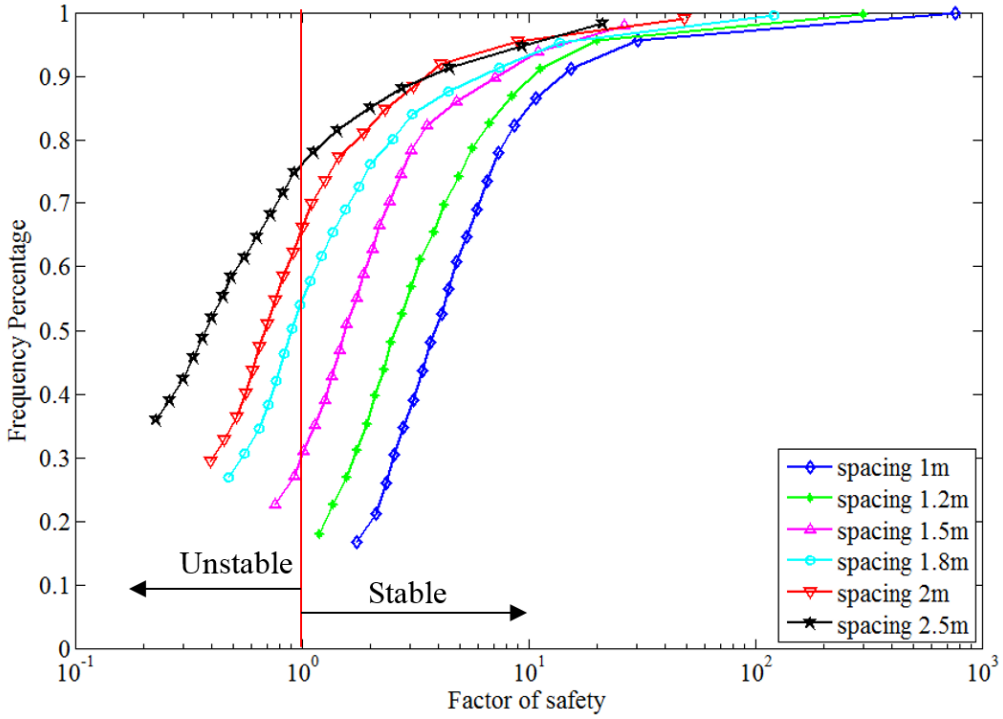

Figure 5.24 FS distribution of 5 m rock bolt installed with capacity 30 kN and different installation spacing

Table 5.3 Alternative design parameters and corresponding POF

Rock bolt design parameters	**Design value**		
Name	Deterministic design	Alternative 1	Alternative 2
Bolt length (m)	3	5	5
Capacity (kN)	50	50	30
Installation angle	Vertical	Vertical	Vertical
Installation pattern	2m by 2m	1.2m by 1.2m	1m by 1m
POF	62%	15%	15%

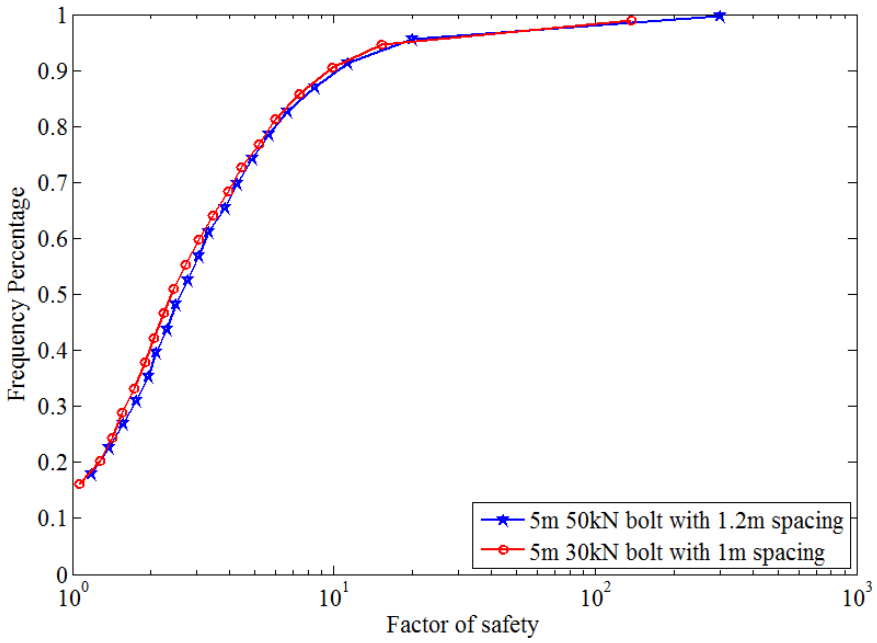

Figure 5.25 Comparison of PoF for two different designs

It is shown from the parametric studies that rock bolt length, bolt capacity and installation spacing have significant impacts on design POF determination. Each of these rock bolt design parameters can differ the design POF; therefore, designer can vary rock bolt design parameters to find design alternatives. For

example, a design criterion is chosen as 85% confidence limit for demonstration (assume 15% of small rock block). Design alternatives are presented in Table 5.3 and associate FS distribution is shown in Figure 5.25. Both alternative 1 and alternative 2 can achieve the design criterion (85%). If secondary reinforcement (such as shotcrete and meshing) is applied to stabilize the small block between rock bolts, rock tunnel can be fully stabilized. Both alternatives use 5m rock bolt. However, alternative 1 uses high capacity rock bolts (50 kN) with a 1.2 m spacing (high cost of single rock bolt but with less total number); whereas, alternative 2 uses low capacity rock bolts (30 kN) with 1m spacing (low cost of single rock bolt but with large total number). Which alternative is more economical should be further investigated.

Owing to time limit of this study, cost analysis among design alternatives is not included. Grenon and Hadjigeorgiou (2003) emphasized that cost difference among design alternatives may be tremendous. Therefore, further studies are clearly needed on this subject matter.

5.6.2 Singapore Jurong Formation (2)

As discussed in Chapter 4, in some circumstance, deterministic analysis can product a reasonable estimation of the mean of rock block size and failure mode. If a reasonable factor of safety is applied, the rock reinforcement design could be sufficient to stabilize the unstable block. However, in some cases, deterministic block analysis can not give a representative block. This case study use a actual case to show that results from deterministic block analysis

with mean orientations is not suitable for rock reinforcement design. Another borehole coring data of Jurong formation is used as example for deterministic rock support design. Its joint orientation contour plot is shown in Figure 5.26. Deterministic block analysis result is shown Table 5.4 and Figure 5.27.

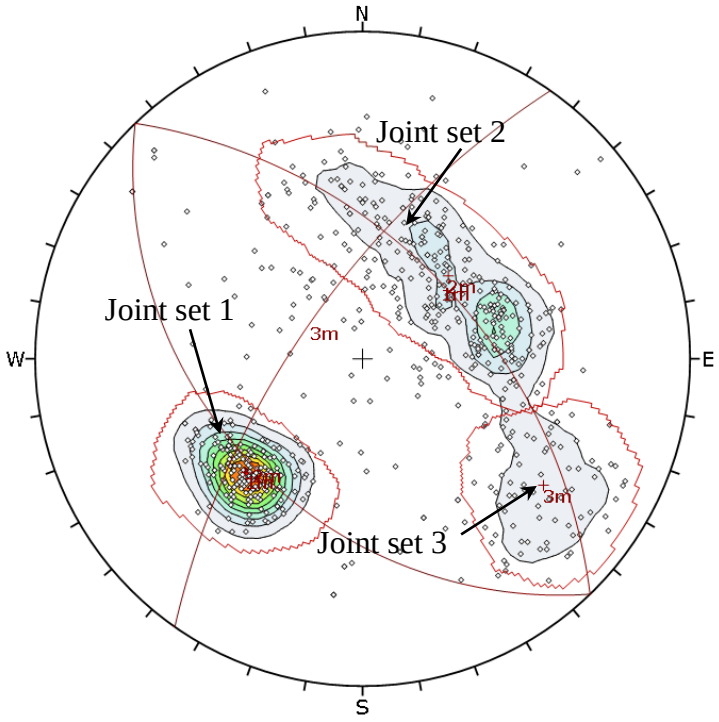

Figure 5.26 Contour plotting and joint set identification (pole plot)

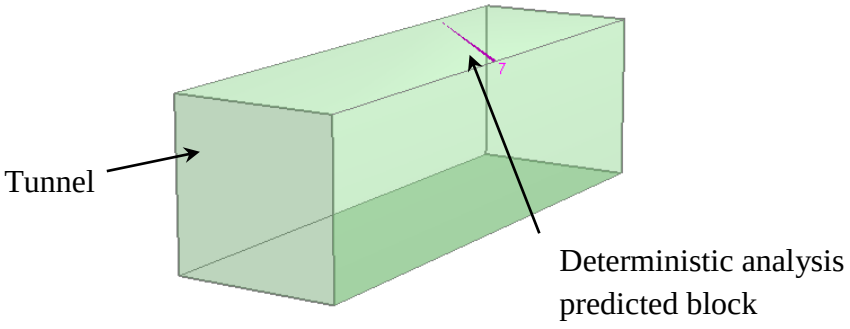

Figure 5.27 Span limited block

Table 5.4 Deterministic block analysis result

Block size (m^3)	0.056
Apex height (m^2)	0.11
Excavation face area (m)	1.53

As shown in Figure 5.27, deterministic block analysis with mean orientations predicts a very small span limited rock block (0.056 m^3) and elongated shape. The failure mode is sliding along discontinuity from joint set 3. If size parameters (trace length and spacing) are considered, the unstable rock block will be restrained to an even smaller size. However, if variation in rock parameters is considered, possible rock block vary in a large range. The probabilistic analysis results are shown in Figures 5.28 to 5.31.

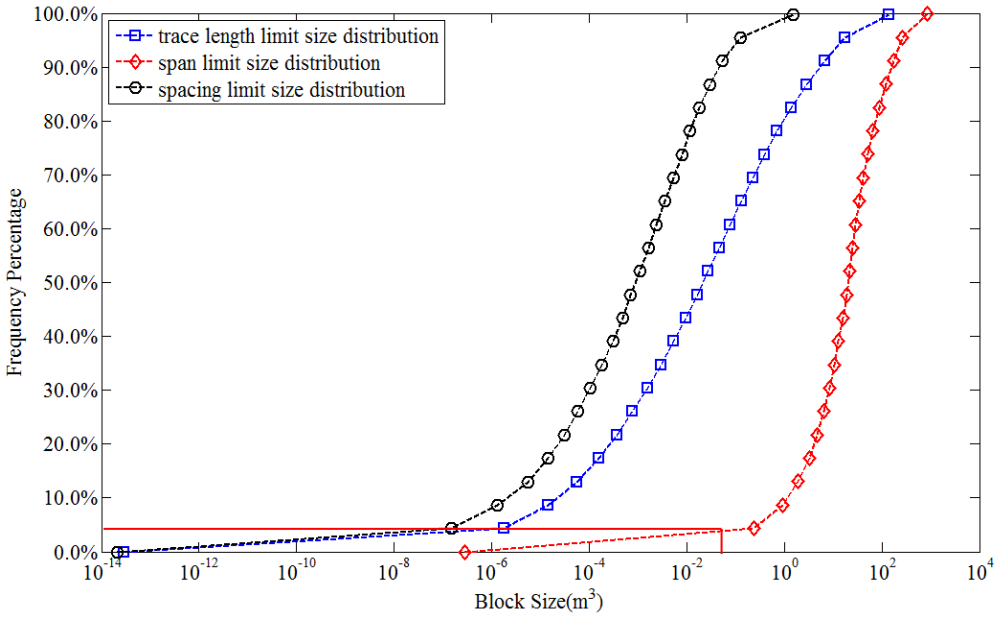

Figure 5.28 CDF of block size considering different size parameters

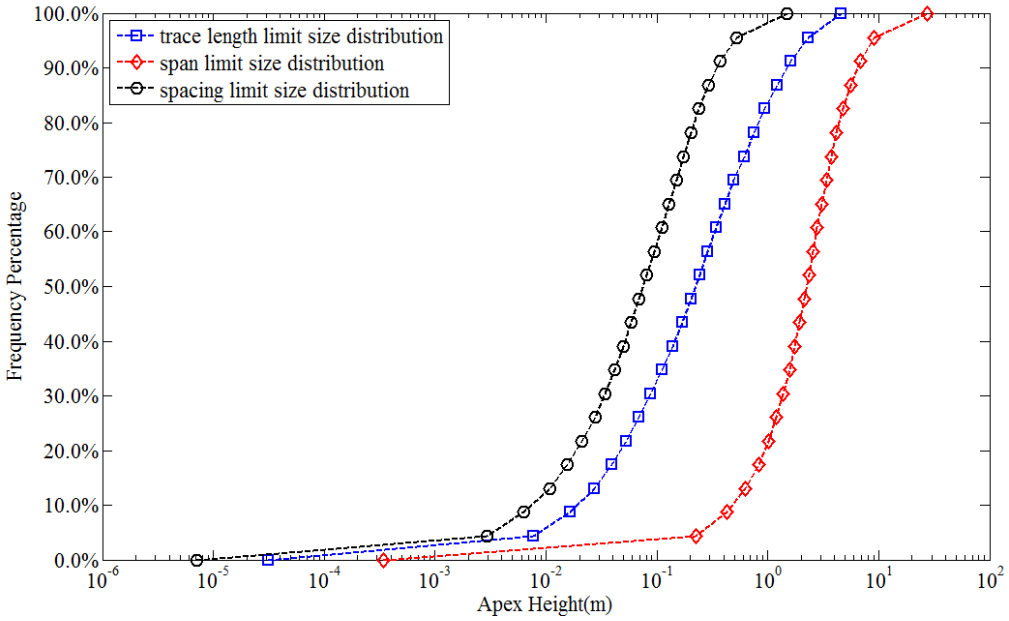

Figure 5.29 CDF of apex height considering different size parameters

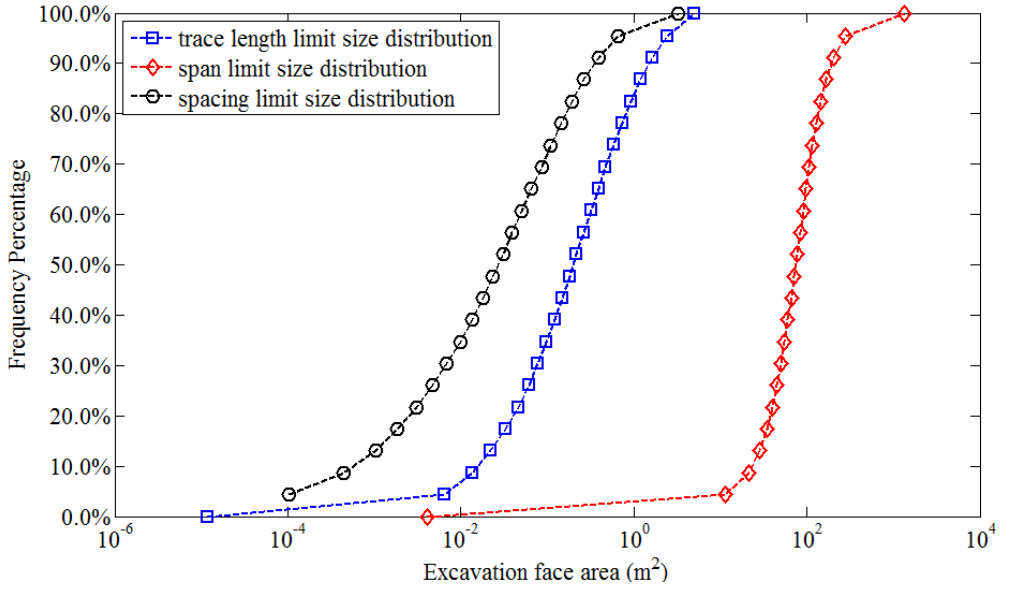

Figure 5.30 CDF of excavation face area considering different size parameters

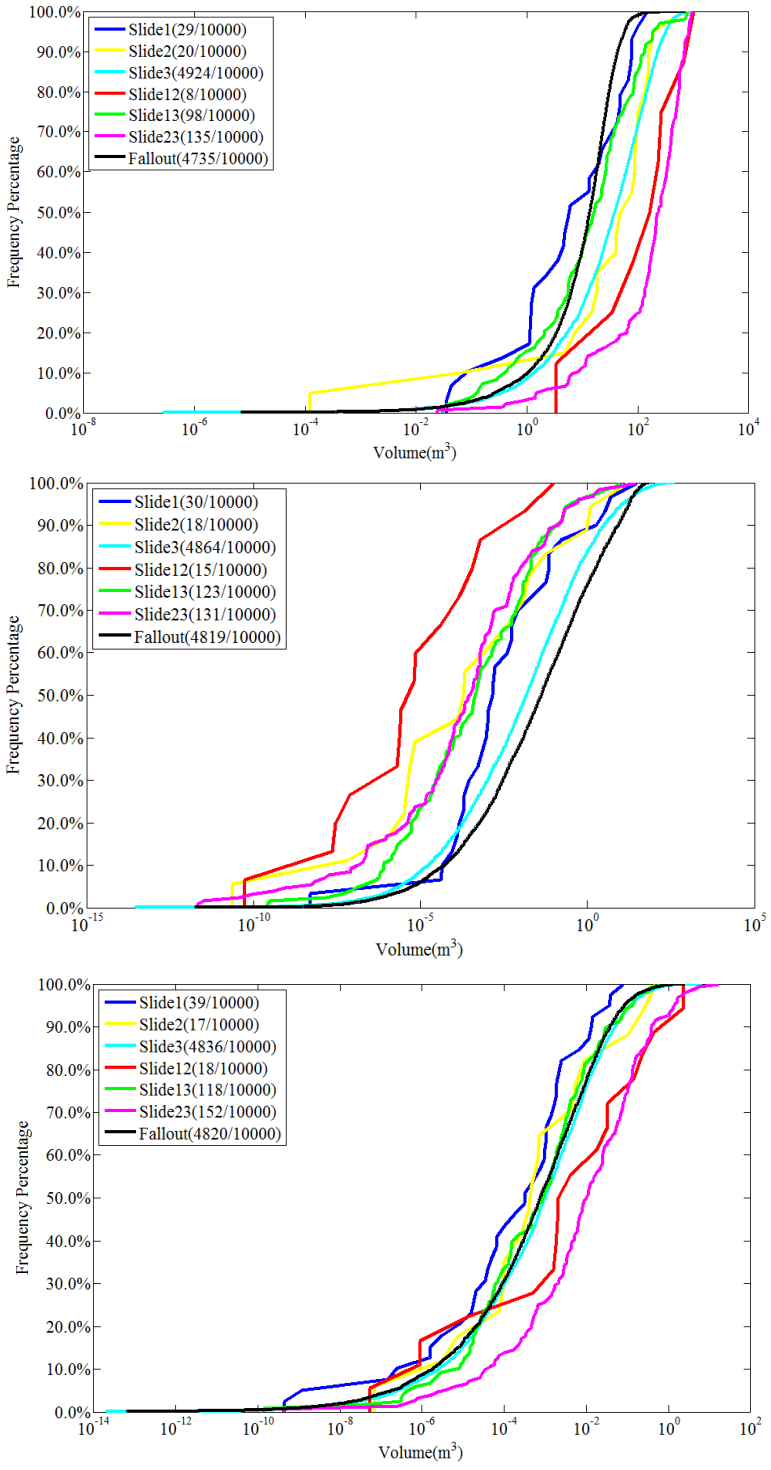

Figure 5.31 Figure 5.31 Volume distribution CDF according to different failure mode (a) span limited analysis result (b) trace length limited analysis result (c) spacing limited analysis result

Table 5.5 Probability of each failure mode out of total simulation number (%)

Failure mode	Span limited size
Sliding along plane 1*	0.29
Sliding along plane 2	0.2
Sliding along plane 3	49.24
Sliding along intersection 12*	0.08
Sliding along intersection 13	0.98
Sliding along intersection 23	1.35
Fallout	47.35
Total	100

* Sliding along plane 1 means unstable block will fail by sliding along discontinuity plane from joint set 1. Sliding along intersection 12 means unstable block will fail by sliding along the intersection of discontinuity planes from joint set 1 and joint set 2.

Probabilistic analysis shows that only about 5% unstable block is smaller than the deterministic predicted block size. Besides, probabilistic analysis also shows that the occurrence of fallout failure is about 50% (Table 5.5), whereas, deterministic block analysis only predicts sliding along discontinuity from joint set 3.Therefore, if rock reinforcement is designed based on this deterministic rock block. Although a large factor of safety is used, it is still cruel.

5.7 Summary

In this chapter, rock support design considerations are presented. Rock bolt design parameters such as bolt length, capacity and installation spacing are the main design criteria and should thus be carefully proposed. Variation in these rock bolt design parameters may have tremendous impacts on rock block stability as discussed in Chapter 4. Therefore, a reinforcement design based

only on deterministic rock block analysis with a factor of safety is deemed to be too cruel and may not be reliable. According to Dunn (2013), a design with a higher factor of safety does not necessarily mean that the design has a lower risk. Hence, the effectiveness of existing design based on deterministic approach is compared to reliability-based design. A case study on Singapore Jurong Formation was conducted using these two design approaches. The analysis result shows that although the largest span-limited block with a factor of safety of 2 is considered in rock bolt design, a 62% of probability of failure (high risk) can occur. In other words, deterministic design with factor of safety is not reliable for this case. Therefore, reliability-based design with POF is adopted to further evaluate the rock block stability. In reliability-based design, the rock bolt design parameters are adjusted until POF of reinforced rock block is less than the acceptable design criteria (POF less than certain amount which depends on the risk level that is acceptable by the designer). Subsequently, parametric study is performed to investigate the effects of above mentioned variation of rock bolt design parameters on POF determination. The analysis results show that rock bolt design parameters have significant effect on reinforced block stability. Generally, increase in rock bolt length and capacity and decrease in bolt spacing will lead to a safer design. However, it was found that these variations in rock bolt design parameters may not be effective under certain conditions such as when a single bolt capacity is achieved, increase in bolt length will not enhance the block stability. This case study coincides with Tyler et al. (1990)'s finding that

the rock bolt length design has an upper limit. Beyond this maximum length, increase of rock bolt length does not enhance the stability of the block. Therefore, cautions should be taken when adjusting rock bolt design parameters to achieve a low POF. It is also observed that rock bolt designs with different rock bolt design parameters may be varied by the designer in order to achieve the acceptable design criteria. Therefore, cost effective analysis should be further investigated to select the most economical reinforcement design.

Chapter 6 Conclusion

6.1 Summary of Findings

The studies presented in preceding chapters aim to study the effect of variation in rock parameters on the rock reinforcement design of unstable rock blocks. The findings of this study are summarized as follows.

1) Variation in joint orientation has demonstrated significant impacts on unstable rock block identification. All rock parameters should be simulated with appropriate distributions. Goodness of fit test results of 6 locations of rock orientation data from Singapore and overseas with a total of 21 joint sets show that over 70% (15 out of 21) of joint sets originate from a non-symmetrical distribution. In other words, non-symmetrical distributed joint sets are usually encountered in rock masses. Commonly assumed Fisher distribution fails to simulate non-symmetrical distributed rock orientation data, whereas, Kent distribution can simulate the distribution well.
2) Probabilistic analysis with Monte Carlo simulation has been conducted to consider variations in all rock parameters. The results show that more failure modes may occur with different probabilities, if joint orientation dispersion is taken account. Whereas, size parameters (joint trace length and spacing) have tremendous influence on rock block size determination. Rock block size would be significantly smaller if size parameters are taken into consideration. Besides, deterministic analysis

predicted failure mode may not be the dominant failure mode in probabilistic analysis and the corresponding block size is not necessarily conservative.

3) If Fisher distribution is adopted for non-symmetrical joint orientation data simulation, unstable rock block size distribution and probability of each failure mode may not be appropriate as compared to the more robust simulation using Kent distribution. Parametric studies show that statistical parameters of Kent distribution (concentration κ, ovalness β, rotation matrix Γ) play important roles in joint orientation simulation and small variation in each of these statistical parameters can lead to a significant variation in unstable block size distribution.

4) A reinforcement design based only on deterministic rock block analysis with a factor of safety is deemed to be cruel and may not be reliable. The effectiveness of existing design based on deterministic analysis is compared to reliability-based design with a case study on Singapore Jurong Formation. The analysis result shows that although the largest span-limited block with a factor of safety of 2 is considered in rock bolt design, a 62% of probability of failure (high risk) can occur. A parametric study is performed to investigate the effects of variation in rock bolt design parameters on reinforcement design probability of rock block failure. The analysis results show that rock bolt design parameters have significant effect on reinforced block stability determination. Generally, increase in rock bolt length and

capacity and decrease in bolt spacing will lead to a safer design. However, it is found that these variations in rock bolt design parameters may not be effective once critical rock block is stabilized.

6.2 Recommendations for Further Studies

In this research, several assumptions and simplifications are used for rock block simulation. However, some improvements can be made for further studies as follows:

1) Ubiquitous approach is assumed for rock block analysis. It assumes rock discontinuity can occur everywhere and anywhere in rock masses in order to capture all possible unstable rock block formed by rock discontinuities. However, in actual field conditions, the locations of rock discontinuities relative to the excavation are specific in rock excavation. Rock discontinuities may not intersect with each other to form unstable rock block, if the position of rock discontinuity is far from each other. Therefore, the position of rock discontinuities can be further considered in future probabilistic rock block analysis.
2) Rock bolt design parameters (e.g. bolt length, capacity and spacing) have shown significant impacts on reinforced rock block stability analysis. Different combination of these rock bolt design parameters can achieve the same design criteria. Grenon and Hadjigeorgiou (2003) emphasized that cost difference among design alternatives may be

tremendous. Therefore, a cost effective analysis is recommended to optimize reinforcement design.

Reference

Babuska, R., and Veen, P.J., Improved covariance estimation for Gustafson-Kessel clustering. IEEE conference. On Fuzzy systems, Vol. 2, pp.1081-1085, 2002.

Baecher, G. B., Lanney, N. A. and Einstein, H. H. Statistical description of rock properties and sampling. In proc. 18th U.S. Symposium. On Rock Mechanics. June 1977, Colorado, USA, pp. 22-24, 1977.

Barton, N., Lien, R., and Lunde, J. Engineering classification of rock masses for the design of tunnel support. Rock mechanics, Vol. 6(4), pp.189-236, 1974.

Berthelsen, O. J. Guide to cavern engineering: Geotechnical Engineering Office, Civil Engineering Dept. 1992.

Bieniawski, Z. T. Engineering classification of jointed rock masses. In International Journal of Rock Mechanics and Mining Sciences & Geomechanics Abstracts, Vol. 11(12), pp. 239-254, 1974.

Bieniawski, Z. T. Rock mechanics design in mining and tunnelling. Amsterdam: A.A. Balkema. 1984.

Bieniawski, Z. T. Engineering rock mass classifications: a complete manual for engineers and geologists in mining, civil, and petroleum engineering. New York: John Wiley & Sons. 1989.

Biron, C. and Arioglu, E. Design of Supports in Mines. pp. 89-117, New York: John Wiley & Sons. 1983.

Brady, B. H. G. and Brown, E. T. Rock Mechanics: For Underground Mining. London: Chapman & Hall. 1993.

Carter, T.G. and Miller, R.I. Crown-pillar risk assessment – planning aid for cost-effective mine closure remediation, Trans. IMM (Sect. A), Vol. 104, pp. 41–57, 1995.

Chen, D. Design of rock bolting systems for underground excavations. PhD thesis, University of Wollongong. 1994.

Coates, D. F. and Cochrane, T. S. Development of design specifications for rock bolting from research in Canadian mines. Report for Department of Energy, Mines and Resources. 1970.

Diederichs, M., Espley, S., Langille, C. and Hutchinson, D.J. A semi-empirical hazard assessment approach to wedge instability in underground mine openings. In Proc. International Conference on Geotechnical and Geological Engineering, November 2000, Melbourne, Australia. 2000.

Driels, M. R. and Shin, Y. S. Determing the number of iterations for Monte Carlo simulations of weapon effectiveness. Report for Defense Threat Reduction Agency. 2004.

Dunn, M. J. Unvertainty in ground support design and implemetation in underground mining. 2013.

Dunn, M. J, Earl, P., and Watson, J. Support design using probabilistic key block methods. In Proc. 6th International Symposium on Ground Support in mining and civil engineering construction, April, 2008, Cape Town, S Africa, Vol. 30, pp. 623-636. 2008.

Earl, P. Report on trail rockbolt spacings for underground surface rock support at Newmont Jundee Operations. Internal Newmont report. 2007.

Engelder, T. and Delteil, J. The orientation distribution of single joint sets. Geological Society, London, Special Publications, Vol. 231(1), pp.285-297. 2004.

Esterhuizen, G.S. JBlock User's Manual and Technical Reference. 1996.

Esterhuizen, G. and Streuders, S. Rockfall hazard evaluation using probabilistic keyblock analysis. Journal-South African institute of mining and metallurgy, pp. 59-64.1998.

Fenton, G. A. Probabilistic Methods in Geotechnical Engineering. Workshop presented at ASCE GeoLogan'97 Conference, Logan, Utah. 15 July 1997.

Fisher, R. Dispersion on a sphere. Proceedings of the Royal Society of London. Series A. Mathematical and Physical Sciences, Vol. 217(1130), pp. 295-305. 1953.

Forgy, E. W. Cluster analysis of multivariate data: efficiency versus interpretability of classifications. Biometrics, Vol. 21, pp. 768-769. 1965.

Goodman, R. E., and Shi, G. Block Theory and its Application to Rock Engineering. Englewood Cliffs, NJ: Prentice-Hall.1985.

Grenon, M., and Hadjigeorgiou, J. Drift reinforcement design based on discontinuity network modelling. International Journal of Rock Mechanics and Mining Sciences, Vol. 40(6), pp. 833-845. 2003.

Grenon, M., and Hadjigeorgiou, J. Applications of fracture system models (FSM) in mining and civil rock engineering design. International Journal of Mining, Reclamation and Environment, Vol. 26(1), pp. 55-73. 2012.

Gustafson, D. E. and Kessel, W. C. Fuzzy clustering with a fuzzy covariance matrix. In decision and Control including the 17th Symposium on Adaptive Processes, Vol.17 pp. 761-766. 1978.

Hanna, T. M. Foundation in Tension-Ground Anchors. Trans Book company, pp. 573. 1982.

Hammah, R. and Curran, J. Fuzzy cluster algorithm for the automatic identification of joint sets. International Journal of Rock Mechanics and Mining Sciences, Vol. 35(7), pp. 889-905. 1998.

Hoek, E. Rock Engineering; Course notes by Evert Hoek (Online), available on the Internet at http://www.rockeng.utoronto.ca/Hoekcorner.htm. 1997.

Hoek, E. and Brown, E. T. Underground excavations in rock. Institution of Mining and Metallury. 1980.

Hoek, E., Kaiser, P.K. and Bawden, W.F. Support of Underground Excavations in Hard Rock, Balkema, Rotterdam, 300 p. 1995.

Jung, S. Generating Von Mises Fisher distribution on the unit sphere (S^2). 2009. Retrived Sep 4, 2012 from http://www.stat.pitt.edu/sungkyu/software/randvonMisesFisher3.pdf

Kemeny, J. and Post, R. Estimating three-dimensional rock discontinuity orientation from digital images of fracture traces. Computers & Geosciences, Vol. 29(1), pp. 65-77. 2003.

Kent, J. T. The Fisher-Bingham Distribution on the Sphere. Journal of the Royal Statistical Society Series B-Methodological, Vol. 44(1), pp. 71-80. 1982.

Kent, J. T. and Hamelryck, T. Using the Fisher-Bingham distribution in stochastic models for protein structure. Quantitative Biology, Shape Analysis, and Wavelets, Vol. 24, pp. 57-60. 2005.

Korsawe, J. Circlefit3d-fit circle to three poits in 3d space. Retrived Jan 4, 2013 from http://www.mathworks.com/matlabcentral/fileexchange/34792-circlefit3d-fit-circle-to-three-points-in-3d-space/content/circlefit3d.m.

Kuszmaul, J. Estimating keyblock sizes in underground excavations: accounting for joint set spacing. International Journal of Rock Mechanics and Mining Sciences, Vol. 36(2), pp. 217-232. 1999.

Lang, T. A. and Bischoff, J. A. Stabilization of rock excavations using rock reinforcement. In proc. 23rd US Symposium on Rock Mechanics, Berkeley, USA. pp. 935-944. August 1982.

Latham, J. P., Van Meulen, J. and Dupray, S. Prediction of in-situ block size distributions with reference to armourstone for breakwaters. Engineering geology, Vol. 86(1), pp. 18-36. 2006.

Leung, C. F. and Quek, S. T. Probabilistic stability analysis of excavations in jointed rock. Canadian Geotechnical Journal, Vol. 32(3), pp 397-407. 1995.

Lewis, T. and Fisher, N. I. Graphical methods for investigating the fit of a Fisher distribution to spherical data. Geophysical Journal of the Royal Astronomical Society, Vol. 69(1), pp. 1-13. 1982.

Löset, F. Using the Q-system for support estimates of small weakness zones and for temporary support (in Norwegian). Internal NGI report no. 548140-1, 40 p. 1990.

Löset, F. Practical application of the Q-system (in Norwegian). Internal NGI report 592046-2, 40 p. 1997.

Lu, P. and Latham, J. P. Developments in the assessment of in-situ block size distributions of rock masses. Rock Mechanics and Rock Engineering, Vol. 32(1), pp. 29-49. 1999.

Lunder, J. Hard rock Pillar strength estimation an applied empirical approach. MSc thesis, University of British Columbia, Canada. 1994.

Luo, J. A new rock bolt design criterion and knowledge-based expert system for stratified. PhD Thesis, Virginia Polytechnic Institute and State University. 1999.

MacQueen, J. Some methods for classification and analysis of multivariate observations. In proceedings of the fifth Berkeley symposium on mathematical statistics and probability. Berkeley, USA. pp. 281-297. 1967.

Mammasis, K. and Stewart, R. W. The Fisher-Bingham Spatial Correlation Model for Multielement Antenna Systems. Vehicular Technology, IEEE Transactions on, Vol. 58(5), pp. 2130-2136. 2009.

Mandl, G. Rock joints. Berlin: Springer. 2005.

Mardia, K. V. and Jupp, P. E. Directional statistics, Vol. 494, John Wiley & Sons. 2009.

Mauldon, M. Keyblock probabilities and size distributions: A first model for impersistent 2-D fractures. International Journal of Rock Mechanics and Mining Sciences & Geomechanics Abstracts, Vol. 32(6), pp. 575-583. 1995.

Mauldon, M., Dunne, W.M. and Rohrbaugh, M.B. Circular scanlines and circular windows: new tools for characterizing the geometry of fracture traces. Journal of Structural Geology, Vol. 23, pp. 247-258. 2001.

Milne, D., Hadjigeorgiou, J.and Pakalnis, R. Rock mass characterization for underground hard rock mines. Tunnelling and Underground Space Technology, Vol. 13(4), pp. 383-391. 1998.

Pahl, P.J. Estimating the mean length of discontinuity traces, International Journal of Rock Mechanics and Mining Sciences & Geomechanics Abstracts, Vol. 18(3). pp. 221-228. 1981.

Palmstrom, A., Blindheim, O. and Broch, E. The Q system–possibilities and limitations. Paper presented at the Norwegian annual tunnelling conference on Fjellsprengningsteknikk/Bergmekanikk/Geoteknikk, Oslo. 2002.

Palmstrom, A. and Broch, E. Use and misuse of rock mass classification systems with particular reference to the Q-system. Tunnelling and Underground Space Technology, Vol. 21(6), pp. 575-593. 2006.

Park, H.J. Risk analysis of rock slope stability and stochastic properties of discontinuity parameters in western North Carolina. PhD thesis, Purdue University.1999.

Park, H. and West, T. Development of a probabilistic approach for rock wedge failure. Engineering geology, Vol. 59(3), pp. 233-251. 2001.

Peel, D., Whiten, W. J. and McLachlan, G. J. Fitting mixtures of Kent distributions to aid in joint set identification. Journal of the American Statistical Association, Vol. 96(453), pp. 56-63. 2001.

Priest, S. D. Hemispherical projection methods in rock mechanics. Wales: George Allen and Unwin, 1985.

Priest, S. D. Discontinuity analysis for rock engineering. Springer. 1993.

Priest, S.D. and Brown, E.T. Probabilistic stability analysis of variable rock slopes, Transactions of the Institution of Mining and Metallurgy, Section A: Mining Industry, IMM, Vol. 92, pp. 1-12.1983.

Priest, S. D. and Hudson, J. A. Estimation of discontinuity spacing and trace length using scanline surveys. In International Journal of Rock Mechanics and Mining Sciences & Geomechanics Abstracts. Vol. 18(3), pp. 183-197. 1981.

Phoon, K. K. Towards reliability-based design for geotechnical engineering. Special lecture for Korean Geotechnical Society. Seoul. 2004.

Rahardjo, H., Aung, K., Leong, E. C. and Rezaur, R. Characteristics of residual soils in Singapore as formed by weathering. Engineering geology, Vol. 73(1), pp. 157-169. 2004.

RIANOVOSTI , Retrieved May 1 2014 from http://en.ria.ru/russia/20130421/180763165/Nine-Miners-Trapped-in-Siberian-Coal-Mine-Accident.html

Shanley, R. J., and Mahtab, M. A., Delineation and analysis of clusters in orientation data. Journal of the International Association for Mathematical Geology Vol. 8 (1), pp. 9-23. 1976.

Song, J. J., Lee, C. I. and Seto, M. Stability analysis of rock blocks around a tunnel using a statistical joint modeling technique. Tunnelling and Underground Space Technology, Vol. 16(4), pp. 341-351. 2001.

Thompson, A.G. and Windsor, C.R. Block formation around excavations using deterministic and probabilistic methods, In Proc. 11th ISRM Conference, The Second Half Century of Rock Mechanics, July 2007, Lisbon, Portugal, Vol.1, pp. 183-186.

Tyler, D., Trueman, R. and Pine, R. A probabilistic method for predicting the formation of key blocks. Mining Science and Technology, Vol. 13(2), pp. 145-156. 1991.

Watson, J. Geotechnical review: ground support standards. Internal Newmont report.2007.

Wesseloo, J. and Read, J. Acceptance criteria, Guidelines for Open Pit slope Design, P, ed by J. Read, pp. 221-236. 2009.

Whitaker, A. E. and Engelder, T. Characterizing stress fields in the upper crust using joint orientation distributions. Journal of structural geology, Vol. 27(10), pp. 1778-1787. 2005.

Windsor, C.R. Systematic design of reinforcement and support schemes for excavations in jointed rock. In Proc. International Symposium on Ground Support and Reinforcement Practice in Mining, ed by E. Villaescusa, C.R. Windsor, A.G. Thompson. pp. 35-58. Rotterdam: A.A. Balkema. 1999.

Windsor, C. R. and Thompson, A. G. Reinforcement design for jointed rock masses. In Proc. 33rd US Symp. on Rock Mech., Santa Fe, Rock Mechanics. Vol. 521, ed by W. R. Tillerson and J. R. Wawersik. pp. 530-539. Rotterdam: A.A. Balkema. 1992.

Wood, A. T. The simulation of spherical distributions in the Fisher-Bingham family. Communications in Statistics-Simulation and Computation, Vol. 16(3), pp. 885-898. 1987.

Zhang, Z., Zhang, J. and Xue, H. Improved K-Means Clustering Algorithm. Image and Signal Processing, 2008. CISP '08. Congress on, Sanya, China. Vol.5, pp.169-172, 2008.

Appendix

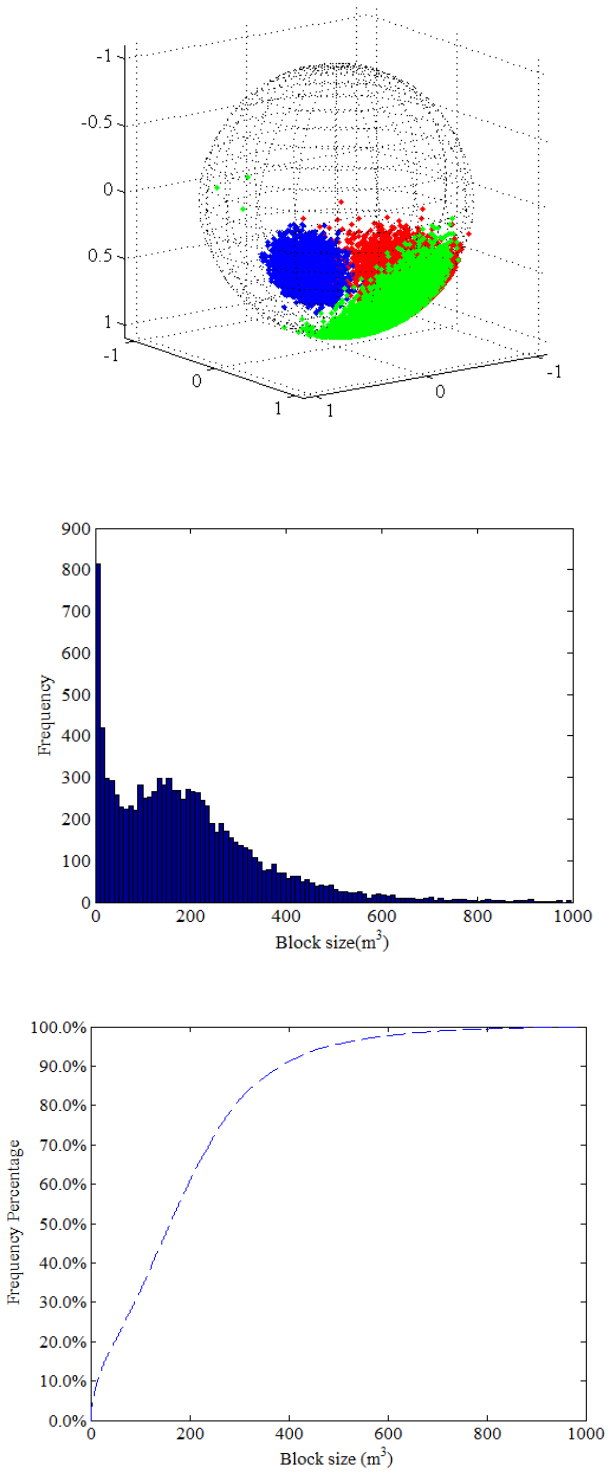

Figure 1 Block size analysis result with case 1

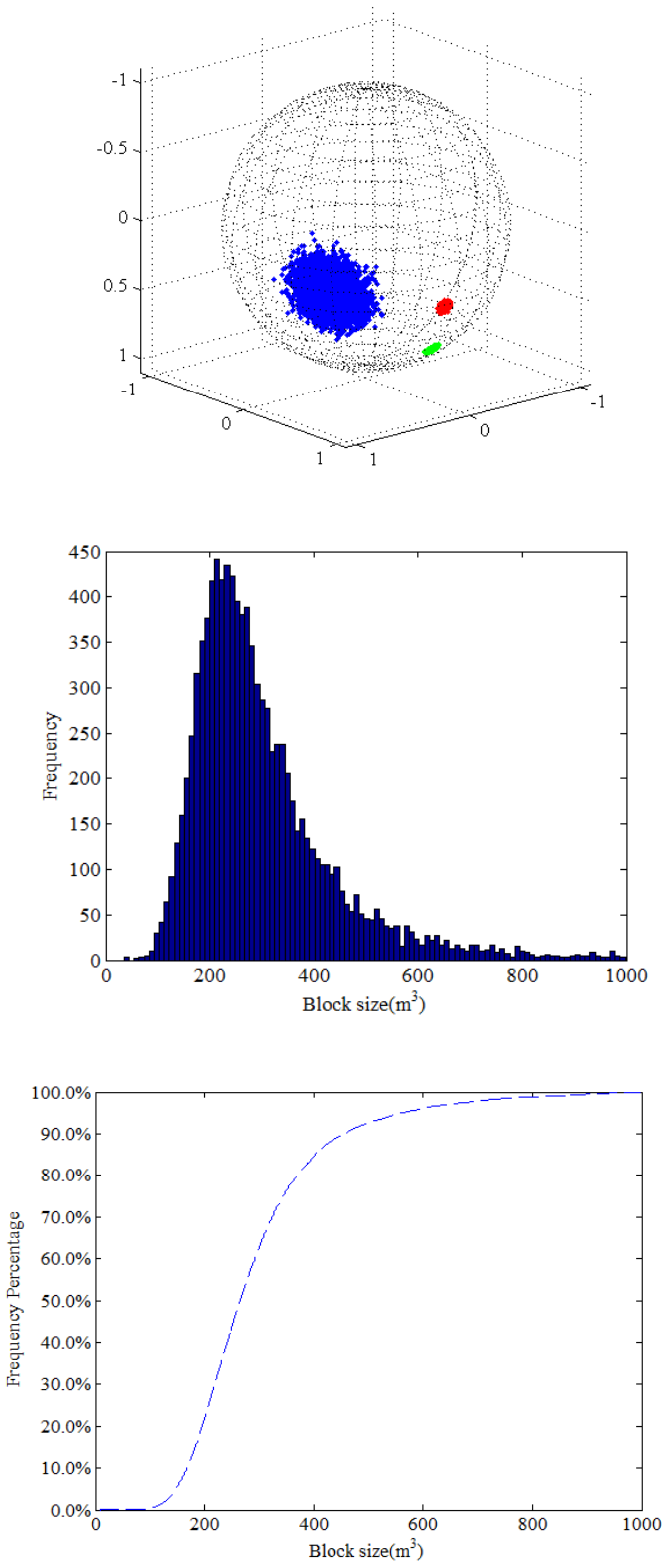

Figure 2 Block size analysis result with case 2

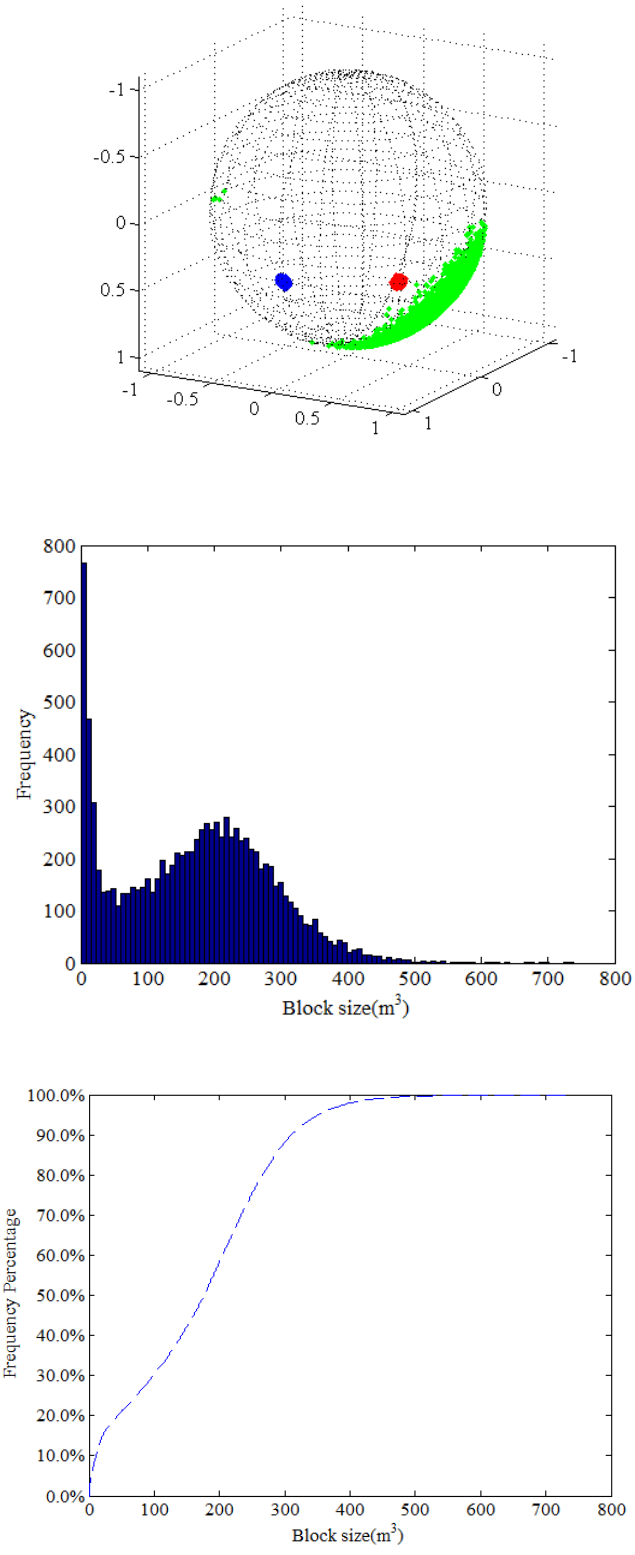

Figure 3 Block size analysis result with case 3

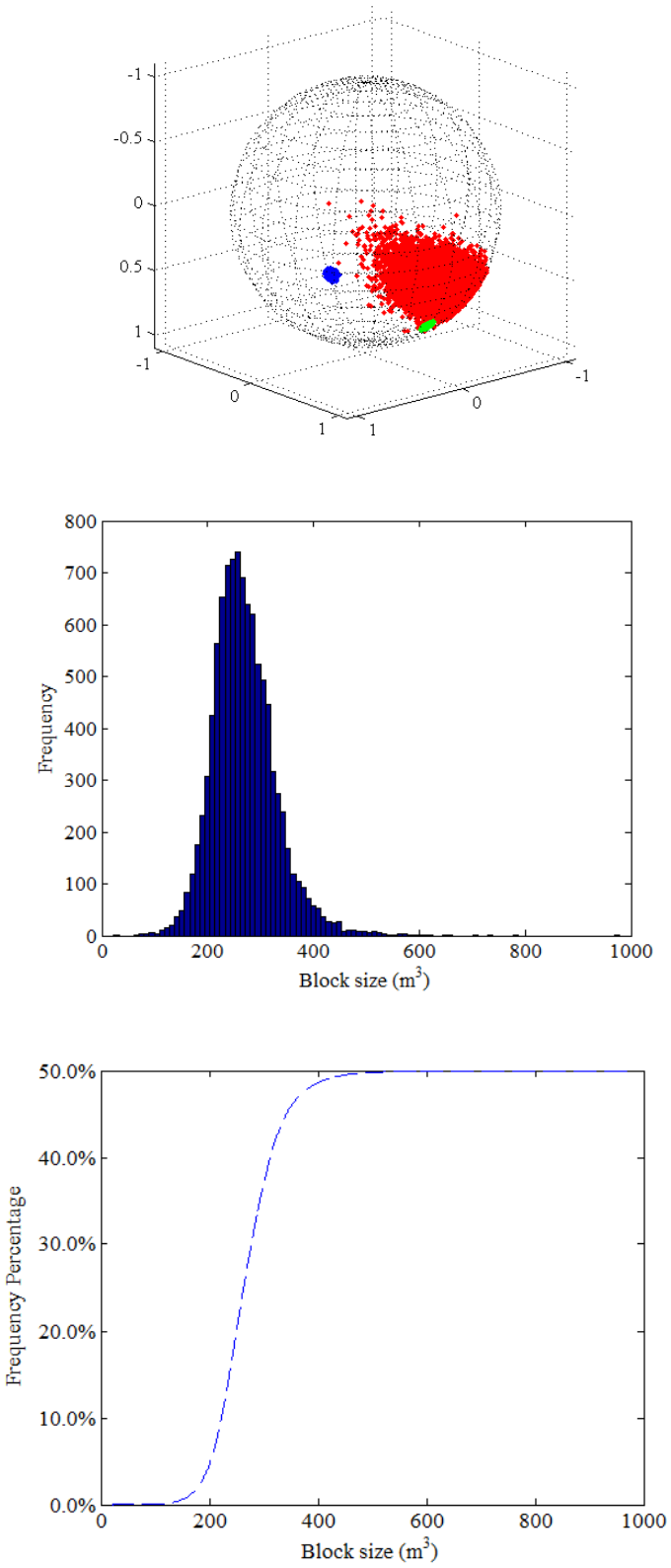

Figure 4 Block size analysis result with case 4

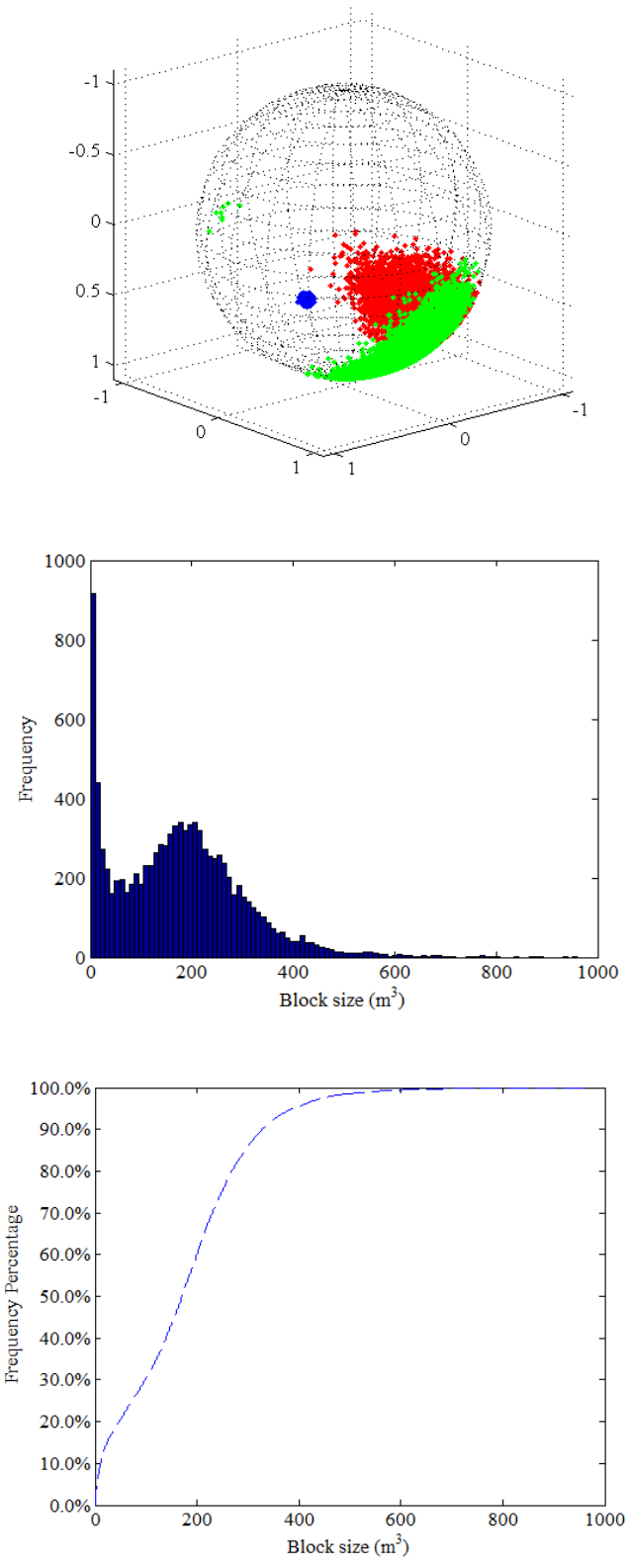

Figure 5 Block size analysis result with case 5

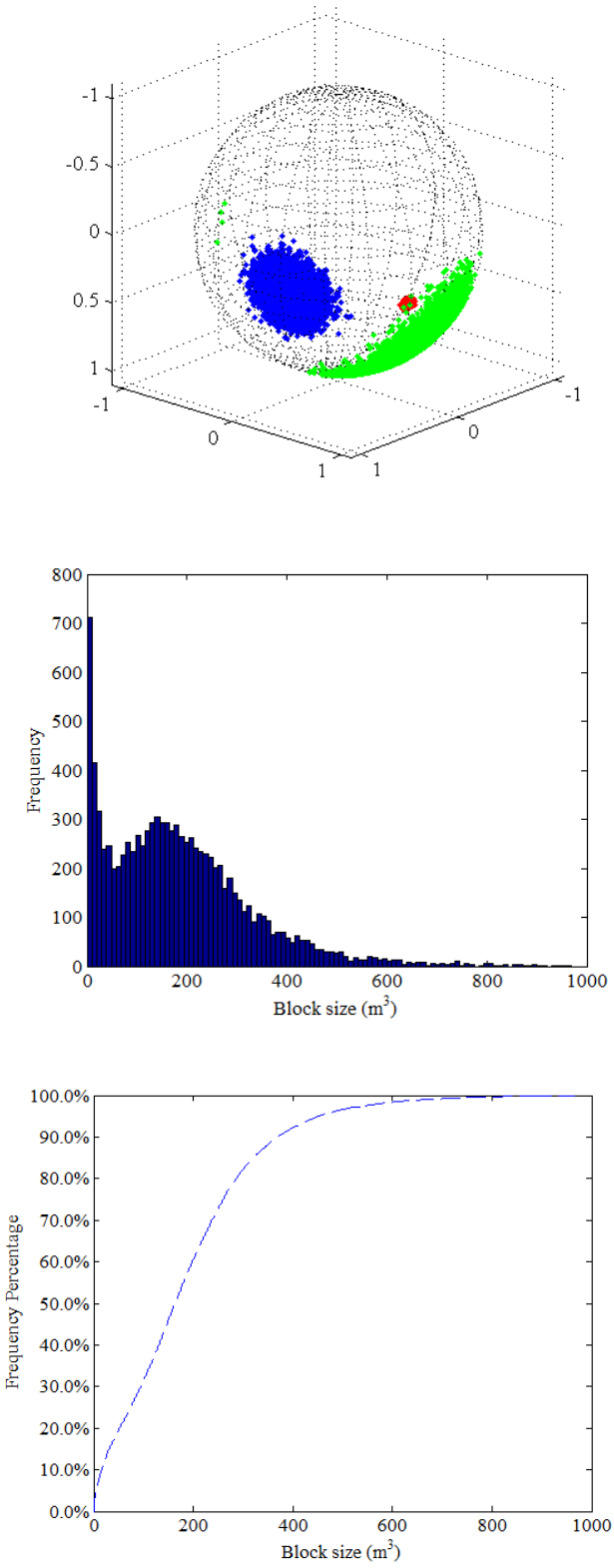

Figure 6 Block size analysis result with case 6

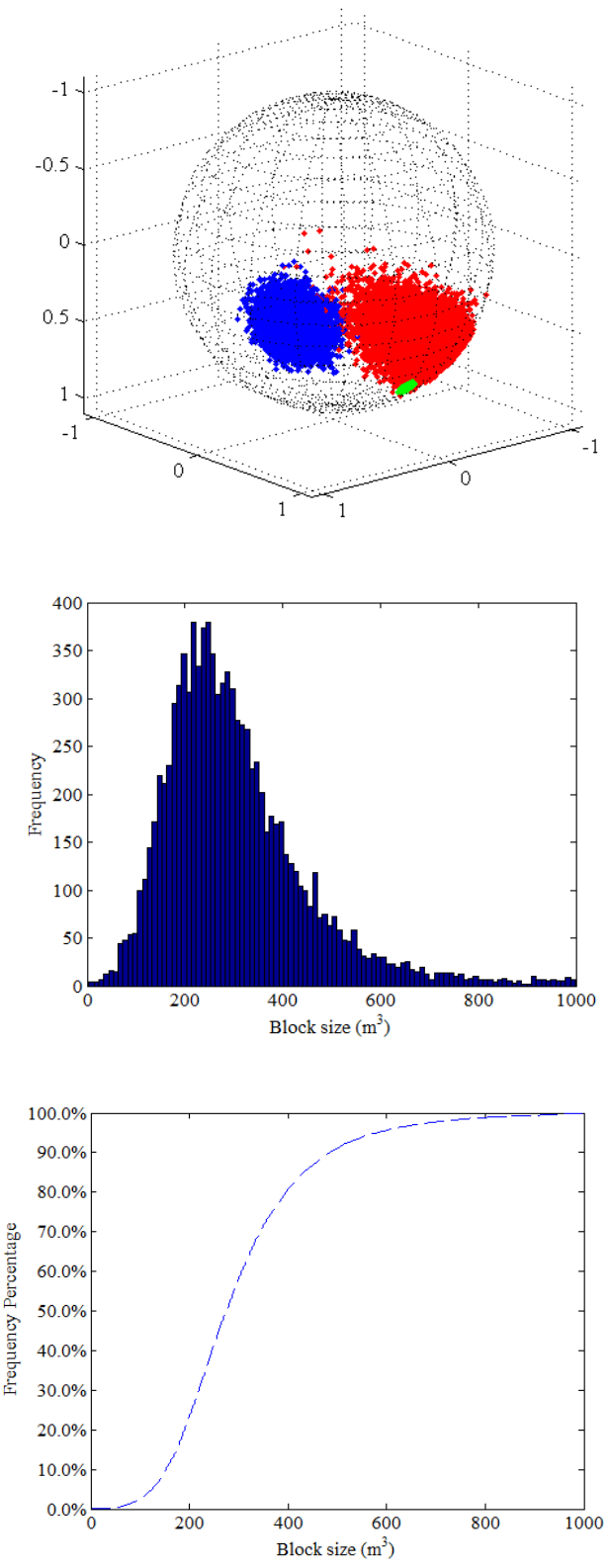

Figure 7 Block size analysis result with case 7

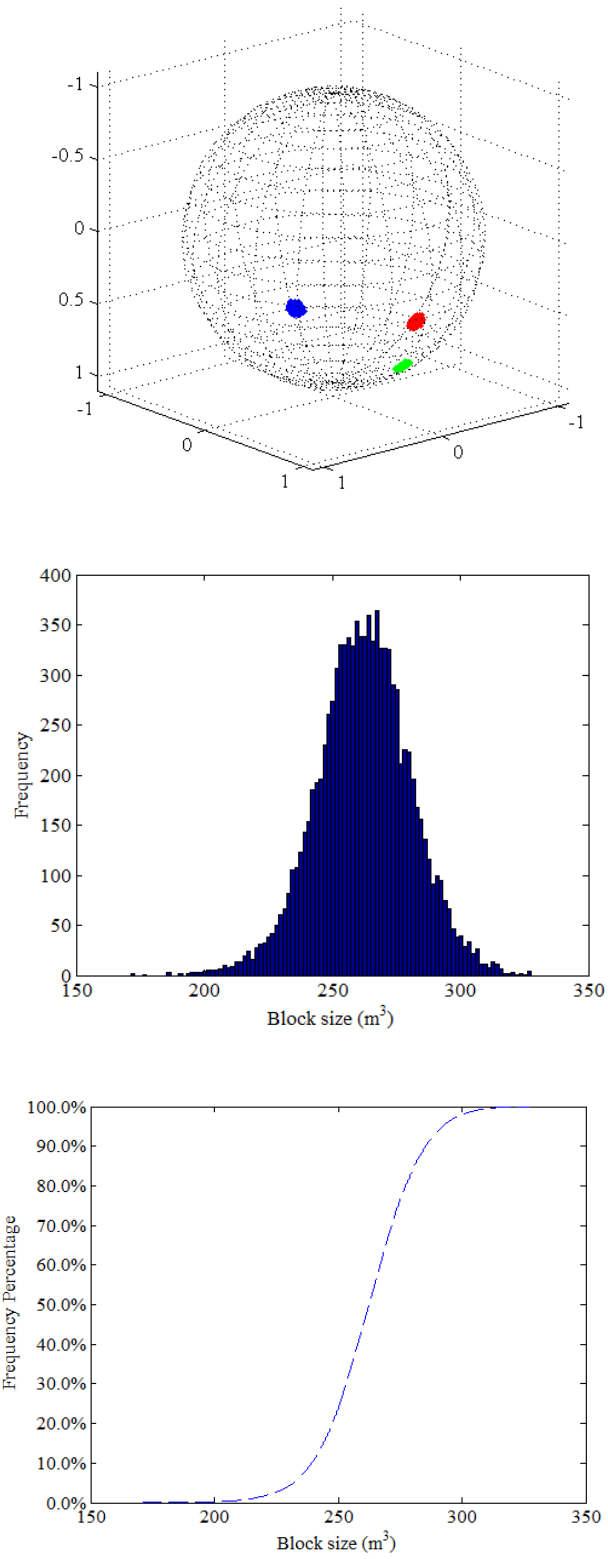

Figure 8 Block size analysis result with case 8